Investigation of Drying Conditions for Dental Practice Loads

By

Ahmed Abdel Rahman

A Thesis Submitted in Partial Fulfilment

of the Requirements for the degree of

Master of Applied Science

in

Mechanical Engineering

Faculty of Engineering and Applied Science

University of Ontario Institute of Technology

Oshawa, Ontario, Canada

April 2019

THESIS EXAMINATION INFORMATION

Submitted by: **Ahmed Abdel Rahman**

Master of Applied Science in **Mechanical Engineering**

Thesis title: Investigation of Drying Conditions for Dental Practice Loads

An oral defense of this thesis took place on April 8, 2019 in front of the following examining committee:

Examining Committee:

Chair of Examining Committee	Dr. Martin Agelin-Chaab
Research Supervisor	Dr. Ibrahim Dincer
Examining Committee Member	Dr. Dipal Patel
External Examiner	Dr. Akramul Azim

The above committee determined that the thesis is acceptable in form and content and that a satisfactory knowledge of the field covered by the thesis was demonstrated by the candidate during an oral examination. A signed copy of the Certificate of Approval is available from the School of Graduate and Postdoctoral Studies.

Abstract

This thesis investigates different drying techniques for dental practice loads experimentally and numerically. Several experiments are carried out by changing both top and bottom wall temperatures while changing the ranges of the pressure pulses during the drying phase. The studies show that both cases result in the best drying quality with only 2 grams of water remaining on the pouches at the end of the cycle under the conditions where the pressure pulse ranges from 14 to 16 kPa at a wall temperature of 170ºC and when the pressure ranges from 14 to 18 kPa at a top wall temperature of 160ºC and a bottom temperature of 170ºC, respectively. In addition, several simulations are presented using the COMSOL Multiphysics software to study the effect of fluid velocity on the evaporation rate of water droplets. Also, the effects of changing the top and bottom wall temperatures on the natural circulation and thus on the average velocity inside the chamber. Finally, the effects of changing both the wall temperatures and the pressure pulses range from 15 kPa to 20 kPa after one complete pressure pulse is presented. The maximum energy and exergy efficiencies are obtained as 78.29% and 30.3%, respectively.

Keywords: Drying; sterilization; Energy; Exergy; Efficiency; Pressure pulses; vacuum drying.

Acknowledgments

I deeply and forever grateful to my supervisor Professor Ibrahim Dincer for his guidance and tolerance. He has guided and encouraged me to carry on throughout this year and motivated me in every way possible. Thank you for guiding me with big doses of patience. His support and confidence in me brought out the best in me and was one of the main sources of motivation during my research and studies. I owe him everything I have learnt in this year and words cannot express how much I learnt from my experience in working with him.

I would like to thank all my colleagues in our lab (ACE3030B) and CERL building, Magd DinAli, Osamah Siddiqui, Haris Ishaq, Shareef Seifden, Khalid Al-Tayeb, Maan Al-Zareer, Ayda Farsi, Mohammad Ezzat, Burak Yuzer, Huseyin Karasu, Farid Safari, Mohammad Ra'fat, Zeynep Demir and Ahmed Hasan for bearing with me the good and the bad times during my wonderful days in MASc. Thank you for supporting me through my Masters in the long hard nights spent working and having fun. I would like to acknowledge Ahmed Hassan (senior) separately for being a friend before a lab mate. He has given me valuable support since the beginning of my project, and who always managed to make me feel better in the stressful times. Also, special thanks to his family, especially to his lovely mom, Ayda Tahoun, for all of her support and amazing food. Special words of gratitude go to my close friend Cilele Zeynep Demir, who have always been a major source of support when things would get a bit discouraging, thank you for the support you have provided me.

A very special word of thank goes to all my family, my brothers Yazan and Mohammad, my sister Razan and my lovely parents, Ali Abdel Rahman and Sawsan Al-Haj for all the emotional and financial support they have given me over the years. None of this would have been possible without them. They have been the light of life and who have given me strength and believe to get anything done. To my parents, there are no proper words to convey my deep gratitude and respect for you.

Table of Contents

List of Tables

List of Figures

Nomenclature

C_p	Specific heat capacity at constant pressure (J/kg K)
m	Mass (kg)
P	Pressure (Pa)
$\dot{Q}$	Heat rate (W)
t	Time (s)
U	Uncertainty of a variable
v	Velocity (m/s)

Greek letters

ρ	Density (kg/m^3)
η	Efficiency

Subscripts and Superscripts

0	Reference state
1,2,3,4	State points
f	Final
fu	Fusion
i	Initial
L	Latent
m	Melting
s	Sensible

Chapter 1: Introduction

In this chapter, worldwide energy needs, drying processes and Health concerns and sterilization are discussed briefly. The motivation and the importance of this topic are presented and finally, the objectives of this work are illustrated.

1.1 Energy Needs

Due to the industrial expansion and the population increase, the consumption of energy is drastically increasing over the years. BP statistical review report [1] shows that the annual growth rates of oil production in 2017 in Canada and the US are 8.1% and 5.6%, respectively, while oil consumption growth rates are 1.2% and 1%, respectively. Figure 1.1 shows the energy consumption by sector since 1970 and projected to 2040. The energy consumed by the industry sector is under an annual demand growth rate of 1% since 1995 to 2017 [1]. On the other hand, global energy demand is expected to increase by 50% by 2030 [2]. Figure 1.2 shows the percentage change in energy consumption, oil consumption, oil production, and total oil proved reserves in Canada and the US. As it's shown, Canada is facing challenges to keep up with the energy demand as it is increasing and the oil

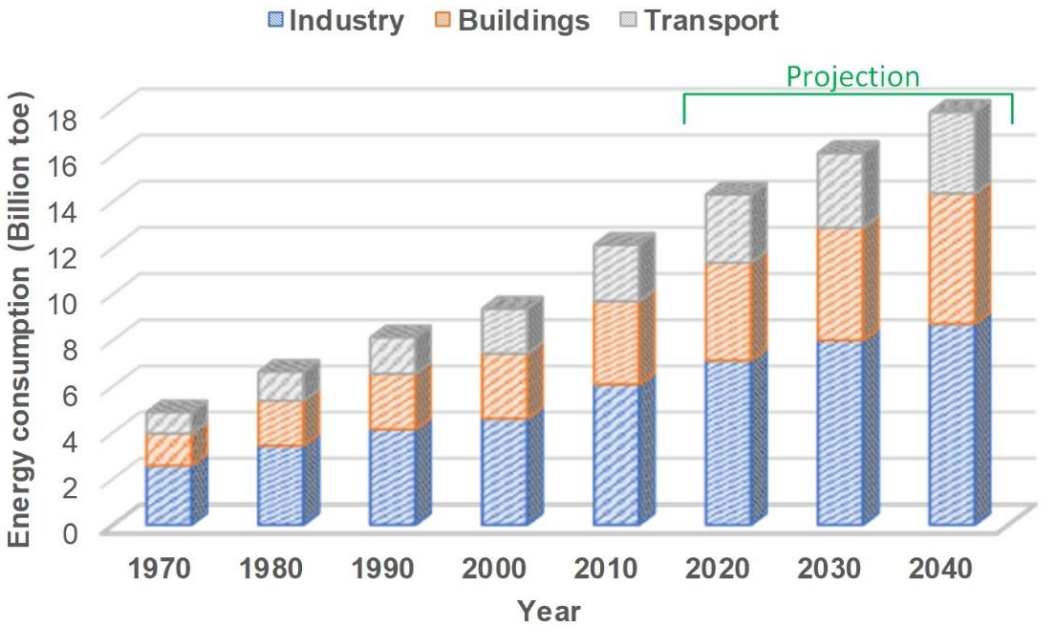

Figure 1.1 Energy consumption by end-user sector (data from [3])

reserves are decreeing. This encourages researchers to find ways to decrease this energy consumption by finding more efficient systems or developing renewable energy resources to meet the increasing demand. One main energy consuming process in the industry is drying. Even though drying consumes a significant amount of energy in the industries, the current available drying technologies are not efficient when it comes to energy consumption. It has been estimated that the efficiency of drying processes in the industry range between 20% to 60% depending on the nature of the process and the product to be dried [4]. This significant contribution to the global energy consumption by drying processes necessitates the need to develop innovation drying techniques and technologies [5]. Drying is among the most energy consuming processes in the industry that represents a significant fraction of the energy consumed depending on the nature of the industry. For example, it consumes 70% of the total energy consumed in manufacturing wood products, 50% in the textile fabrics industry and 27% of paper industry [6]. The total energy saving by utilizing the waste heat from drying processes in the industry is 377 trillion BTU which translates into $1240 million annually [7]. So, aiming for more efficient drying technologies will help, significantly, to reduce the total energy consumption in the world.

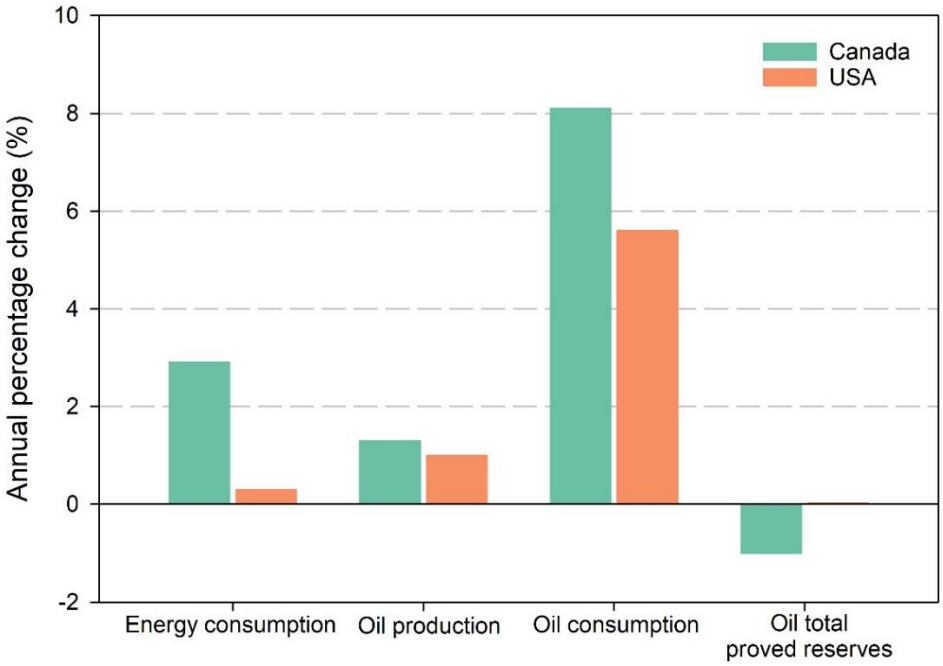

Figure 1.2 Energy consumption, oil production, oil consumption, and oil total proved reserves percentage change between 2016 and 2017 in Canada and the US (data from [1])

1.2 Drying Processes

The removal of moisture from a wet solid, solution or gas is usually referred to as drying process and it's often found in various industrial operations. For example, washed and centrifuged sugar crystals are being dried to get the finished product ready for packaging. Also, Soap bars are dried to decrease the water content before being ready to be used. Milk powder is produced by drying milk in a spray chamber. In the previous examples, there is a direct contact between the product and a hot gas that causes moisture loss from the wet material. For other heat sensitive products, heat is supplied by a heating medium like the wall of the dryer. Or even by the expulsion of moisture under vacuum which decreases the amount of required heat [8]. The causes of moisture are very different and the consequences of it can vary too depending on the nature of the industrial process. The causes of moisture include, but not limited to:

- Cooling. Products are cooled as the last stage of production in many industrial processes. Water might be used for cooling which creates the problem of leaving water droplets on the product. For example ready meals, cans, and pet food.
- Cleaning. Products usually have to be cleaned as the last step in production by being washed or rinsed which leaves some water droplets on the products. For example jam, sauces and soft drinks. Or even during the production phase, for example: when the outer surface of steel pipes should be rinsed with water after being washed with acids prior to the galvanizing process.
- Steam. Some products are exposed to steam at the end of the process to be cleaned which causes the problem of having condensate on the product. For example: fruits and juices.

Moisture which may cause many problems includes:

- Contaminated environment. Moisture is difficult to control and it contaminates the space in which it's presented. This becomes critical in products in which hygiene is of great importance like food.
- Ink spills. Printing on a wet surface is not possible since whatever being printed is going to run out and become invisible. Some products require important codes or

dates to be printed on them and having a wet outer surface makes the product illegible.

- Adhesive labels. As long as the outer surface of any product is wet, it's not possible to stick labels on it. The glue used to stick labels work when the surface is completely dry. Labels might be very important for some products to include codes, date or any other information.
- Damaging machines. Some machines during any industrial process are not designed to accept wet products. Having moist products can cause damages to machines during the manufacturing process.

The drying process of any moist material is a complicated process that requires analysis of mass and heat transfer coupled since they occur simultaneously inside the material to be dried [9]. Due to the complications of drying of moist materials, extensive efforts have been made to understand and develop theoretical models that include both heat and mass transfer to accurately describe the drying phenomena [10]. Luikov [11] suggested that mass transfer potential is a more crucial variable than moisture content in moisture movement in porous bodies. Also, temperature gradient is an important driving force for mass flow in porous media as was suggested by Mukherjee et al. [12]. According to Yilbas et al. [9], the quantitative understanding of the drying process is what makes the process complicated and it's mainly due to the following difficulties:

- All the involved physical processes are non-linear.
- Complicated exchanges and interactions
- The dominating phenomena keep changing during the drying process based on the drying conditions.
- The transport properties inside the material are function of both the moisture content and temperatures which means that they keep changing during the drying process.

1.3 Health Concerns and Sterilization

In the field of health care, safety is a critical issue in which every patient have the right to receive safe and reliable health services in which they should be kept free from any risks

of injuries in the hospital or any form of health care. The possibality for patients to experience adverse events in hospitals is significant, According to publishes reports and studies in Canada, the United States, the United Kingdom, Australia, New Zeland, and other countries show that between 4% to 16.6% of patients suffered some sorts of harm in hospitals, including permanent disability and death. However, 50% of those recorded cases were preventable types of harms, which are called preventable adverse events [13]. A preventable adverse event is defined as the unintended harm or injury that causes disability, death or prolonged hospital stay caused by health care management rather the ptient's disease that got him or her in the hospital in the first place. Even though modern health care systems provide high-quality services, patients can still suffer from any sort of preventable harms which might include death.

Dental health is an important part of our overall health since it affects the ability of eating, speech, social function, and self-esteem. Dental instruments can be either manually driven, air driven or electrically driven are used by dentists to prepare a tooth for receiving a restoration or to clean, polish and any other dental procedures. Those dental headpieces should be cleaned and sterilized between patient use since they become internally and externally contaminated after being used [14–19]. The sterilizing process is a widely used practice for the cleaning and the disinfection of medical and dental tools which is followed by a drying process to ensure no moisture is present in the pouches. The presence of moisture in pouches will promote bacteria growth, which is why the drying process is just as important as the other processes.

1.4 Research Challenge and Motivation

There are two types of table top autoclaves that are commonly used in the industry, a cassette type, and a chamber type. For this thesis, the focus is going to be on the chamber type. These devices sterilize loads by removing air from the chamber and exposing the load to saturated steam conditions of approximately 134°C and 2 bar for a number of minutes. Typical sterilizer loads, in the dental environment, consist of several pouches containing approximately 300 grams of dental instruments each. These pouches are typically fabricated with one side of transparent plastic and the other of a steam permeable paper. At

the end of the sterilization, this typical loaded pouch has approximately 4 ml of liquid water on the load, saturating the paper and forming droplets on the plastic layer. Sterilized loads can be handled when there is no visible water in the loaded pouch. Sterilizer manufacturers must define complete cycle times based on dry output for the worst case load configuration. The user of the sterilizer is interested in achieving the shortest overall cycle time. It is therefore desirable to achieve the shortest possible drying time. The current limiting issue is typically small droplets which remain on the plastic inner side of the pouch. This droplet takes a long time to evaporate as there is a low thermal mass to provide the energy needed, the local environment in the pouch is moist and there is a low movement of the drying medium local to the droplet. So, the key challenge is to provide the least drying times for dental practice loads in a more efficient and cost effective manner.

1.5 Objectives

Improving the drying quality for the sterilization process is of great importance for a wide range of dental tools industries in Canada and worldwide. The main objective of this thesis is to develop new models and technologies for the drying phase at the end of the sterilization process for dental tools to decrease the time required for the process and enhance the quality of drying by having fewer water droplets on the instruments to be dried. So, this thesis aims to experimentally improve the drying quality and develop new mathematical models.

The specific objectives of the thesis are listed below:

- To study the effect of changing the flow velocity from 1.5 m/s to 3 m/s on the evaporation rate of water by measuring the amount of evaporated water over a certain period of time for different flow velocities.
- To model and study the effect of changing the top and bottom wall temperatures on the natural circulation and thus on the average magnitude of the velocity of the fluid inside the chamber, the homogeneity of the mixture and average temperature of the fluid inside the chamber.

- To model and study the effect of changing both top and bottom wall temperatures from 150^{o}C to 170^{o}C and the pressure pulses ranges from 15 kPa to 20 kPa on the drying quality for the pouches after one complete pressure pulse.
- To compare the drying quality, experimentally, by varying the top wall temperature from 150°C to 170°C while keeping the bottom wall temperature as 170°C and changing the upper limit of the pressure pulses created during the drying phase from 16 kPa to 20 kPa while keeping the lower limit pressure as 14 kPa.
- To measure and study the influence of varying the pressure pulses ranges and the varying the top wall temperatures on the energy and exergy efficiencies of the drying phase.

Chapter 2: Literature Review

In this chapter, drying in general and vacuum and dental load drying in particular are discussed. Furthermore, a literature review about phase change material (PCMs) is performed. Finally, the sterilization process in discussed

2.1 Drying

Drying is a widely used industrial process in which mass is transferred, usually water or moisture, from a solid or liquid. It's a thermally driven process of great importance in many industries like pharmaceutical, chemical, agriculture, food, paper, wood, mineral, and solid fuel preparation. The drying process considered as energy-intensive industrial process [20]. For example, 15% of the energy consumption in North America is consumed in drying energy processes [21]. There are, mainly, two different types of drying: vacuum and conventional drying. The difference between conventional and vacuum drying is that in the vacuum drying, the total pressure difference is the driving force. Two main processes occur during the drying process, heat transfer that takes place from the surrounding environment to the moist object or surface to evaporate the moisture and the transfer of the internal moisture from inside the object to be dried to its surface [20].

2.1.1 Vacuum Drying

Vacuum drying has been used since the early 1900s for wood drying [22], as the first US patent was issued in 1904, "Process for Drying Timber" [23]. Vacuum can be classified based on the heating source into four groups: Cyclic vacuum, dielectric vacuum, superheated steam vacuum and conductive heating vacuum [22]. Vacuum drying is recommended since it aids to decreases the overall cycle time [24]. In vacuum food drying process, the removal of moisture usually takes place under low pressure while heat is supplied from the heated plates in which the food is placed on top of the heating coils. This heat is used to supply the latent heat needed for the boiling of the water droplet. Usually, hot water is the source of heat in such applications. Jaya and Das [25] Studied the effect of mango pulp thickness and vacuum chamber plate temperature on the drying of mango pulps. The pulp thickness was varied from 2 to 4 mm while the vacuum chamber plate

temperature was ranging from 65ºC to 75ºC. It was found that the drying process should be carried out below 72.3 ºC with a maximum pulp thickness of 2.6mm. Sahari et al. [26] Studied the effects of temperature, pressure, and thickness on the dehydration of date powder. Four various scenarios were considered, (100^0C and 20.4 kPa, 93^0C and 40.5 kPa, 84 C and 72.8 kPa, 68 C 80.1 kPa). The optimum operation parameters were 85^0C, 72 kPa and 1 cm thickness during 7 hours in total drying time. Many factors were considered when choosing the optimum conditions, like moisture reduction, color quality, energy consumption, and economical feasibility. Zotarelli et al. [27] Studied the effect of multi-flash drying on the water content of fruits. Based on the finding of this study, pressure pluses help cooling down the temperature of the surface of the fruit which increases the temperature differences between the fruits and surrounding air which will enhance the heat transfer process.

2.1.2 Dental Load Drying

During the drying process of dental loads placed inside pouches, condensation occurs inside the pouches as a result of contacting the steam with the load cooler surface. To complete the cycle, the load removed from the chamber should be completely dry since the presence of water droplets can cause re-contamination of the tools. The recommended drying phase pressure is 1 to 2 psi (6.9 to 13.8 kPa). Water at 6.9 kPa will boil at 38.7^0C, and the condensation will be removed during the vacuum process as it boils from the energy of the load itself. After a fixed amount of time, the load is cooled, and the temperature dropped to below the boiling temperature at the vacuum pressure. Keeping the load inside the chamber after the set drying time has no added benefit since evaporation is negligible after this point. The optimal drying time depends on the load density and the distribution of the load inside the chamber. For example, plastic may require additional drying time since it cools rapidly. Pulsed heated air or pulsed air can be used as an additional drying process [28]. So, some heating is required to keep the object temperature from falling below the boiling point at the vacuum pressure using one of the following methods: 1- Raising the temperature of the tools before starting the drying process. 2- Using radiant heat to warm up the entire chamber. 3- Heat up the tools inside the chamber using conduction heat transfer plate inside the chamber [29]. For wrapped instruments, the

recommended drying time is 20-30 minutes [30]. Drying an object at 25^0C in a vacuum is three times faster than drying it with air at 30^0C and 50% relative humidity [29]. Dion and Parker [28] Suggest that heavier pouches should be placed at the top shelf since condensation droplets are created due the contact of steam with cooler surface (pouches), and condensation droplets will fall from the top shelf to the lower shelves. In addition, it's suggested to place a cotton sheet or line free towel in between the shelves to prevent condensation droplets from falling to the lower shelves which will aid the drying process and also increase the condensate surface area which will increase the evaporation rate. In addition, the positioning of the pouches plays a significant role in a successful drying process. The pouches should be positioned so that the condensate will is allowed to flow downward and not allowed to be collected. Dry air should be introduced to the chamber passing through a bacteria-free filter which will break the vacuum and help to complete the drying process [29].

2.2 Phase Change Materials

Phase change material (PCM) is an energy storage material that releases heat in the form of sensible and latent heat. During melting and solidification, PCMs are capable of releasing a large amount of latent energy for a small volume [31,32]. PCM determines the temperature that the thermal energy is released when discharge occurs. PCMs are reusable and could be sourced from organic resources. They are usually hydrated salts that have great extent of heat energy stored in the form of latent heat which is absorbed or released when the materials alter state from solid to liquid or liquid to solid. The PCM retains its latent heat without any alteration in physical or chemical properties over thousands of cycles. So, PCMs absorbs energy when heating and undergo a phase change, and then releases that heat when cooled [33]. Sensible heat is stored as thermal energy as the material, solid or liquid; temperature is increased. The amount of heat absorbed is a function of the material's temperature difference, specific heat capacity, and mass. On the other hand, latent heat is absorbed when the material undergoes a phase change which is the most efficient thermal energy storage mode. Equations 2.1 and 2.2 show the amount of heat absorbed for the two modes.

$$Q_s = \int_{T_i}^{T_f} mC_p dT = mC_p(T_f - T_i) \quad (2.1)$$

$$Q_L = \int_{T_i}^{T_m} mC_p dT + mL_{fu} + \int_{T_m}^{T_f} mC_p dT \quad (2.2)$$

In general, the phase change materials act as thermal batteries. When it is cooled down and frozen liquid, the temperature remains at the freezing temperature until a significant amount of heat is removed, releasing stored energy and allowing it to freeze. By using PCMs, the wires, the heater, the maintenance, can be eliminated and the temperature levels can remain high with lower costs.

The PCMs freeze and thaw at the desired temperature, storing or releasing energy in the phase change process. PCMs can be derived from bio materials which bring higher sustainability and environmentally benign option.

Inorganic PCM are engineered hydrated salt solution made from natural salts with water. The chemical composition of salts is varied in the mixture to attain essential phase-change temperature. Distinctive nucleating agents are added to the mixture to minimize phase-change salt separation and to minimize super cooling that is otherwise characteristic of hydrated salt PCM. Salt hydrates are characteristic of being non-toxic, non-flammable and economical.

Bio-based PCMs are organic materials that are naturally present fatty acids such as vegetable oil. Based on their chemical composition, their phase-change temperature can change. These products are non-toxic, non-corrosive and have infinite life cycles. However, they can be expensive and flammable at high temperatures.

Organic PCMs are naturally existing petroleum bi-products that have their unique phase-change temperature. Paraffin wax consists of a mixture of mostly straight chain n alkanes $CH_3–(CH_2)–CH_3$. The crystallization of the (CH_3)-chain releases a large amount of latent heat. These products are generally produced by major petrochemical companies causing availability limitations. They can be toxic and expensive depending on the substance. They have infinite life cycles and the price varies with changes in petroleum prices globally.

The PCM systems are expected to have the following properties:

- Appropriate PCM with its melting point in the desired temperature range,
- Appropriate heat exchange surface,
- Appropriate container compatible with the PCM.

PCMs can be classified into three main categories: a) low-temperature PCMs where the transition temperature is below 15ºC b) medium temperature PCMs where the transition occurs between 15ºC and 90ºC c) high-temperature PCMs where the transition takes place above 90ºC [34,35]. Table 2.1 shows a potential PCMs that can be used to enhance the drying process.

Table 2.1 Different PCMs compounds

Compound	Heat of fusion (kJ/kg) Heat of phase transition (kJ/kg)	Melting Temperature (^{0}C) Phase transition temperature (^{0}C)	Category	Ref. No.
$AlCl_3$	280	192	Inorganic (solid-liquid)	[36]
$MgCl_2.6H_2O$	169	117	Salt hydrate (solid-liquid)	[37][38]
Erythritol	344	117	Organic (solid-liquid)	[39]
Tris[Hydroxymethyl]aminomethane	285.3-295.6	132.4-134.5	Polyalcohols (solid-solid)	[40]–[42]

Solid-solid PCMs release lower latent heat when phase change compared to solid-liquid PCMs. However, the main advantage of solid-solid PCMs is the smaller volume and the fact that they can easily be contained without leaking problems [43].

In this study, our focus is going to be on the drying process considering the properties in the sterilizing process as our initial state since we cannot change sterilizing time, pressure and temperature because it's regulated, and the final state should be a dry product in the least possible time. In the developed process we should avoid poor performance, lower productivity, and high operation and maintenance costs.

The use of PCMs inside the chamber of the system is suggested, however, due to health concerns and regulations, nothing should be placed inside the chamber during the sterilization process.

2.3 Sterilization

Sterilization is any process in which all biological agents such as bacteria and viruses are eliminated, killed, removed or deactivated from a specified region of the surface. Any medical device that is used in contact with patient's tissues involves the risk of infection. Such equipment must be properly disinfected or sterilized. Depending on the use of the tools or the equipment, high-level disinfection or low-level disinfection is required. Proper cleaning should proceed with any high-level disinfection and sterilization [44]. Rational and logical approach to disinfection and sterilization of medical equipment were developed over 45 years ago and the scheme is still used by professionals in this field to plan for disinfection and sterilization methods [45–48].

The steam sterilization method has been used for than a century as the main infection control method for objects that can withstand high pressure and temperature because it's non-toxic, generally available and easy to control [28]. Six factors are fundamentally critical for a successful steam sterilizing process: a) time b) temperature c) moisture d) direct steam contact e) air removal f) drying [28]. The cycle time for the sterilizing process is defined when the output is completely dry at the worst load configuration. The dryness of the object is measured by the weight difference between the pouches before and after going through the sterilization process. For the safe use of dental and medical instruments, disinfection and sterilization should be used properly.

Based on the literature, there are no experimental or numerical studies for the drying process for any sterilization machine for dental practice load. In this thesis, several experiments are conducted to measure the effects of several parameters on the quality of the drying process. In addition, different simulations are carried out to develop possible solution to enhance the drying quality.

Chapter 3: Experimental Apparatus and Procedure

In this chapter, the experimental setup is presented to study the effects of several operational parameters on the performance of the drying phase by measuring the improvement in the drying quality by measuring the weight of the water droplets remaining on and inside the pouches.

3.1 Process Description

This section defines the three different phases during the sterilization cycle, namely: Conditioning phase, sterilization phase, and drying phase. First, air is removed from the chamber by creating one or two pressure pulses in the first stage which is known as the conditioning phase. Saturated steam at 300 kPa at 134ºC is then introduced for 4 minutes to sterilize the pouches during the sterilization phase. Finally, the drying phase takes place to remove the water droplets from the pouches. The pouches in the chamber are made from a transparent plastic from one side and steam preamble paper from the other side that allows the stem and air to flow inside the pouches and clean the load. Figure 3.1 (a) shows the pouches when the tools are packed, and the pouches are sealed. Each pouch is 300 grams and the maximum number of pouches in a single process is 16, so the maximum total load to be dried is 4.8 kg.

3.1.1 Conditioning and Sterilization Phases

The time taken during the conditioning phase depends if it's the first run of the machine or the machine is used before. The conditioning phase is defined as the phase in which the chamber is being pressurized to the required sterilization pressure. During the conditioning phase, saturated steam is introduced to the chamber to pressurize it. During this phase, both pressure and temperature inside the chamber increase until they reach the desired values of pressure and temperature which are 300 kPa at 134 ºC, respectively. The steam should be saturated which is defined as 97% dry and 3% moisture [49]. This can be done through multiple pressure pulses to ensure sufficient air removal from the chamber [28,29]. Then, the sterilizing phase takes place where both pressure and temperature are held constant.

The minimum sterilization time should be 4 minutes to kill any microorganisms [50]. At the end of the sterilization phase, the pressure starts to drop marking the start of drying.

Figure 3.1 a) The transparent plastic side and the steam permeable paper side of the packed pouches. b) The trays inside the chamber without any load inside

3.1.2 Drying phase

The drying phase for this specific machine starts when the pressure drops after the end of the sterilization phase to 80 kPa and ends when it reaches up again to 80 kPa marking the end of the cycle. The total drying phase time is set by the user before running the cycle, it can be set between 0 minutes to 30 minutes. Zero minute drying time means that the cycle will end right after the sterilization phase, so no drying is taking place within the cycle. During the drying phase, the pressure can keep dropping the whole time by the built-in Venturi device or pressure pulses can take place instead of only dropping the pressure as it's going to be shown later in chapter5. The number of the pressure pulses created during the drying phase depends on the total drying time and the range of the pressure pulses. Obviously, the larger the range of the pressure pulses, the more time it takes to create each pressure pulse and thus less number of pressure pulses are created during a period of time.

3.2 Experimental Setup and Procedure

Figure 3.1 (b) shows the chamber without any load inside. As it can be seen, it consists of 4 racks to hold the pouches. Each rack is designed to hold 4 to 5 pouches which is equivalent to 1.2 kg-1.5 kg of load.

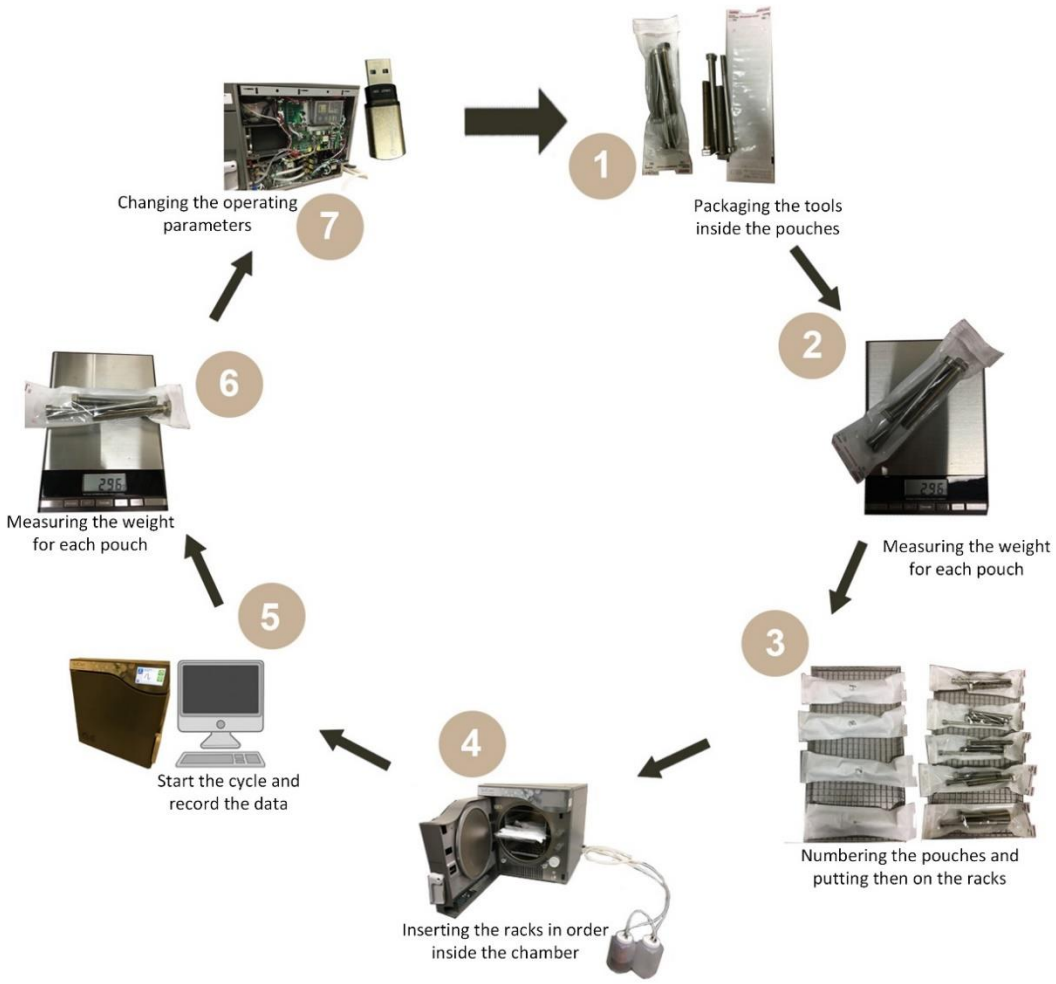

Figure 3.2 Experimental steps

Figure 3.2 shows the experimental steps followed while conducting the experiments. The first step is packaging the dental loads. Each pouch is design to carry 4 tools, the average weight for each tool is 75 grams. The second step is weighing the pouches. After packaging each pouch, the weight is measured and recorded. Then, the third step is to number all the pouches and arrange them on the racks. The fourth step is to put all the 4 racks with all the numbered pouches inside the chamber. The fifth step is to run

the sterilization cycle and logging the required the values of pressure and temperature to monitor the performance of the cycle. The sixth step is to take weight measurements again to compare them with the original weights measured before putting then in the chamber. The seventh step to update the machine's software to change either the wall temperatures or the pressure pulses ranges to run the cycle again for different drying conditions.

Chapter 4: Modeling and Analyses

In this chapter, the uncertainty analyses used for the experimental part is shown. In addition, the performance analyses used to calculate both energy and exergy efficiencies are illustrated.

Depending on the flow type, different set of equations should be used to describe the flow. Choosing the type of flow to solve for the pressure and velocity is a crucial step in the simulation since the solution of the fluid flow is going to be used to solve other physical interferences like heat transfer and transport of concentrated species. In addition, the simpler and the more accurate the assumptions are to solve for the fluid flow, the easier it's to solve, and the less time it takes in computations.

In the analysis of any drying process, the ideal gas theory is essential since water vapor generated from the moisture removal behaves like idea gas. The idea gas theory states that the ideal gas can be described in terms of three physical parameters: the volume of the gas, its temperature, and pressure. When designing a drying process, both the mathematical model and equipment limitations should be considered to choose the best-operating conditions for the drying process. A set of boundary and initial conditions should be appropriately chosen and then solved to accurately characterize the system and accurately predict the process parameters at any given time during the drying process. In addition, there are many correlations available in the literature to evaluate different parameters related to the drying process and required to develop the mathematical model.

4.1 Uncertainty Analyses

Uncertainty analysis is a technique that is performed to ensure the accuracy of the results. The total uncertainty can be expressed as follows:

$$U_y = \sqrt{\sum_i \left(\frac{\partial y}{\partial x}\right)^2 U_x^2} \tag{4.1}$$

where $U = \text{Uncertainty of variable}$

Random and symmetric errors are the two components of the experimental uncertainty and it's expressed as follows:

$$U_i = \sqrt{S_i^2 + R_i^2} \tag{4.2}$$

where $S_i = \text{Systematic errors}$ and $R_i = \text{Random errors}$

Relative standard deviation is:

$$RSD = \frac{S}{\bar{x}} 100\% \tag{4.3}$$

where $S = \text{Systematic errors}$ and $\bar{x} = \text{Mean of results}$

4.2 Performance Analyses

Energy efficiency is of great importance for understanding how well a drying process performs [51]. Al-Ali and Dincer [52] highlighted the importance of energy and exergy analyses for any thermodynamic system through the analysis of the first and the second law of thermodynamics In the following analyses, the kinetic and potential energy values they are negligible. The main performance variables include heat, work, and energy transferred by mass. Therefore, $\frac{v_i^2}{2} + gz = 0$. The simplified scematic of the drying process is shown in Figure 4.2.

Energy efficiency can be defined as the useful output over the required input. The energy efficiency of the drying process can be defined/expressed as follows:

$$\eta_{en} = \frac{(m_2 - m_3) \times h_{fg}}{m_1 h_1} \tag{4.4}$$

where the enthalpy of the drying air is defined as follows:

$$h_1 = (h_a)_1 + \omega_1 \left(h_g\right)_1 \tag{4.5}$$

Similar analysis was carried out by Dincer and Rosen [53], for the process of drying food items. The mass of the water on the pouches was calculated experimentally for each of the experimental runs before and after the drying process. The mass of the drying air

was calculated based on the pressure pulses ranges. The average values of the pressure pulses were considered. The relative humidity of the drying air was assumed to be 0.1 for all the cases.

The second law of thermodynamics is used with the conservation of mass and conservation of energy to conduct exergy analysis. According to Dincer and Rosen [53], the exergy of a system is defined by finding the maximum shaft work that can provided by the system in its current state. The exergy efficiency for this system is defined as follows:

$$\eta_{ex} = \frac{m_{w2} ex_{ph,2} - m_{w3} ex_{ph,3}}{m_1 ex_{ph,1}} \tag{4.6}$$

where the physical exergy for the drying air includes the physical exergy of both air and humidity carried by the air, it is calculated as follows:

$$ex_1 = \left(h_{a,1} - h_{a,0}\right) - \left[T_0 \times C_{p,a} \times \ln\left(\frac{T_1}{T_0}\right) - R \times \ln\left(\frac{P_1}{P_0}\right)\right] + \left[\omega_1 \times \left(h_{w,1} - h_{w,0}\right) - T_0 \times \left(s_{w,1} - s_{w,0}\right)\right] \tag{4.7}$$

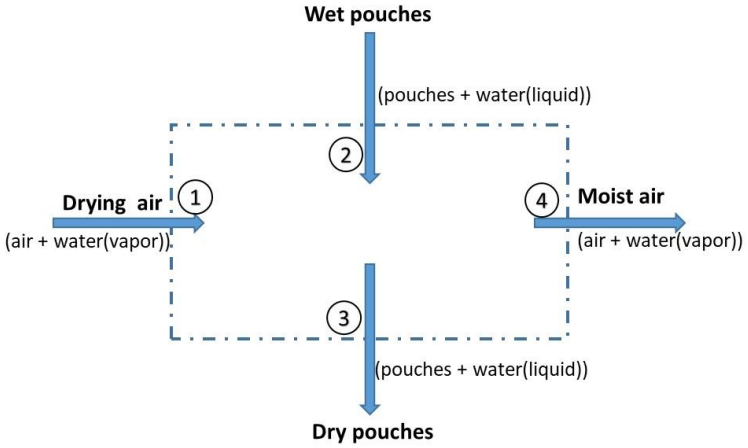

Figure 4.1 Schematic of a drying process showing input and output terms

Chapter 5: Results and Discussion

In this chapter, the experimental results obtained by changing pressure pulses ranges and inner walls temperatures are presented. Moreover, the energy efficiency of the drying process for the different experimental configurations is presented. In addition, the results of the simulation obtained from the COMSOL Multiphysics software [54] are discussed. The simulations are mainly focusing on improving the evaporation mechanism inside the chamber. The effect of the flow velocity on the evaporation rate of a wet surface is studied. Methods to improve the circulation and increase the flow speed inside the chamber will be discussed in detail. Some methods for improving the circulation within the chamber include: a) wall temperature gradient b) condenser to create a cold zone on the back wall of the chamber to condense the moisture in one area. Finally, the effects of varying both pressure pulses ranges and top wall temperatures on the drying quality after one complete pressure pulse is presented in detail.

5.1 Experimental Work

In this section, 9 different experimental cases are analyzed to study the combined effect of changing the inner wall temperatures and the pressure pulses ranges experimentally. In addition, the energy and exergy efficiencies for each of the experimental cases are calculated.

5.1.1 Different Walls Temperatures and Pressure Pulses Ranges

In order to study the effects of both changing the range of pressure pulses and having different wall temperatures during the drying process, several experiments are conducted to investigate the combined effect of changing both pressure pulses ranges and the top wall temperatures. The lower limit of the pressure pulses was set as 14 kPa while the upper limit was increased with an increment of 2 kPa with a range of 16 kPa to 20 kPa. The reason for the 2 kPa increments is that not all the pressure values between 15 kPa and 20 kPa can be tested and there is not too much variation effect on small pulses due to control tolerance and similar results are expected due to this. For example for 14 kPa to 16 kPa pulses, the actual pressure pulses will be between 14 kPa $\pm$1 kPa for bottom control and 16 kPa $\pm$ 2

kPa for top control. For this reason, the top pressure is varied as 16 kPa, 18 kPa, and 20 kPa. In addition to varying the pressure pulses range, the top and the bottom wall temperatures are varied to compare the performance of the drying process to the original 170°C constant walls temperatures. As the cold fluid has higher density, it's expected to be trapped in the down half of the chamber. In order to enhance the mix and the circulation inside the chamber, the lower wall temperature is always set to either equal of higher temperature compared to the top wall temperature. For the following experiments, the top wall temperature is varied as 170°C, 160°C, and 150°C. So, the parameters for the 9 experiments are as follows:

- Pressure pulses range: 14 kPa to 16 kPa. Top wall temperature: 170°C. Bottom wall temperature: 170°C. Represented as: **14-16 (170-170)**
- Pressure pulses range: 14 kPa to 16 kPa. Top wall temperature: 160°C. Bottom wall temperature: 170°C. Represented as: **14-16 (170-160)**
- Pressure pulses range: 14 kPa to 16 kPa. Top wall temperature: 150°C. Bottom wall temperature: 170°C. Represented as: **14-16 (170-150)**
- Pressure pulses range: 14 kPa to 18 kPa. Top wall temperature: 170°C. Bottom wall temperature: 170°C. Represented as: **14-18 (170-170)**
- Pressure pulses range: 14 kPa to 18 kPa. Top wall temperature: 160°C. Bottom wall temperature: 170°C. Represented as: **14-18 (170-160)**
- Pressure pulses range: 14 kPa to 18 kPa. Top wall temperature: 150°C. Bottom wall temperature: 170°C. Represented as: **14-18 (170-150)**
- Pressure pulses range: 14 kPa to 20 kPa. Top wall temperature: 170°C. Bottom wall temperature: 170°C. Represented as: **14-20 (170-170)**
- Pressure pulses range: 14 kPa to 20 kPa. Top wall temperature: 160°C. Bottom wall temperature: 170°C. Represented as: **14-20 (170-160)**
- Pressure pulses range: 14 kPa to 20 kPa. Top wall temperature: 150°C. Bottom wall temperature: 170°C. Represented as: **14-20 (170-150)**

For all the previous cases, the experiments were done in which the drying time was set to be 15 minutes for each one of them. The values of the pressure during the cycle are recorded and shown in Figure 5.1. Three different lines are shown for each of the three

pressure pulses ranges: 14 kPa to 16 kPa, 14 kPa to 18 kPa and 14 kPa to 20 kPa. As it is shown, the drying phase starts when the pressure drops to 80 kPa after the sterilization phase and ends when it reaches 80 kPa again after the last pressure pulse as it was explained earlier in Chapter 3. It's noted that the control of the pressure pulses is not perfect when it comes to the upper limit. However, for the lower limit of the pressure pulses, the pressure hits 14 kPa for all the cases before it starts increasing again which represents a good control over the lower limit. When the pressure range is set to be from 14 kPa to 16 kPa, the actual measured average value of the upper limit of the pressure pulses is 17.55 kPa which shows 9.67 % difference from the original set value of 16 kPa. When the pressure range is set to be from 14 kPa to 18 kPa, the actual measured average value of the upper limit of the pressure pulses is 20.53 kPa which shows 14.06 % difference from the original set value of 18 kPa. When the pressure range is set to be from 14 kPa to 20 kPa, the actual measured average value of the upper limit of the pressure pulses is 22.38 kPa which shows 11.88 % difference from the original set value of 18 kPa. The detailed values for the pressure at the upper limits of the pressure pulses seen in Figure 5.1 are shown in Table 5.1.

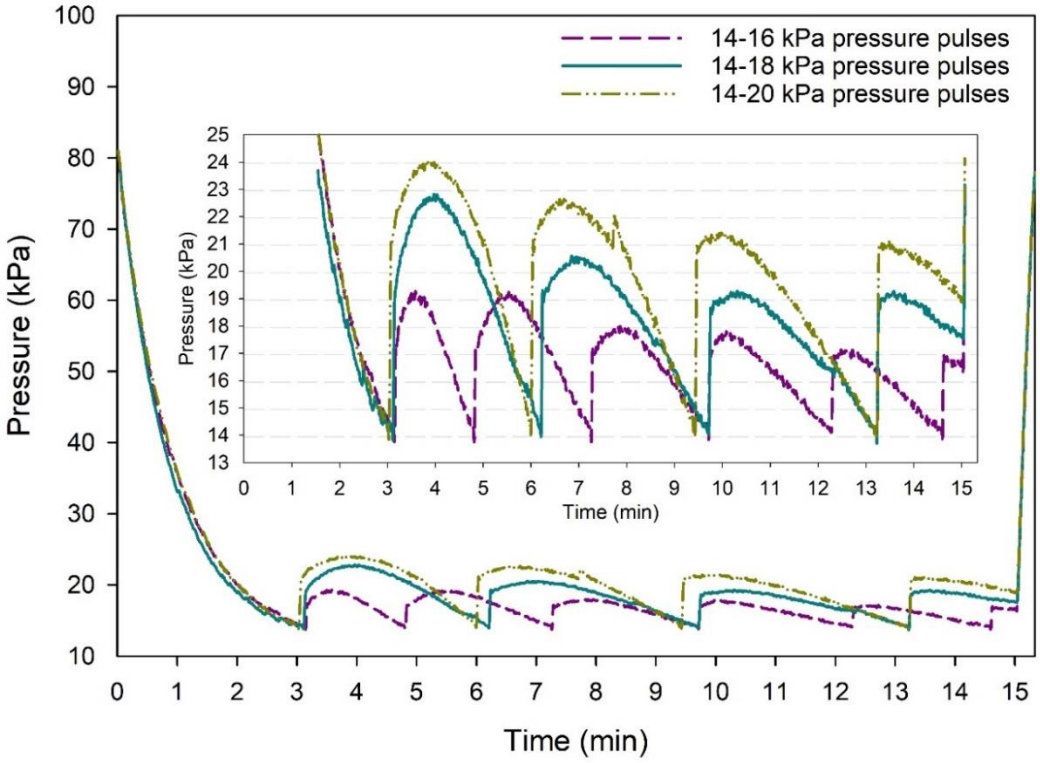

Figure 5.1 Pressure variation during the drying phase of the cycle for the different pressure pulses ranges: 14 kPa to 16 kPa, 14 kPa to 18 kPa and 14 kPa to 20 kPa.

For the 15 minutes of total drying time, the number of pulses vary depending on the pressure pulses range. When the pressure pulses are from 14 kPa to 16 kPa, the number of pressure pulses are 6 complete pulses and one incomplete pulse where the pressure drops only to 16.3 kPa instead of 14 kPa before it starts rising again. When the pressure pulses are from 14 kPa to 18 kPa, the number of pressure pulses are 4 complete pulses and one incomplete pulse where the pressure drops only to 17.5 kPa instead of 14 kPa before it starts rising again. When the pressure pulses are from 14 kPa to 20 kPa, the number of pressure pulses are 4 complete pulses and one incomplete pulse where the pressure drops only to 18.9 kPa instead of 14 kPa before it starts rising again.

Table 5.1 The variation between the set value of the upper limit of the pressure pulses and the actual measurements

Pressure pulse range (kPa)	**14-16**	**14-18**	**14-20**
Actual upper limit pressure (kPa)	16	18	20
1st pressure pulses upper limit pressure (kPa)	19.31	22.76	24.08
2nd pressure pulses upper limit pressure (kPa)	19.27	20.74	22.76
3rd pressure pulses upper limit pressure (kPa)	18.14	19.27	21.48
4th pressure pulses upper limit pressure (kPa)	17.84	19.35	21.18
5th pressure pulses upper limit pressure (kPa)	17.25	-	-
6th pressure pulses upper limit pressure (kPa)	16.96	-	-
Average measurements (kPa)	17.55	20.53	22.38
Error	9.67%	14.06%	11.88%

5.1.2 Uncertainty Analyses

Any experimentally measured value are subjected to error based on the device being used and the surrounding conditions. Table 5.2 summarizes the error value for the pressure measurements.

Table 5.2 Pressure measurements uncertainty

Variable	**Reference value (kPa)**	**Relative Bias Error %**	**Relative precision Error %**	**Total Statistical Uncertainty %**
Upper limit of the pressure pulse	20	8.94	5.93	10.73
	18	9.74	7.95	12.58
	16	11.03	1.13	11.09

5.1.3 Experimental Results

16 pouches are used for each of these experiments. Each pouch has a different load that was recorded before the start of any of the experiments. The total drying time for these runs was set as 15 minutes. As it can be seen in Figure 5.2, each of the pouches No. 6 and 10 has one gram of water for the 14-16 (170-170) configuration. The performance is good in this configuration due to having a lot of pressure pulses since the range is relatively small and more pulses can be created. However, smaller pressure pulses mean less amount of dry air being introduced to the chamber which allows the moist air and the steam to remain inside the chamber. Figure 5.3 shows the drying results for the 14-16 (170-160) configuration. It's noted that the performance is worse compared to the original fixed wall temperature and that's due to the decrease in the average temperature of the chamber during the drying process. Pouches No. 8, 11 and 14 has one gram of water each while pouch No. 12 has two grams of water. As the average temperature drops inside the chamber due to having lower wall temperatures, the products after the drying process are wetter. As it's clear in Figure 5.4, pouches No. 6, 7, 9 and 10 has one gram of water each, while pouches No. 12, 13 and 14 has two grams of water for the 14-16 (170-150) configuration.

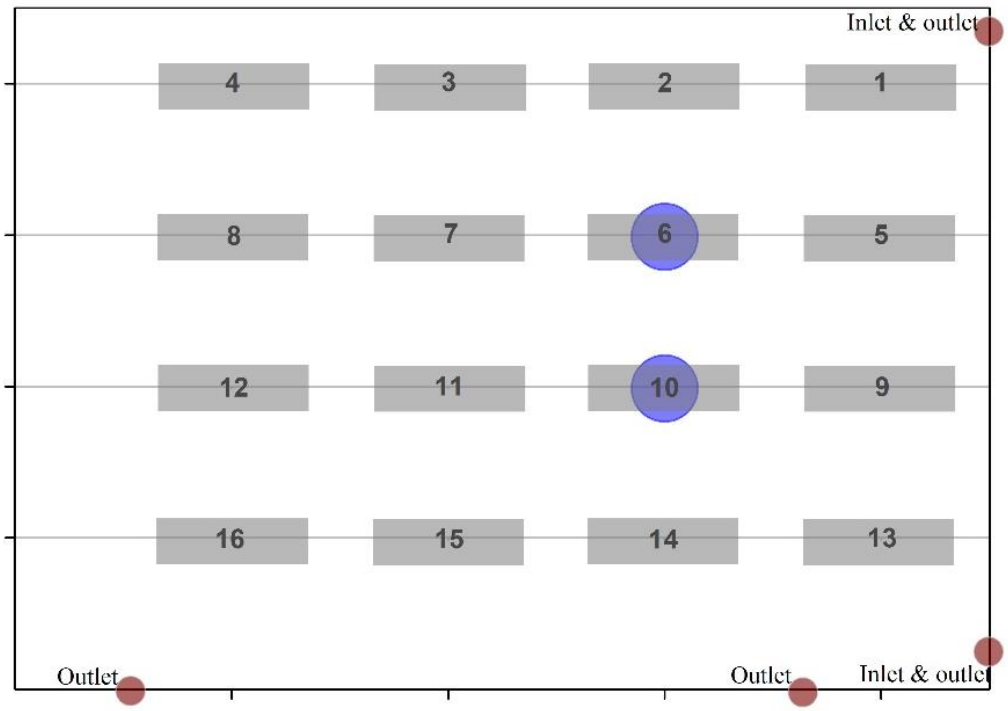

Figure 5.2 Water droplets after the drying process for the 14-16 (170-170) configuration

Figure 5.5 shows the drying results of the configuration 14-18 (170-170). As can be seen, the performance is weak due to having less number of pulses which means that the pouches don't breath and water is being trapped inside. Pouches No. 1, 2, 5, 8, 9, 10, 11, 14, 15 and 16 have one gram of water each, while pouch No. 7 has two grams of water as shown in Figure 5.4. When changing the top wall temperature to 160°C, the performance is almost the same if not worse as it's shown in Figure 5.6. Pouches No. 4, 5, 9, 11 and 15 have one gram of water each while pouches No. 7, 10 and 15 have two grams of water each. Surprisingly, when changing the wall temperature to 150°C for the same range of pressure pulses, the performance improves and becomes similar to 14-16 (170-170) configuration. It can be noted in Figure 5.7 that only pouches No. 14 and 16 have one gram of water each.

Changing the pressure pulses range to 14 kPa to 20 kPa make the drying process even worse. As it can be seen in Figure 5.8, pouches No. 5 and 13 have one gram of water each while pouches No. 6, 7, 9, 11 and 12 have two grams of water each. Changing the top wall temperature to 160°C doesn't show any merit as it's clear in Figure 5.9. Pouches No. 3, 5, 13 and 15 have one gram of water each, while pouches No. 6, 7, 9, 11, 12 and 16 have two grams of water each. Lowering the top wall temperature to 150°C for the 14 kPa to 20 kPa results in the worst drying process quality. As it's noted in Figure 5.10, pouches No. 2, 4, 5, 13, 14, 15 and 16 have one gram of water each, while pouches No. 6, 7, 9, 11 and 12 have two grams of water each.

The summary for all the results can be found in tables 5.1, 5.2 and 5.3. Figure 5.11 shows the total water content remaining in all the punches at the end of each of the 9 cases. It's noted that as the range of the pressure pulses increases, the drying quality decreases by having more water presented on top and inside the pouches. As it can be seen, both 14-16 (170-170) configuration and 14-18 (170-150) configuration result in the best drying quality compared to all the other studies cases. Both of them results in only 2 grams of water droplets, in total, on all the pouches. The worst configurations are when the pressure pulses range is the highest, between 14 kPa and 20 kPa, and the top wall temperatures are 160°C and 150°C.

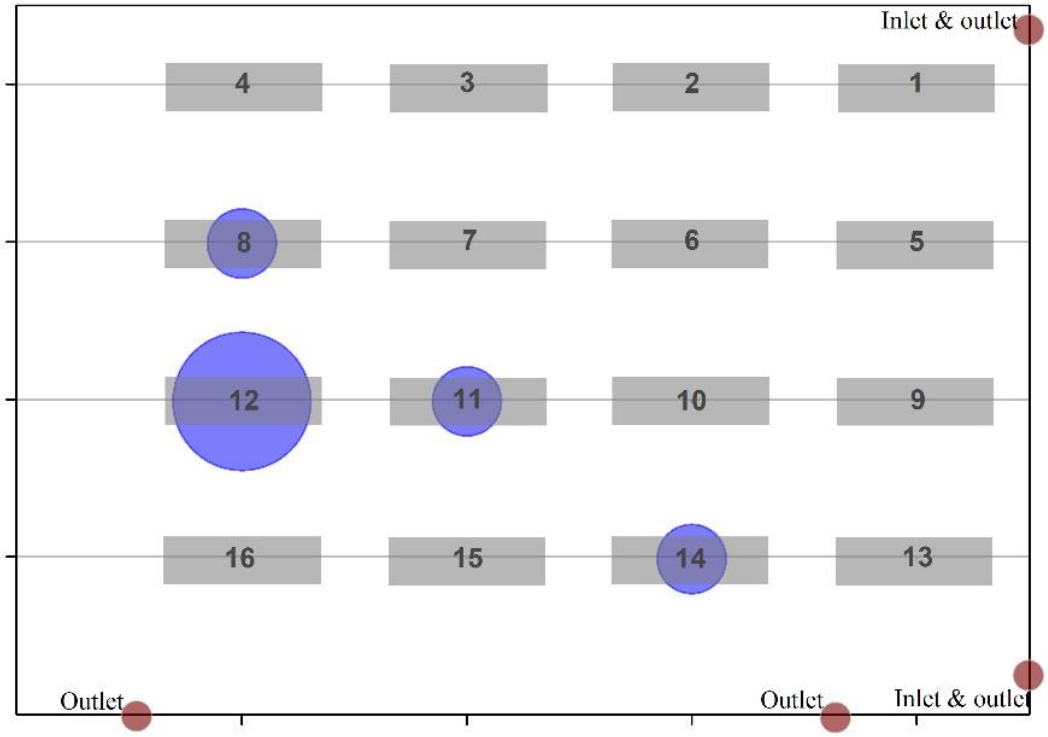

Figure 5.3 Water droplets after the drying process for the 14-16 (170-160) configuration

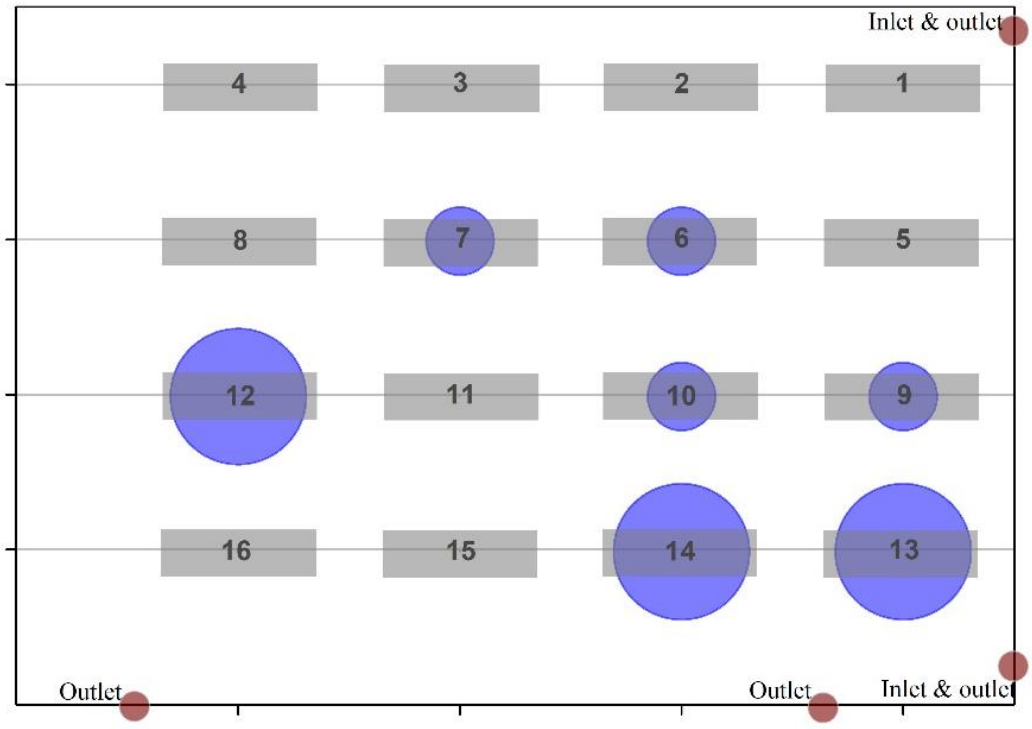

Figure 5.4 Water droplets after the drying process for the 14-16 (170-150) configuration

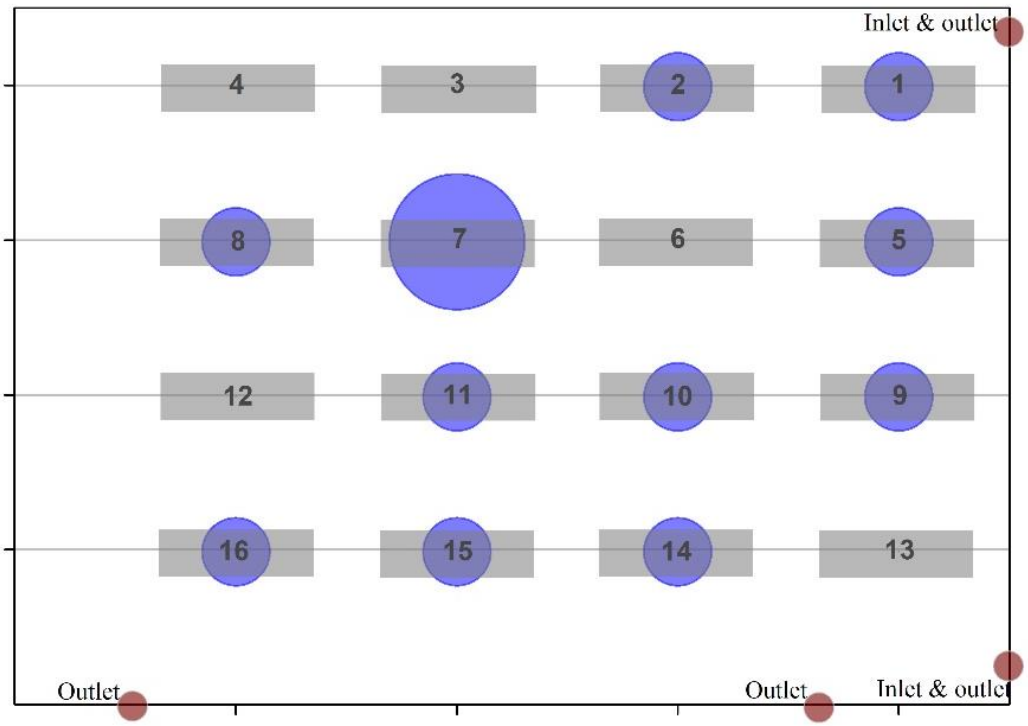

Figure 5.5 Water droplets after the drying process for the 14-18 (170-170) configuration

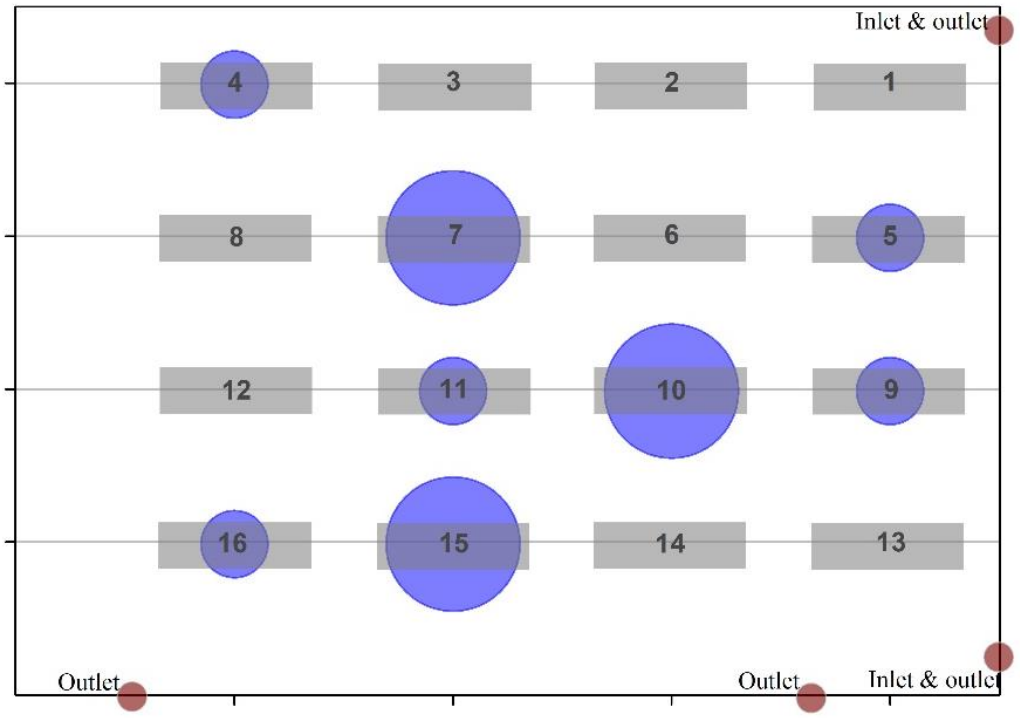

Figure 5.6 Water droplets after the drying process for the 14-18 (170-160) configuration

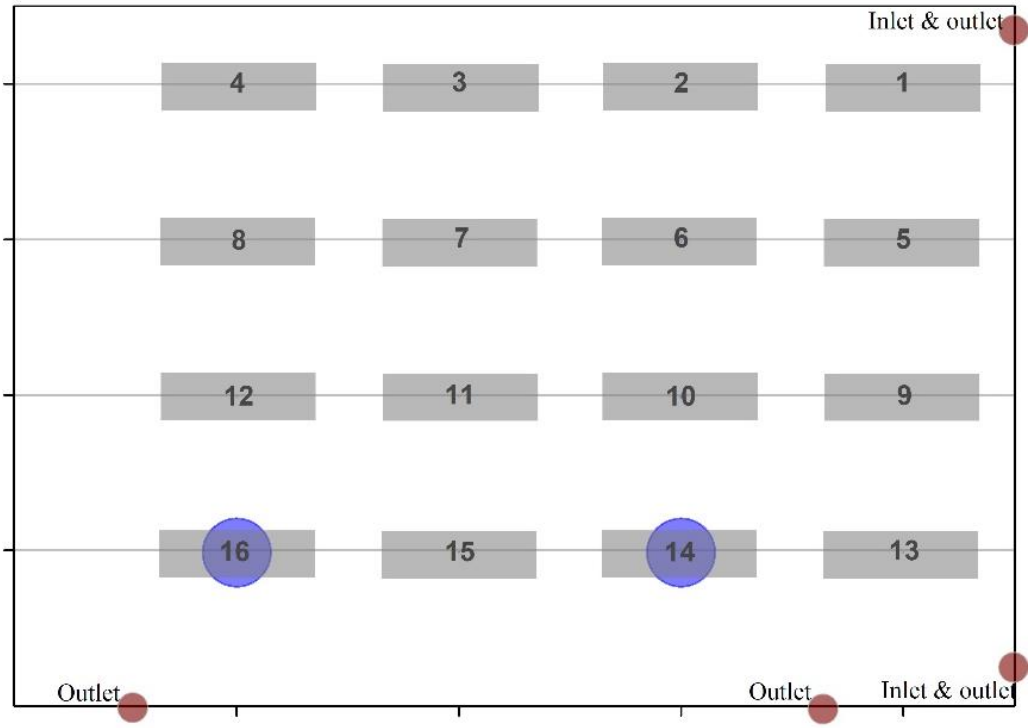

Figure 5.7 Water droplets after the drying process for the 14-18 (170-150) configuration

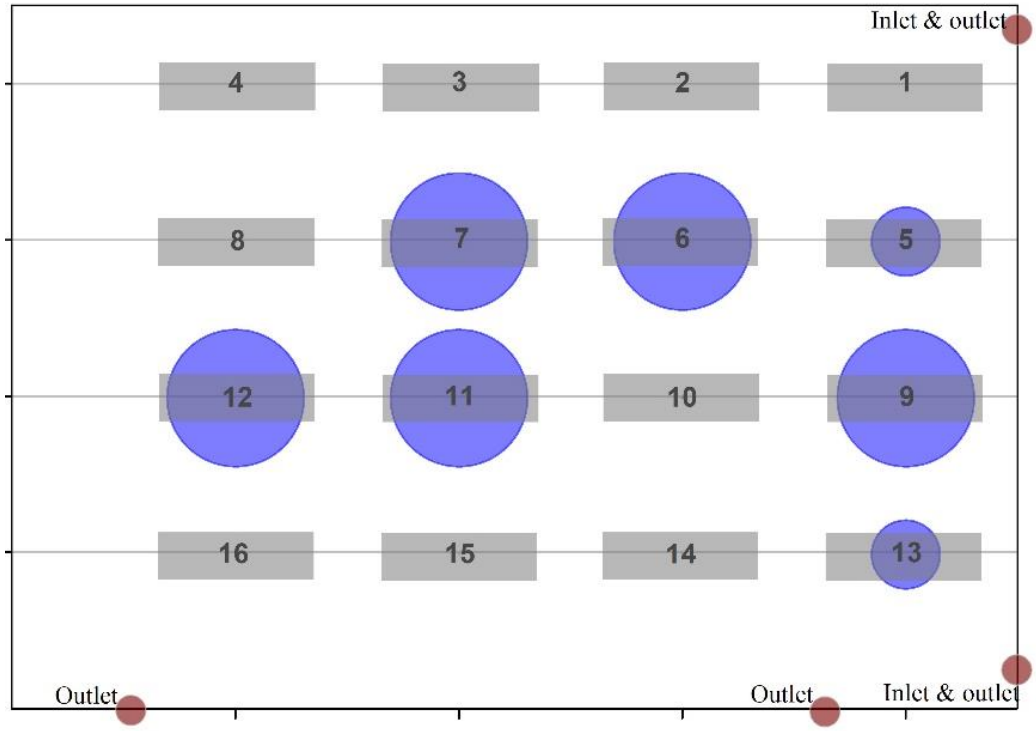

Figure 5.8 Water droplets after the drying process for the 14-20 (170-170) configuration

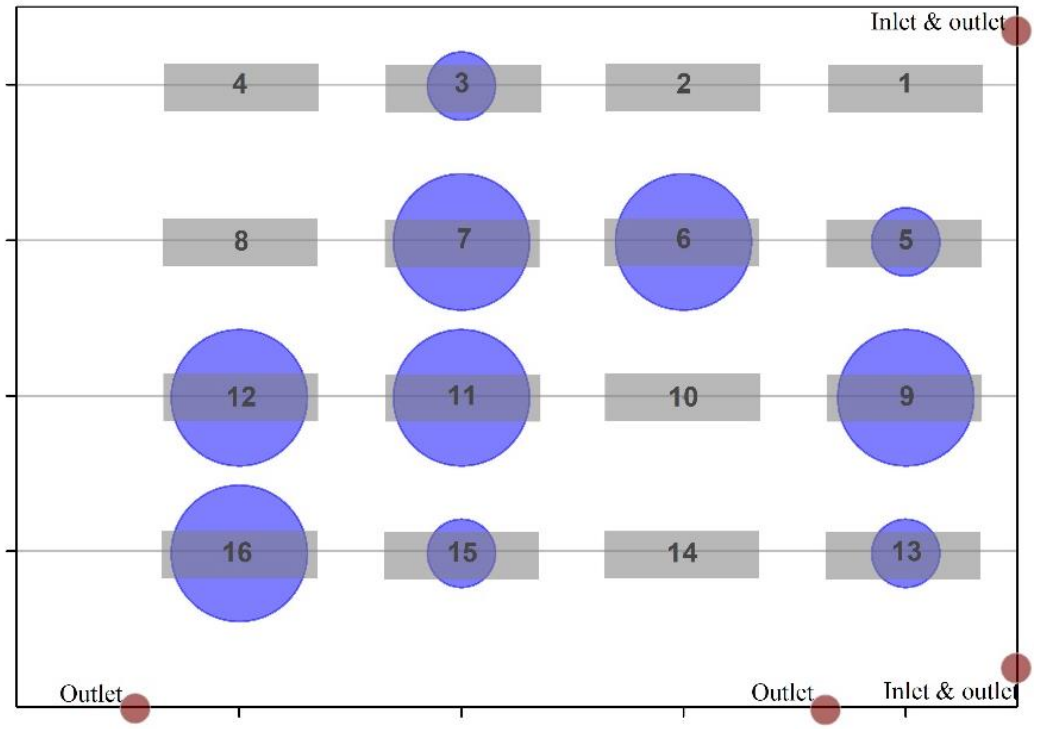

Figure 5.9 Water droplets after the drying process for the 14-20 (170-160) configuration

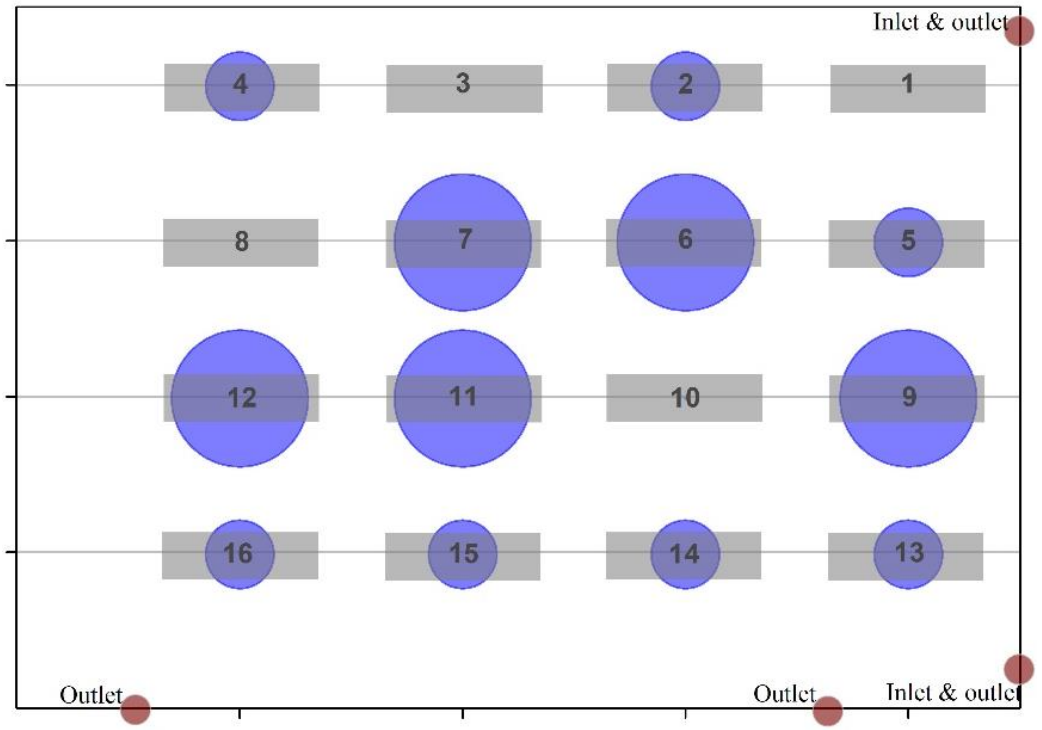

Figure 5.10 Water droplets after the drying process for the 14-20 (170-150) configuration

Table 5.3 Drying results for the 14 kPa to 16 kPa pressure pulses and different wall temperatures configurations

14-16 (170-170)				14-16 (170-160)				14-16 (170-150)			
Pouch No.	Weight before (g)	Weight after (g)	Difference (g)	Pouch No.	Weight before (g)	Weight after (g)	Difference (g)	Pouch No.	Weight before (g)	Weight after (g)	Difference (g)
1	294	293	-1	1	296	296	0	1	295	295	0
2	293	291	-2	2	295	295	0	2	295	294	-1
3	291	291	0	3	295	295	0	3	295	295	0
4	295	293	-2	4	298	298	0	4	298	297	-1
5	292	292	0	5	296	296	0	5	297	296	-1
6	235	236	1	6	239	239	0	6	238	239	1
7	234	234	0	7	237	237	0	7	236	237	1
8	294	294	0	8	297	298	1	8	297	297	0
9	294	294	0	9	298	298	0	9	297	298	1
10	235	236	1	10	239	239	0	10	238	239	1
11	238	237	-1	11	238	239	1	11	236	236	0
12	293	292	-1	12	295	297	2	12	295	297	2
13	295	293	-2	13	298	298	0	13	297	299	2
14	237	237	0	14	240	241	1	14	239	241	2
15	235	234	-1	15	238	238	0	15	239	239	0
16	235	234	-1	16	240	239	-1	16	239	238	-1

Table 5.4 Drying results for the 14 kPa to 18 kPa pressure pulses and different wall temperatures configurations

14-18 (170-170)				14-18 (170-160)				14-18 (170-150)			
Pouch No.	Weight before (g)	Weight after (g)	Difference (g)	Pouch No.	Weight before (g)	Weight after (g)	Difference (g)	Pouch No.	Weight before (g)	Weight after (g)	Difference (g)
1	295	296	1	1	295	295	0	1	295	295	0
2	294	295	1	2	294	294	0	2	295	294	-1
3	294	294	0	3	294	294	0	3	295	293	-2
4	297	297	0	4	297	298	1	4	297	295	-2
5	296	297	1	5	296	297	1	5	295	294	-1
6	239	238	-1	6	238	238	0	6	238	237	-1
7	236	238	2	7	236	238	2	7	236	235	-1
8	296	297	1	8	297	297	0	8	297	297	0
9	297	298	1	9	296	297	1	9	297	296	-1
10	238	239	1	10	237	239	2	10	238	237	-1
11	237	238	1	11	237	238	1	11	237	237	0
12	295	295	0	12	295	295	0	12	295	294	-1
13	298	298	0	13	297	296	-1	13	297	297	0
14	240	241	1	14	240	240	0	14	239	240	1
15	238	239	1	15	237	239	2	15	238	238	0
16	238	239	1	16	237	238	1	16	238	239	1

Table 5.5 Drying results for the 14 kPa to 20 kPa pressure pulses and different wall temperatures configurations

14-20 (170-170)				14-20 (170-160)				14-20 (170-150)			
Pouch No.	Weight before (g)	Weight after (g)	Difference (g)	Pouch No.	Weight before (g)	Weight after (g)	Difference (g)	Pouch No.	Weight before (g)	Weight after (g)	Difference (g)
1	296	295	-1	1	295	295	0	1	295	295	0
2	294	293	-1	2	295	293	-2	2	294	295	1
3	294	294	0	3	295	296	1	3	294	294	0
4	298	296	-2	4	297	296	-1	4	297	296	-1
5	295	296	1	5	295	296	1	5	296	297	1
6	238	240	2	6	238	240	2	6	239	241	2
7	236	238	2	7	236	238	2	7	236	238	2
8	296	296	0	8	297	296	-1	8	296	296	0
9	297	299	2	9	297	299	2	9	297	299	2
10	238	238	0	10	238	239	1	10	238	238	0
11	236	238	2	11	236	238	2	11	236	238	2
12	295	297	2	12	295	297	2	12	295	297	2
13	297	298	1	13	297	298	1	13	297	298	1
14	240	240	0	14	240	240	0	14	240	241	1
15	238	238	0	15	238	239	1	15	238	239	1
16	238	238	0	16	238	240	2	16	240	241	1

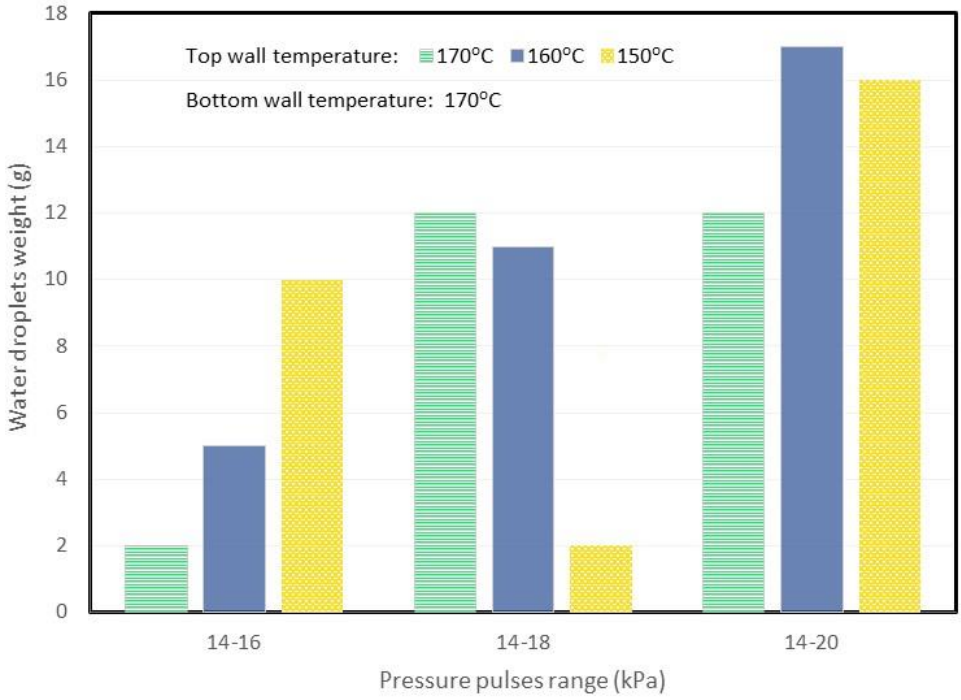

Figure 5.11 Total amount of water after the complete cycle for different ranges of pressure pulses and top wall temperatures

5.1.4 Drying Energy and Exergy Efficiencies

Figure 5.12 shows the energy efficiencies for the different ranges of the pressure pulses and top wall temperatures. The highest energy efficiency was found to be 78.29%, which was achieved when the pressure pulses range was between 14 kPa to 16 kPa and the top wall temperature was 170°C. The lowest energy efficiency was found to be 35.17%, when the pressure pulses range was between 14 kPa to 20 kPa and the top wall temperature was 160°C. Figure 5.13 shows the exergy efficiencies for the different ranges of the pressure pulses and top wall temperatures. The highest exergy efficiency was found to be 30.3%, which was achieved when the pressure pulses range was between 14 kPa to 18 kPa and the top wall temperature was 150°C. The lowest energy efficiency was found to be 15.46%, when the pressure pulses range was between 14 kPa to 20 kPa and the top wall temperature was 160°C. It's noted from the energy and exergy analyses that when the pressure pulses range is the largest, 14 kPa to 20 kPa, both energy and exergy efficiencies drop which shows the worst performance in terms of energy and exergy efficiencies. Unlike the energy efficiency, the exergy efficiency doesn't vary significantly with varying the humidity of

the drying air. This mainly due to the fact that the amount of water carried by air at low temperatures is relatively small and thus its physical exergy content becomes negligible.

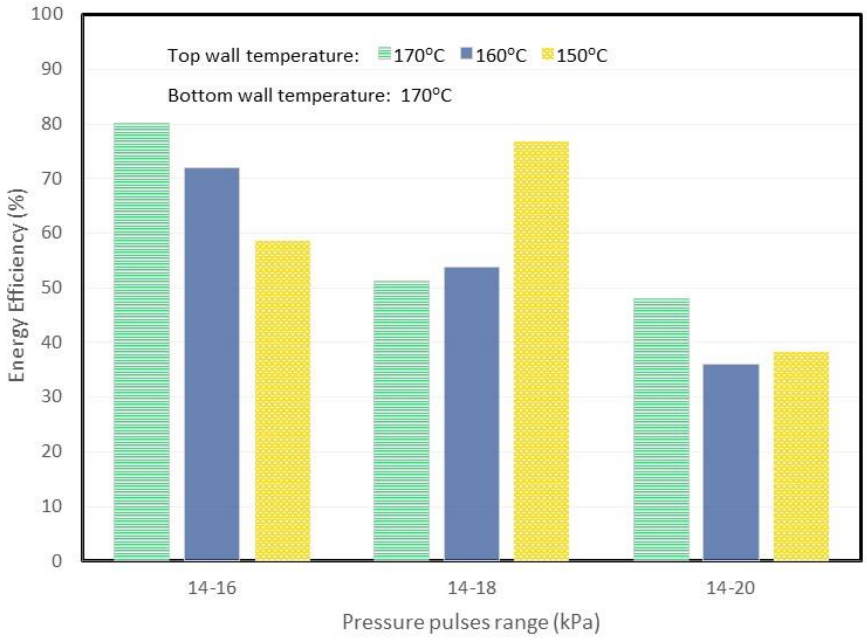

Figure 5.12 Energy efficiency for the different pressure pulses ranges and top wall temperatures

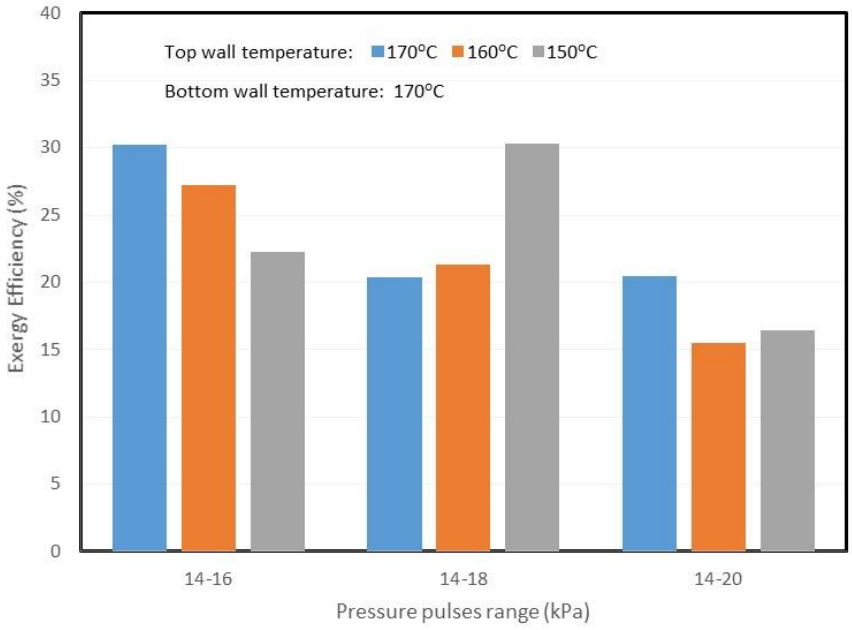

Figure 5.13 Exergy efficiency for the different pressure pulses ranges and top wall temperatures

5.2 Numerical Study Results

In this section, the results of the simulation carried out by the COMSOL Multiphysics software is presented. First, the effect of the flow velocity on the evaporation rate is shown by simulating a flow of air over a glass filled with water. In addition, the effect of varying wall temperatures on the velocity of the fluid inside the chamber is shown by simulating a simple 3D cylindrical chamber with the exact same geometry of the real chamber. In addition, the effects of installing a condenser inside the chamber instead of varying the wall temperatures and the velocity of the fluid inside the chamber is also shown. Moreover, the development of a mathematical model to come up with correlations for the drying process relating the change of pressure inside the chamber with time using artificial intelligent algorithm by the software Eureqa-Formalize is shown. Finally, the effect of both varying wall temperatures and pressure pulses ranges on the mixing of steam and air inside the chamber and the average magnitude of the velocity of the fluid inside the chamber is also presented using a 2D model with a full load of pouches. The effect of Flow Velocity on the evaporation rate

5.2.1 The Effect of Air Velocity on the Amount of Evaporated Water

In this section, the effect of the dry air velocity and temperature on the amount of evaporated water is analyzed and modeled numerically. For this simulation, a beaker filled with water is used to test the evaporation rate. The beaker is surrounded by an air domain as shown in Figure 5.14. The airflow transports the water vapor. The approach used here neglects volume change of the water inside the beaker. This is a reasonable assumption for problems where the considered time is short compared to the time needed to evaporate a noticeable amount of water. The beaker is made of aluminum and contains hot water at 80°C and enters the modeling domain with this temperature. For modeling evaporative cooling, three effects must be taken into account: the turbulent flow of the air around the beaker, heat transfer in all domains, and transport of water vapor in the air. The results of the simulations show that the velocity of the dry air has a major effect on the amount of evaporated water.

Turbulent Flow is used to simulate the air flow in this simulation. Namely Low Re k-ε interface, because the Reynolds number is low and turbulent effects must be considered. All the turbulence variables are solved for the whole domain to provide accurate input values for the transport equation. Assuming that the velocity and pressure field is independent of the air temperature and moisture content. This allows to calculate the turbulent flow field in advance and then use it as input for the heat transfer and species transport equations. Heat Transfer, the heat transfer inside the beaker and water is due to conduction only. For the moist air, convection dominates the heat transfer, and the turbulent flow field is required. The material properties are determined by the moist air theory. Moister Transfer, to obtain the correct amount of water which is evaporated from the beaker into the air, the Moisture Transport in Air interface is used. The initial relative humidity is assumed to be 20%.

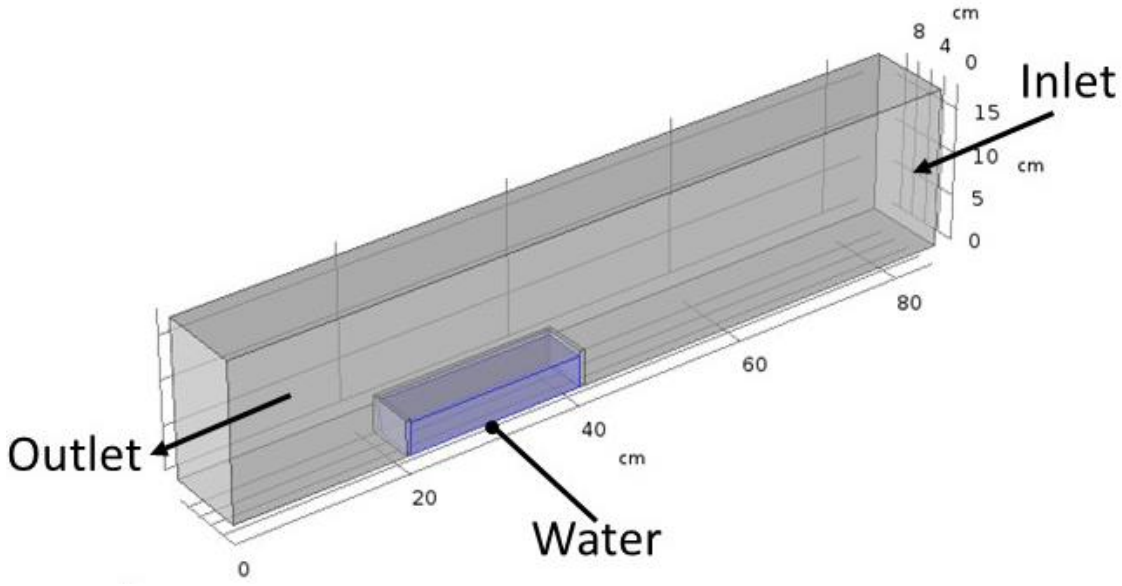

Figure 5.14 The geometry used in the first simulation

This simulation shows the effect of the flow velocity on the evaporation mechanism. Bansal and Zealand [55] Presented simple empirical correlation to predict the rate of water evaporation from small exposed water bodies. The correlation is a function of air velocity and the difference between the saturated vapor pressure of the water body and partial vapor pressure of the surrounding air.

Different mesh sizes were used to choose the perfect mesh size, yet the one that requires less computational time, to carry on with the simulations. The Figure 5.15 shows the mesh independent study to choose the perfect mesh for this simulation. Going from 195,496 elements to 236,971 elements results in 3.8 % difference in the results which is considerably high. Another finer mesh was chosen with 296,434 elements and the difference in the results from the previous mesh was only 0.9 % which is acceptable. So, in this simulation, a mesh with 236,971 elements was used as it's shown in Figure 5.15. The assumed initial and boundary conditions for this model is shown in Table 5.6

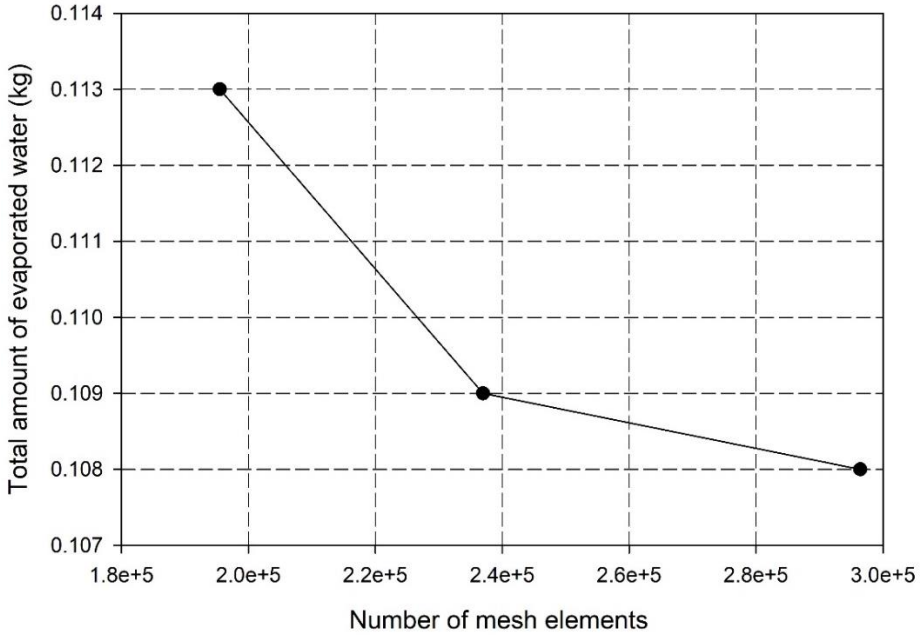

Figure 5.15 Variation of the total amount of evaporated water with different mesh sizes

Table 5.6 Initial and boundary conditions used in the simulation

Flow type	Turbulent
Compressibility type	Incompressible flow
Turbulence model type	RANS, Low Reynolds number k-e
Initial pressure	Ambient pressure 101.325 kPa
Inlet conditions	velocity of 1.5 m/s, 2 m/s, 2.5 m/s and 3 m/s at 100°C and 20% relative humidity
Outlet condition	Normal stress of 0 N/m^2
Initial temperature	100°C
Solid type	Glass
Water initial temperature	50°C
Initial relative humidity	100%

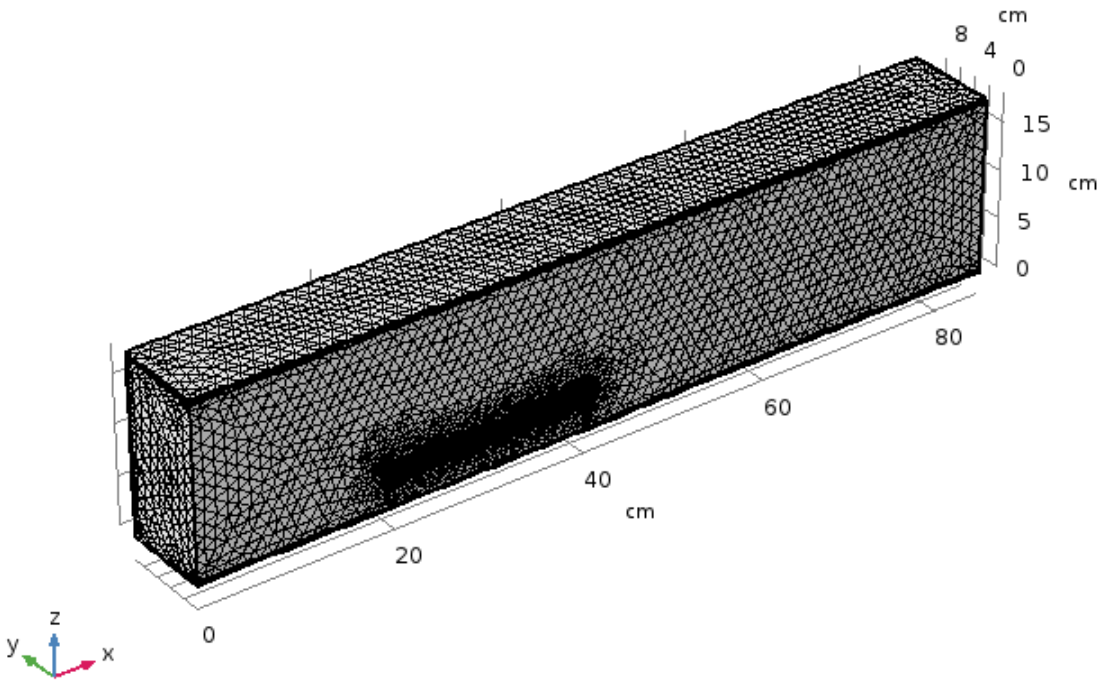

Figure 5.16 The mesh with 382,350 elements used in the simulation

Figure 5.17 shows the variation of the total amount of evaporated water over different flow velocities. This was calculated by multiplying the average normal moisture flux value over the simulation by the total time of the simulation. The amount of evaporated water increases as the air velocity over the wet surface increases. These results are expected as was suggested by [55]. In the drying process, the only non-mechanical way to increase the flow velocity is by enhancing the natural circulation inside the chamber. As it can be seen, doubling the value of the velocity from 1.5 m/s to 3 m/s increases the amount of evaporated water from 2.4 grams to 49 grams which shows the high effect of flow velocity on the evaporation rate. In the next sections, some methods to increase the flow velocity over the wet pouches during the drying process to improve the evaporation rate.

5.2.2 The Effects of Varying Wall Temperatures on the Flow Velocity

For these simulations, a 3D cylinder representing the chamber containing a mixture of steam and air initially as shown in Figure 5.18. To simplify the simulation, air is assumed to occupy the bottom half of the cylinder while steam is at the top part of the chamber due to the fact that steam being less dense than dry air and thus, steam will occupy the top half

of the chamber. The initial temperature of the air and steam is assumed to be 134°C while the walls have different constant temperatures that range between 150°C to 170°C. The main objective of these simulations is to compare varying both the top and the bottom wall temperatures with the original configuration in which both the top and the bottom wall temperatures are 170°C. It's expected that having a higher wall temperature at the bottom will results in better circulation and mixing since the clod fluid mainly accumulates in the bottom half. However, both ways were simulated. In other words, both top and bottom wall temperatures are being varied between 150°C and 170°C. The walls temperatures configurations used were as follows:

Bottom wall temperature = 170°C, Top wall temperature = 160°C **(170-160 configuration)**

Bottom wall temperature = 170°C, Top wall temperature = 150°C **(170-150 configuration)**

Bottom wall temperature = 160°C, Top wall temperature = 170°C **(160-170 configuration)**

Bottom wall temperature = 150°C, Top wall temperature = 170°C **(150-170 configuration)**

Bottom wall temperature = 170°C, Top wall temperature = 170°C **(150-170 configuration)**

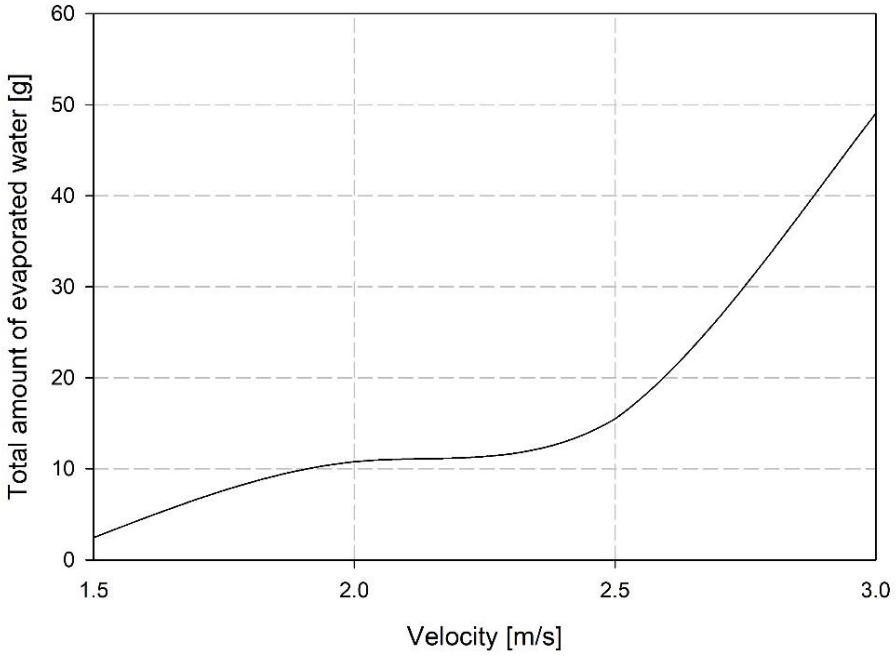

Figure 5.17 Total amount of evaporated water variation with changing air flow velocity

The simulations in this sections are meant to show the effect of having different wall temperatures to enhance the natural circulation and thus increase the velocity of the fluid inside the chamber during the drying process. The assumed boundry and initial conditions of the simulations are shwon in Table 5.7

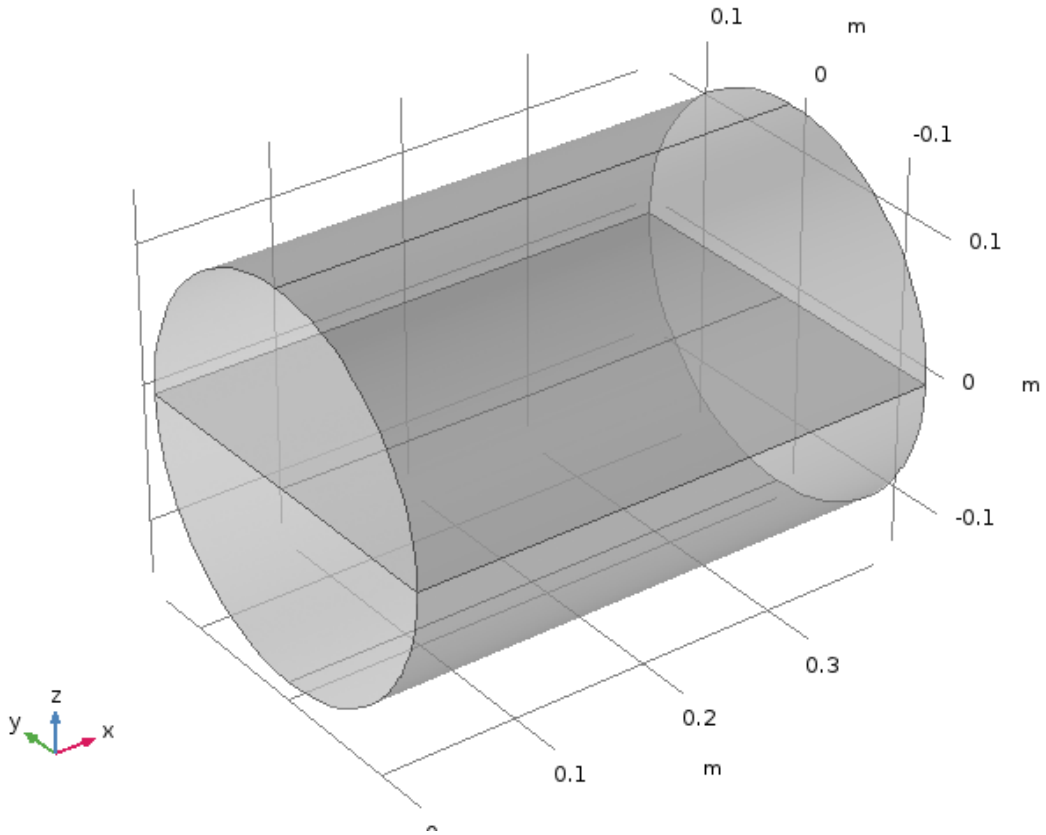

Figure 5.18 The geometry of the chamber used in the simulation

Table 5.7 Initial and boundary conditions used in the simulation

Flow type	Laminar
Compressibility	Incompressible flow
Turbulence model type	None
Initial pressure	Ambient pressure 101.325 kPa
initial temperature	134°C
Lower wall temperature	varied between 150°C, 160°C and 170°C
Upper wall temperature	varied between 150°C, 160°C and 170°C
Initial composition of the lower half of the chamber	100% water vapor
Initial composition of the bottom half of the chamber	100% dry air

For these simulations, different mesh sizes were tested and simulated for 2 seconds to obtain the best mesh that requires the least computational time. Figure 5.19 shows the average velocity of the flow in the top half of the chamber after 2 seconds. As it can be seen, going from 48,598 elements to 137,849 elements results in 3.6% error in the average value of the velocity. So, another mesh size of 460,032 elements results in only 1.5% error value. So, the mesh size of 137,849 elements is used for this simulation. The mesh is shown in Figure 5.20.

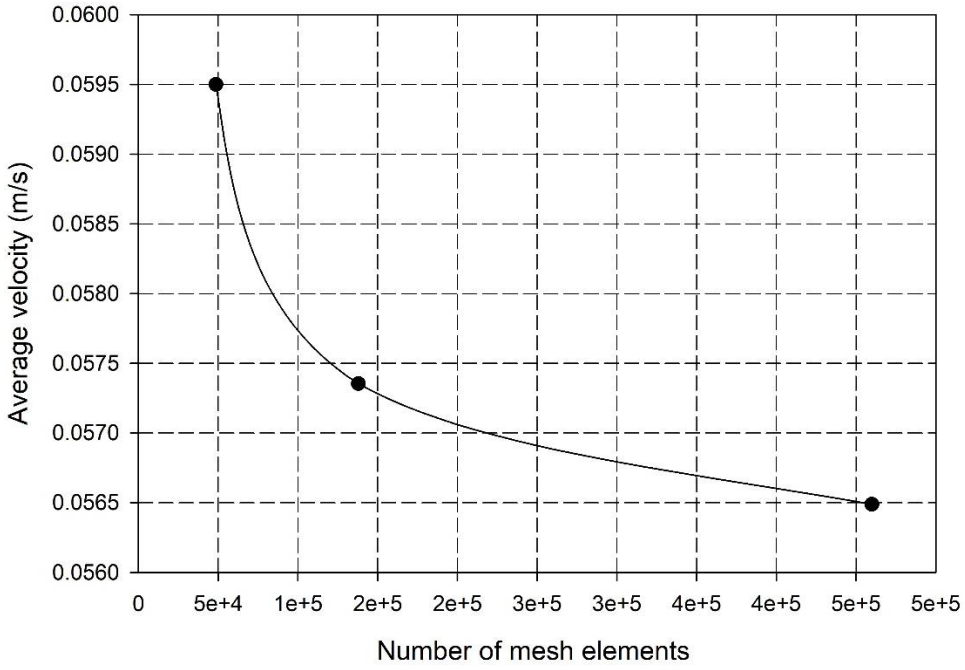

Figure 5.19 The variation of the average velocity in the top half of the chamber with different mesh sizes for the (170-160) configuration

As it can be seen in Figure 5.21, the 170-150 configuration results in the highest circulation velocity inside the chamber compared to other wall temperatures configurations. While as the temperature difference between the top and the bottom wall decreases in the 170-160 configuration, the natural circulation is not as effective to force the air and steam to circulate and interact. On the other hand, having a high wall temperature for the top wall is not going to enhance the circulation as it's the case for the other configurations. It's shown that the average velocities inside the chamber after 20 sec. are 0.044 m/s, 0.031 m/s, 0.017 m/s 0.014 m/s, 0.024 m/s for the (170-150), (170-160), (160-170), (150-170) and (170-170) configurations. The configuration in which the top

wall temperature is 150°C and the bottom wall temperature is 170°C is the best configuration for enhancing the circulation inside the chamber. In other words, the (170-150) configuration enhances the average velocity inside the chamber by 83.6% compared to the current situation in which both the top and the bottom walls have the same temperature of 170°C.

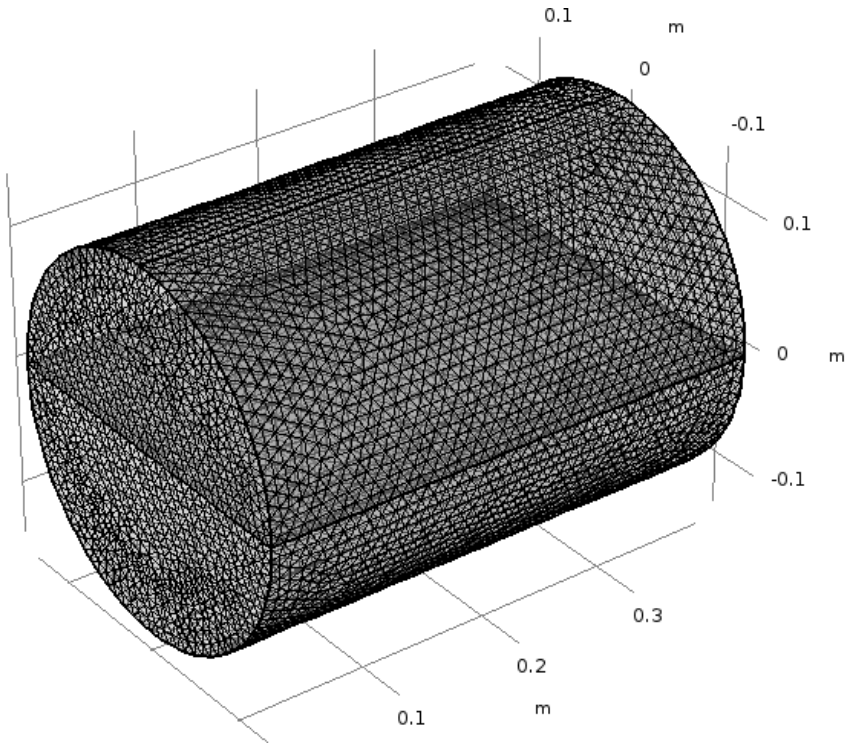

Figure 5.20 The mesh used for the simulation of the 3D chamber

Figure 5.22 shows the steam concentration over time in the different scenarios that were used in the study. The optimum point is to go for 0.5 mass fraction since the mass fraction is shown in Figure 5.21 is only for the top half of the chamber. Initially, the steam concentration at the top half of the chamber is assumed to be 100% and preferably, enhancing the circulation should results in 50% steam concentration eventually, the 170-150 configuration results in the closet value to the desired value of the distribution. However, running the simulations for more than 20 sec. will results in finally having the 50% concentration for all the configurations, however, to minimize the time needed for that, both the170-170, 170-150 and 170-160 configurations show the best potential since it's going to take less time to reach the desired homogeneity level of 0.5.

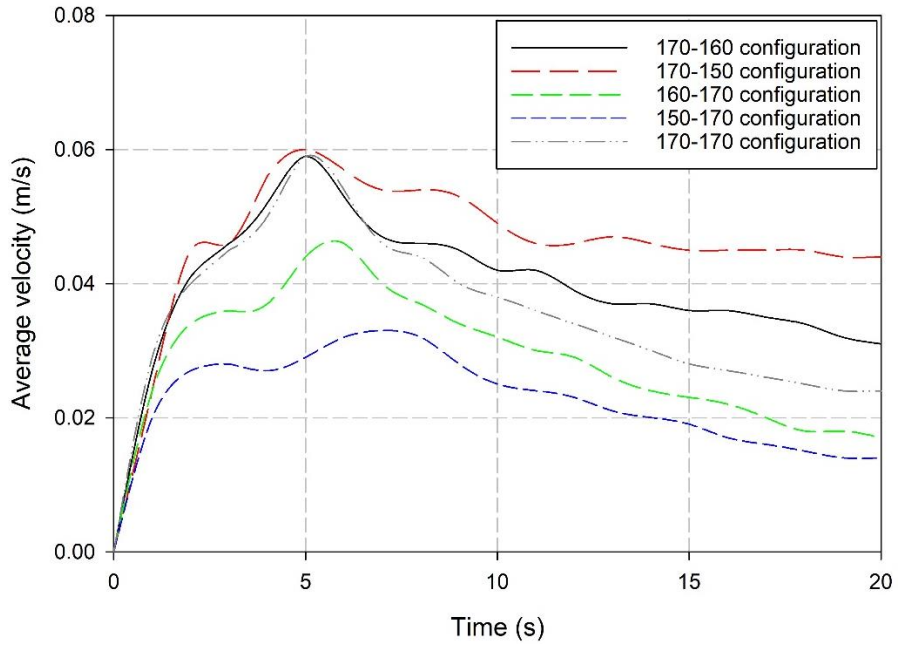

Figure 5.21 Average magnitude of the velocity variation of the fluid in the chamber variation with time for the different wall temperatures configurations

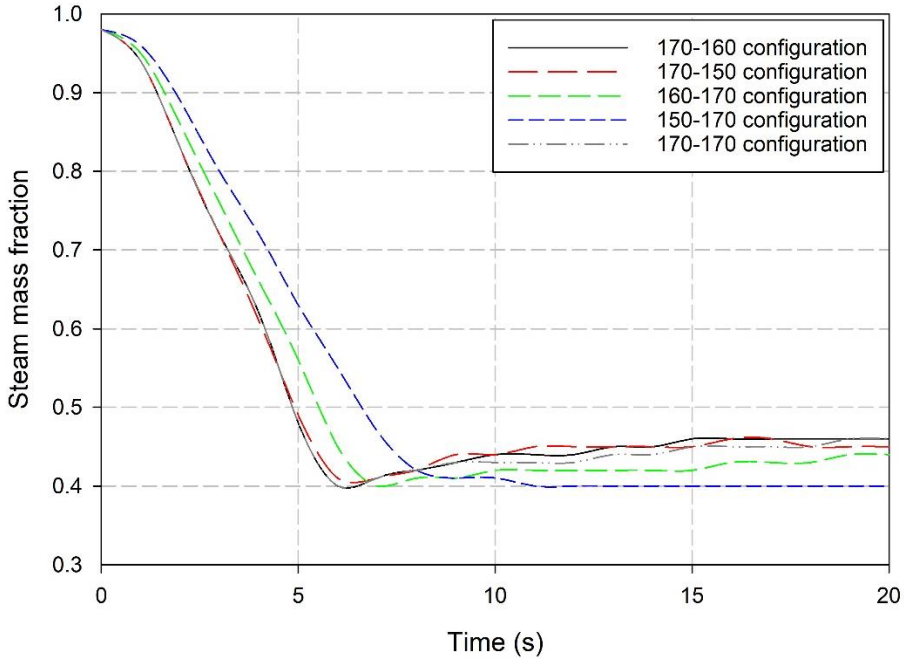

Figure 5.22 Average steam mass fraction variation in the top half of the chamber comparison between different wall temperatures configurations

Figure 5.23 shows surface plots for the steam concentration the all the considered configurations after 5 sec., 10sec., and 20sec. The best scenario is to have a uniform

distribution throughout the chamber. It's noted that the 170-150 configuration results in the most uniform distribution for both steam and air after 20 sec. The enhancement of the distribution of both steam and air is going to help in venting more steam during the vacuuming part during the cycle which is desirable. Since air has a higher density than steam, it's going to be more concentrated in the bottom half of the chamber, and all the holes in the chamber act like outlet during the vacuuming phase in which 3 of them are located in the bottom half of the chamber while only one hole is located in the top section. Enhancing the mixing between air and steam will decrease the mass of air venting out the chamber during the pressure pulses and increase the amount of vapor out.

Table 5.8 shows the magnitude of the average velocity of the fluid in the chamber, the steam mass concentration in the top half of the chamber and the average fluid temperature in the temperature over the total time of the simulation which is 20 seconds for all the 5 previously mentioned configurations. Compared to the 170-170 configuration, setting the top wall temperature as 150°C results in increasing the average velocity of the fluid in the chamber from 0.024 m/s to 0.044 m/s after 20 seconds which represents 83.6% improvement. While the average velocity of the fluid when the top wall temperature is 160°C, the average velocity is 0.031 m/s which represents 31.2% improvements. The other two configurations in which the bottom wall temperature is less than the top one results in lower average velocity than the base 170-170 configurations. On the other hand, changing the top wall temperature in the 170-160 and 170-150 configurations don't show any noticeable improvements in the homogeneity of the mixture compared to 170-170 configuration. While changing the bottom wall temperature in the 160-170 and 150-170 configurations results in a less homogenous mixture which is not desired. Even though that changing the top wall temperature shows merit in enhancing the average magnitude of the velocity, it negatively affects the average temperature of the fluid inside the chamber. It's common sense that when both the top and bottom wall temperatures are 170°C, the average fluid in the chamber is going to be higher compared to when having lower wall temperatures. After 20 seconds, the average fluid temperature inside the chamber drops from 158.1°C to 149.8°C and 154.1°C when the top wall temperatures change to 150°C and 160°C, respectively. So, the 170-150 configuration results in a 5.2% drop in the average temperature while the 17-160 configuration results in a 2.5% drop.

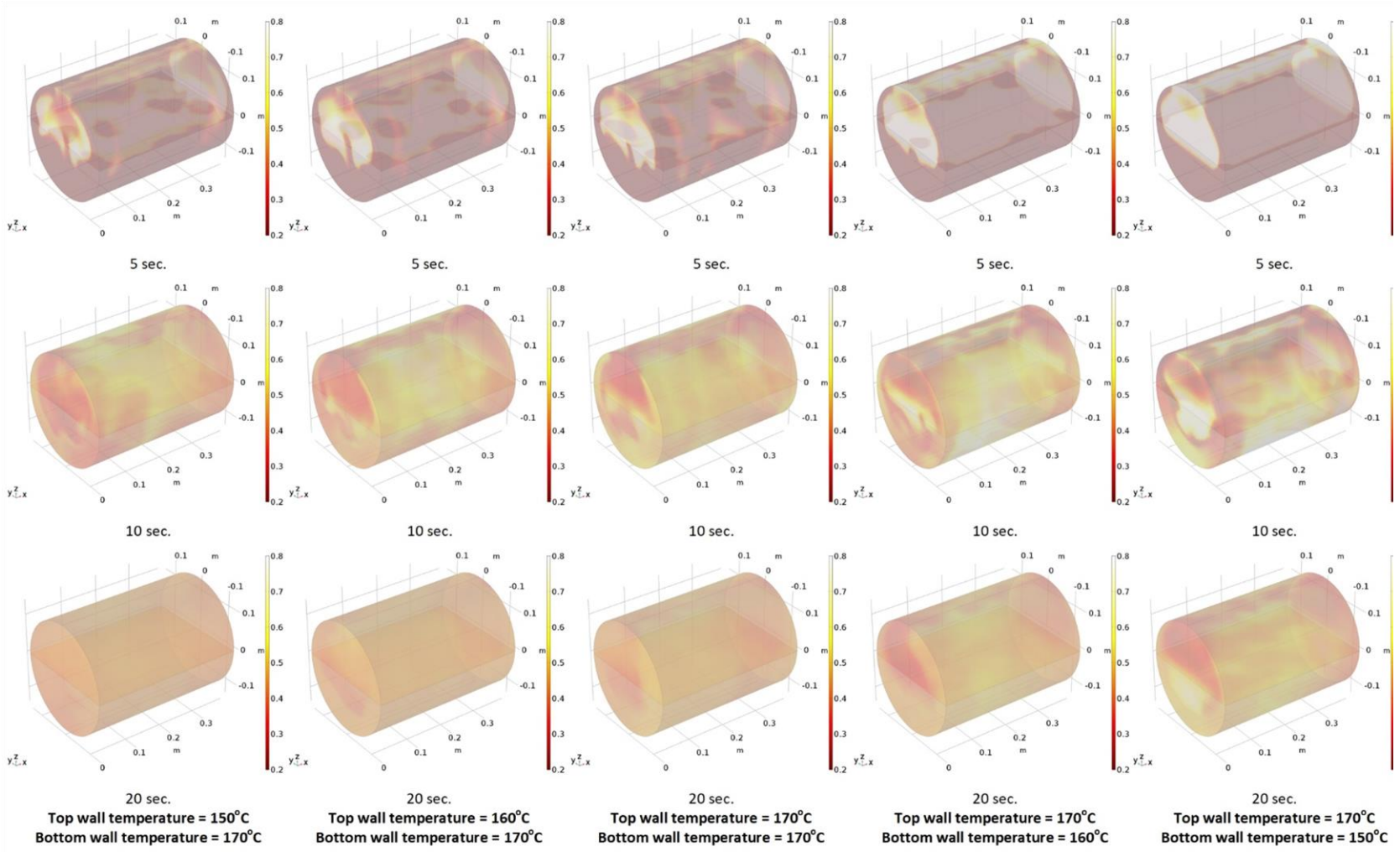

Figure 5.23 Steam mass fraction distribution after 5, 10 and 20 sec. for the different studied configurations

Table 5.8 Average velocity magnitude and average steam concentration in the top half and the average temperature of the chamber results variation over time for the different wall temperatures configurations

Time (s)	Average velocity magnitude (m/s)					Steam concentration fraction in the top half					Average temperature (°C)				
	170-150	170-160	170-170	160-170	150-170	170-150	170-160	170-170	160-170	150-170	170-150	170-160	170-170	160-170	150-170
0	0	0	0	0	0	0.98	0.98	0.98	0.98	0.98	134.1	134.1	134.2	134.1	134.2
1	0.024	0.027	0.029	0.024	0.020	0.94	0.94	0.94	0.95	0.96	135.9	136.3	136.7	136.4	136.9
2	0.045	0.041	0.040	0.034	0.027	0.83	0.83	0.83	0.86	0.89	136.8	137.5	138.2	137.6	138.9
3	0.046	0.046	0.045	0.036	0.028	0.72	0.72	0.72	0.76	0.80	137.7	138.7	139.7	138.8	140.9
4	0.056	0.052	0.050	0.037	0.027	0.61	0.62	0.62	0.66	0.72	138.8	140.0	141.2	140.1	142.9
5	0.060	0.059	0.059	0.044	0.029	0.49	0.48	0.48	0.56	0.63	139.8	141.2	142.8	141.3	144.7
6	0.057	0.053	0.054	0.046	0.032	0.41	0.40	0.40	0.45	0.55	140.8	142.5	144.3	142.6	146.5
7	0.054	0.047	0.046	0.040	0.033	0.41	0.41	0.41	0.40	0.47	141.7	143.7	145.7	143.8	148.1
8	0.054	0.046	0.044	0.037	0.032	0.42	0.42	0.42	0.41	0.42	142.6	144.8	147	144.9	149.4
9	0.053	0.045	0.040	0.034	0.028	0.44	0.43	0.43	0.41	0.41	143.4	145.9	148.2	145.9	150.6
10	0.049	0.042	0.038	0.032	0.025	0.44	0.44	0.43	0.42	0.41	144.2	146.8	149.4	146.9	151.7
11	0.046	0.042	0.036	0.030	0.024	0.45	0.44	0.43	0.42	0.40	144.9	147.7	150.5	147.9	152.7
12	0.046	0.039	0.034	0.029	0.023	0.45	0.44	0.43	0.42	0.40	145.6	148.6	151.5	148.8	153.6
13	0.047	0.037	0.032	0.026	0.021	0.45	0.45	0.44	0.42	0.40	146.2	149.4	152.5	149.6	154.5
14	0.046	0.037	0.030	0.024	0.020	0.45	0.45	0.44	0.42	0.40	146.8	150.2	153.4	150.4	155.3
15	0.045	0.036	0.028	0.023	0.019	0.45	0.46	0.45	0.42	0.40	147.4	150.9	154.3	151.2	156.0
16	0.045	0.036	0.027	0.022	0.017	0.46	0.46	0.45	0.43	0.40	148.0	151.6	155.2	151.9	156.7
17	0.045	0.035	0.026	0.020	0.016	0.46	0.46	0.45	0.43	0.40	148.5	152.3	156.0	152.6	157.3
18	0.045	0.034	0.025	0.018	0.015	0.45	0.46	0.45	0.43	0.40	149.0	152.9	156.7	153.3	157.9
19	0.044	0.032	0.024	0.018	0.014	0.45	0.46	0.46	0.44	0.40	149.4	153.5	157.4	153.9	158.4
20	0.044	0.031	0.024	0.017	0.014	0.45	0.46	0.46	0.44	0.40	149.8	154.1	158.1	154.4	158.9

5.2.3 The Effects of Having a Cold Condensing Zone on the Flow Velocity

One suggestion to improve the circulation inside the chamber was to install a condenser at the back of the chamber. The reason for placing the condenser at the back wall of the chamber is to prevent any condensation from drooping on top of the pouches and causes them to be wet. In this section, the merit of installing a condenser is studied and compared with the results of having two different wall temperature in terms of enhancing the natural circulation phenomena and the average magnitude of the velocity inside the chamber. The geometry of the chamber with the condenser is shown in Figure 5.24. The condenser is assumed to have a constant temperature of 20°C, while the wall temperatures are kept constant at 170°C. For this simulation, the same mesh from the previous section was used since they have similar geometries. The results of this simulation in terms of enhancing the circulation inside the chamber and increasing the flow velocity is going to be compared with the (170-150) configuration since it showed the best performance in the previous section and with the current 170-170 configuration to show how much improvement can be obtained by installing a condenser. Figure 5.25 shows the mesh with 183,759 elements used for this simulation. The boundary and initial conditions of these simulations are shown in Table 5.9.

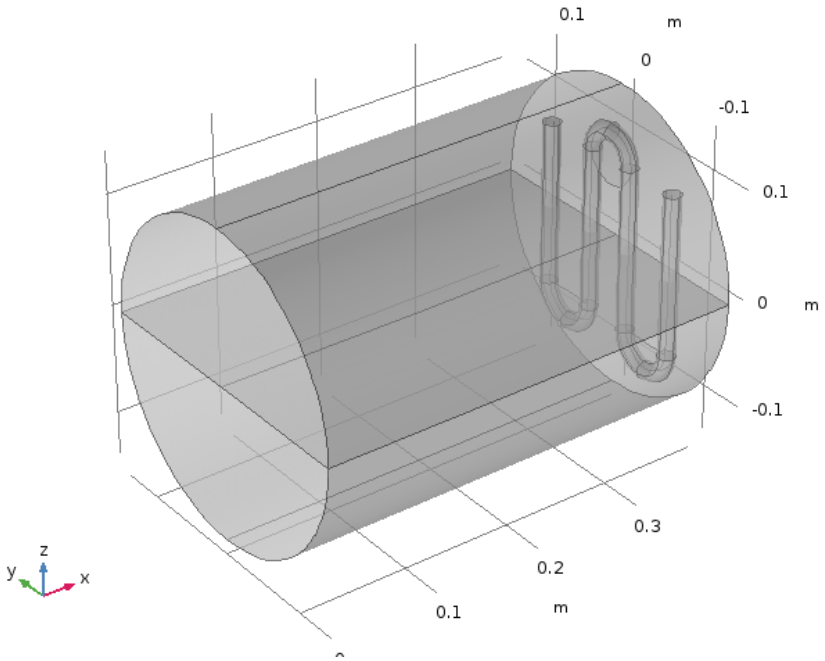

Figure 5.24 Geometry of the 3D chamber with a condenser

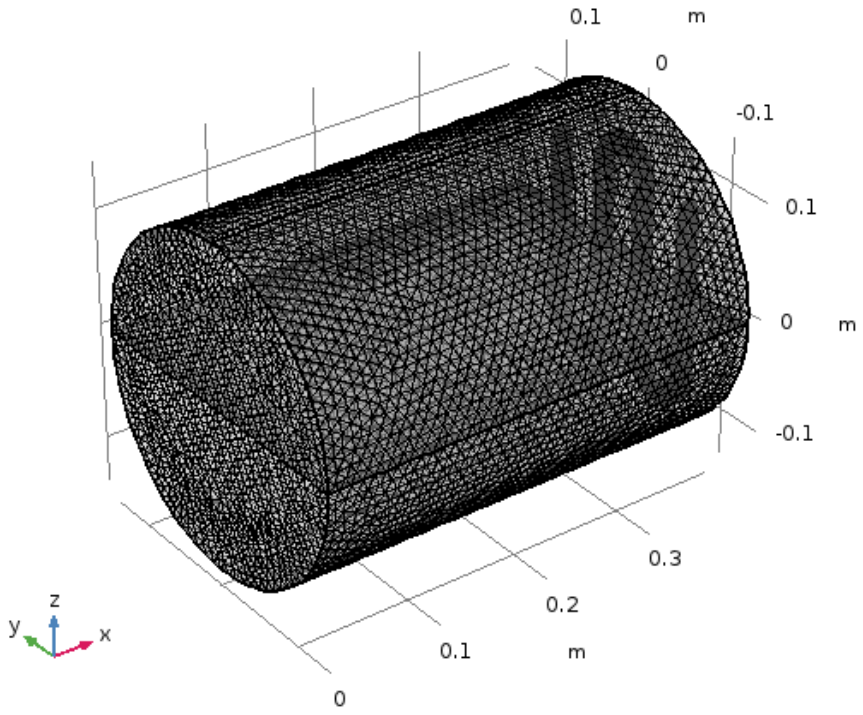

Figure 5.25 The mesh used for the simulation of the chamber with a condenser

Table 5.9 Initial and boundary conditions used in the simulation

Flow type	Laminar
Compressibility	Incompressible flow
Turbulence model type	None
Initial pressure	Ambient pressure 101.325 kPa
initial temperature	134°C
Lower wall temperature	varied between 150°C, 160°C, and 170°C
Upper wall temperature	varied between 150°C, 160°C, and 170°C
Initial composition of the lower half of the chamber	100% water vapor
Initial composition of the bottom half of the chamber	100% dry air
Condenser initial and fixed temperature	20°C

Figure 5.26 shows the velocity variation in the average magnitude of the velocity of the fluid inside the chamber with time comparing both the (170-150) and the (170-170) configurations with velocity variation when having a condenser at 20°C. As can be seen, the condenser acting like a cold zone in the chamber enhances the velocity distribution significantly. The temperature difference created by the condenser is larger than the temperature difference between the two walls in the (170-150) configuration which

improves the natural circulation mechanism much more compared to the (170-150) configuration. After 20 sec., the average magnitude of the velocity inside the chamber with a condenser is 0.142 m/s compared to 0.044 m/s in the (170-150) configuration and 0.024 m/s using the current (170-170) configuration.

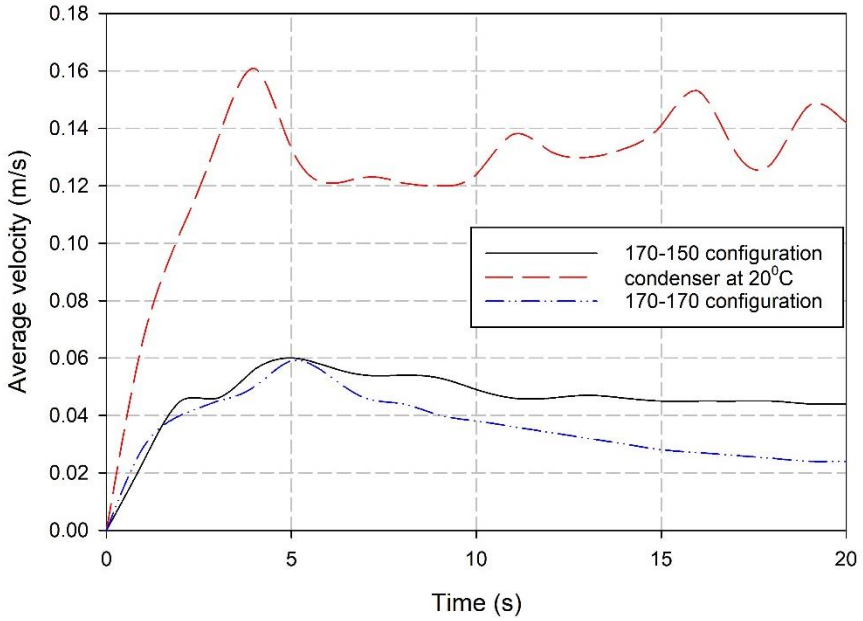

Figure 5.26 Average magnitude of the velocity variation of the fluid in the chamber variation with time for the 170-150 configuration, 170-170 configuration and with a condenser

Figure 5.27 shows the average steam mass fraction variation with time in the top half of the chamber comparing the performance between changing the wall temperatures and installing a condenser. It's clear installing a condenser doesn't show a huge enhancement in the distribution of both steam and air inside the chamber compared to both the (17-150) and the (170-170) configurations after 20 seconds since the change in the mixture homogeneity stops after the first few seconds. However, a condenser helps in reaching a better homogeneity level in less time compared to the other two configurations as shown. Figure 5.28 shows the steam mass fraction distribution variation with time in surface plots to compare the performance of the chamber with a condenser and the chamber with the (170-150) and the (170-170) configurations. It's clearly shown the mixture of steam and air reaches a better homogeneity level in less time compared to the other two configurations.

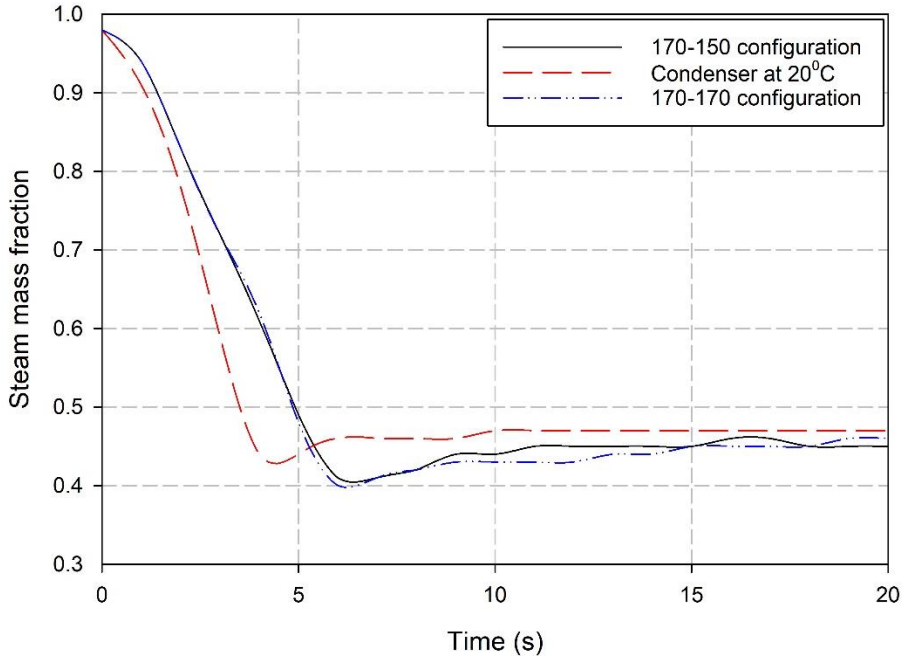

Figure 5.27 Average steam mass fraction variation in the top half of the chamber variation with time for the 170-150 configuration, 170-170 configuration and with a condenser

Table 5.10 shows the results of the simulations comparing the average magnitude of the velocity, steam mass fraction in the top half of the chamber and the average temperature during the simulation time of 20 seconds for the (170-150) configuration, (170-170) configuration and with a condenser. As it can be seen and discussed earlier, installing a condenser drastically improves the average flow velocity inside the chamber compared to the best scenario which is the (170-150) configuration. Installing a condenser increases the average magnitude of the velocity after 20 seconds by 496.8% compared to the original (170-170) configuration, it also improves it by 225.0% compared to the (170-150) configuration. In addition, the condenser enhances the homogeneity of the mixture by helping in reaching a more homogeneity level in less time. As it's shown, the chamber with a condenser required around 6 seconds to reach to almost a steady state of homogeneity level while it takes 11 seconds and 15 seconds for the (170-150) configuration and the (170-170) configuration, respectively. However, installing a cold coil acting as a condenser in the chamber will cause the temperature of the fluid to decrease which will increase the relative humidity of the air inside the chamber for the same water content carried by air flowing inside the chamber while creating the pressure pulses. This is going to decrease

the air ability to carry moisture from the pouches. After 20 seconds, the average temperature inside the chamber is 139.8°C compared to 158.1°C for the (170-170) configuration, this represents 11.6% decrease in the average fluid temperature.

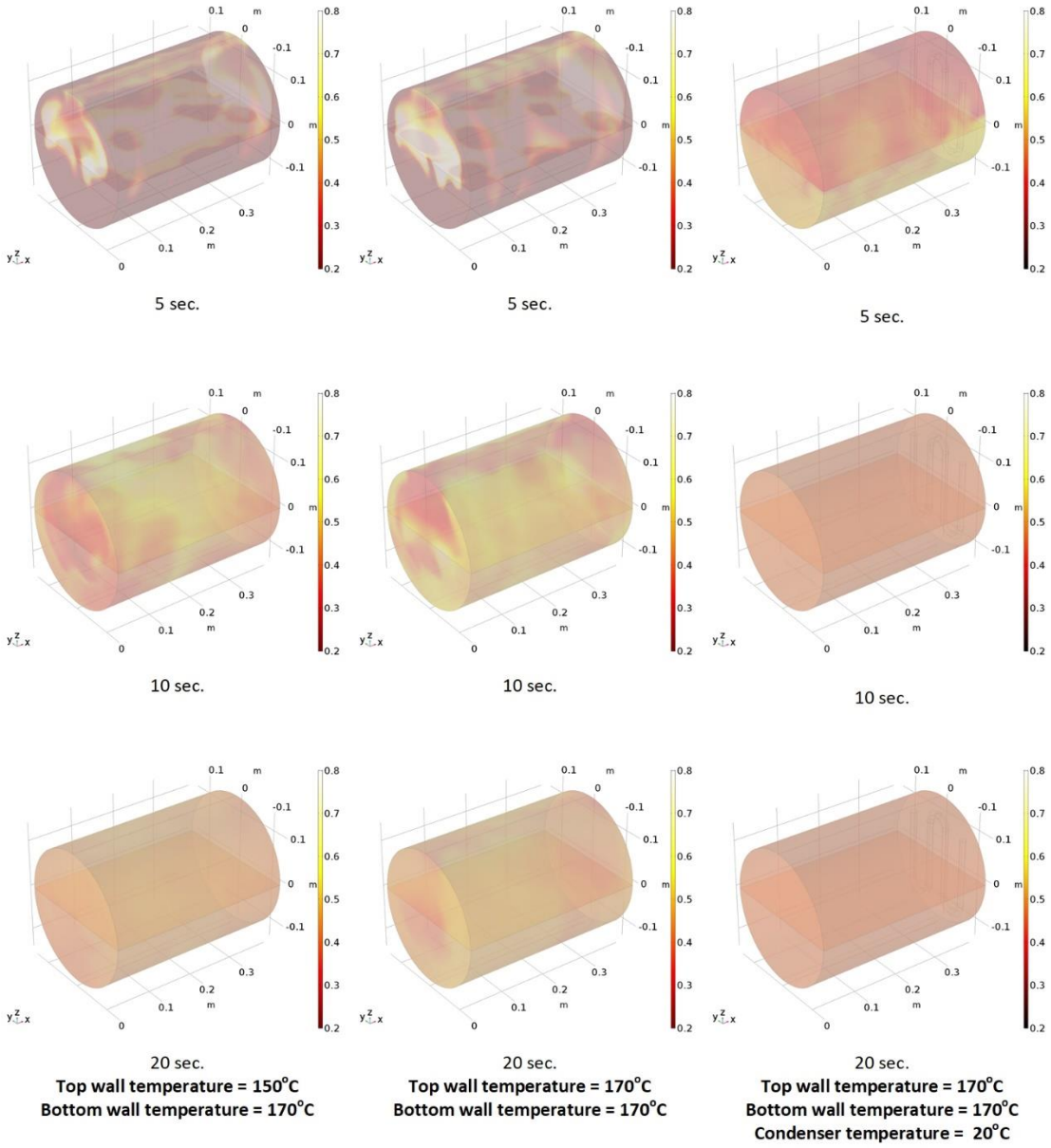

Figure 5.28 Steam mass fraction distribution after 5, 10 and 20 sec. for the (170-150) configuration, (170-170) configuration and with a condenser

Table 5.10 Average velocity magnitude and average steam concentration in the top half and the average temperature of the chamber results variation over time for the (170-170) configuration, (170-150) configuration and with a condenser

Time (s)	Average velocity magnitude (m/s)			Steam concentration fraction in the top half			Average temperature (°C)		
	170-150	170-170	condenser	170-150	170-170	condenser	170-150	170-170	condenser
0	0	0	0	0.98	0.98	0.98	134.1	134.2	134.0
1	0.024	0.029	0.067	0.94	0.94	0.91	135.9	136.7	135.1
2	0.045	0.040	0.104	0.83	0.83	0.78	136.8	138.2	136.2
3	0.046	0.045	0.136	0.72	0.72	0.59	137.7	139.7	136.9
4	0.056	0.050	0.161	0.61	0.62	0.44	138.8	141.2	137.9
5	0.060	0.059	0.133	0.49	0.48	0.44	139.8	142.8	138.7
6	0.057	0.054	0.121	0.41	0.40	0.46	140.8	144.3	139.2
7	0.054	0.046	0.123	0.41	0.41	0.46	141.7	145.7	139.8
8	0.054	0.044	0.121	0.42	0.42	0.46	142.6	147.0	140.1
9	0.053	0.040	0.120	0.44	0.43	0.46	143.4	148.2	140.4
10	0.049	0.038	0.124	0.44	0.43	0.47	144.2	149.4	140.5
11	0.046	0.036	0.138	0.45	0.43	0.47	144.9	150.5	140.3
12	0.046	0.034	0.132	0.45	0.43	0.47	145.6	151.5	140.2
13	0.047	0.032	0.130	0.45	0.44	0.47	146.2	152.5	140.4
14	0.046	0.030	0.133	0.45	0.44	0.47	146.8	153.4	140.4
15	0.045	0.028	0.141	0.45	0.45	0.47	147.4	154.3	140.8
16	0.045	0.027	0.153	0.46	0.45	0.47	148.0	155.2	141.0
17	0.045	0.026	0.132	0.46	0.45	0.47	148.5	156.0	140.4
18	0.045	0.025	0.128	0.45	0.45	0.47	149.0	156.7	140.2
19	0.044	0.024	0.148	0.45	0.46	0.47	149.4	157.4	139.9
20	0.044	0.024	0.142	0.45	0.46	0.47	149.8	158.1	139.8

5.2.4 Mathematical Model for the Pressure Pulses

As it was explained earlier, the drying process starts when the pressure in the chamber reaches 80 kPa and ends when it reaches this pressure level again. The time required for drying is defined as the time when the pressure inside the chamber is 80 kPa at the initial state and going back to 80 kPa again after the pressure pulses take place in between. Usually, the pressure goes down to 14 kPa as suggested by [24] for the optimum pressure required to enhance the boiling of water droplets at low temperature and pressure. During the drying process, pressure pulses are created by vacuuming and pressurizing the chamber several times creating what we called pressure pulses to allow the pouches to breathe and enhance the boiling of the water droplet stuck inside the pouches. The number of pressure pulses created depends on the total drying time and the range of pressure pulses. As time increases, more pressure pulses can be created. In addition, the lower range of pressure pulses allows more pulses to occur during a specific time. The objective of this model is to find the effects of the range of pressure pulses that maximizes the amount of air inlet the chamber. Maximizing the amount of dry air introduced to the system helps to capture the water droplet presented in the pouches.

Figure 5.29 shows pressure measurements during one complete sterilizing cycle. The pressure is decreased to 15 kPa and the drying process took around 10 minutes. Figure 5.30 shows the temperature variation throughout the cycle. As air is being replaced by steam in the conditioning phase, the temperature in the chamber is increased to 134ºC to initiate the sterilization process. Different thermocouples give different readings of the temperature during this phase. However, during the sterilization phase, the temperature is uniform throughout the chamber since it's filled with saturated steam. After 4 minutes of sterilization, the drying process takes place and the temperature of the steam drops. Any pressure pulses during the drying process means that air is being introduced to the chamber which mixes with the steam and causes the temperature to drop. For the cycle shown in Figure 5.30, the average temperatures of the fluid inside the chamber at the beginning and the end of the drying phase are 95ºC and 89ºC, respectively. While the average temperature throughout the drying phase is 82ºC.

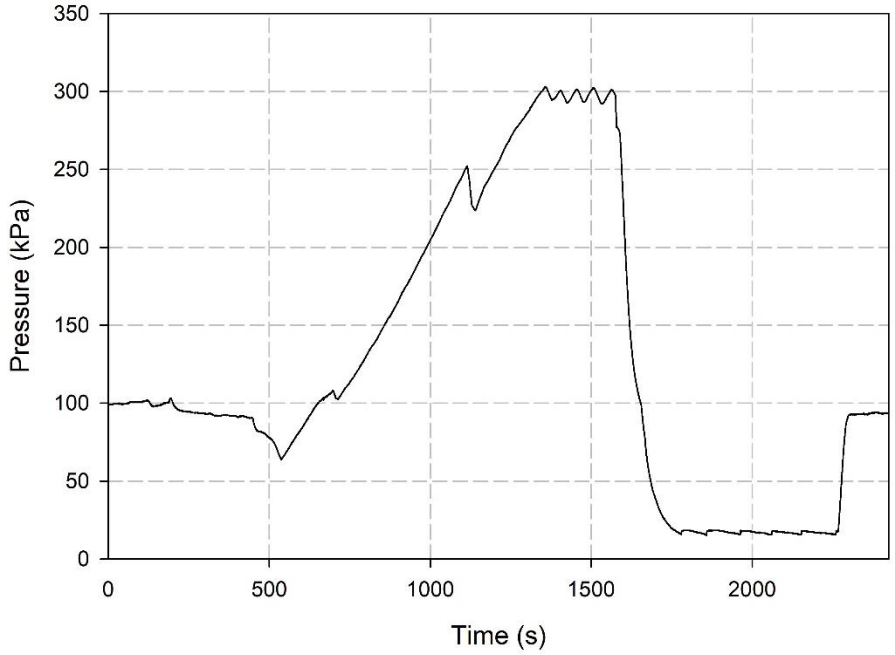

Figure 5.29 Pressure profile in one full sterilization cycle

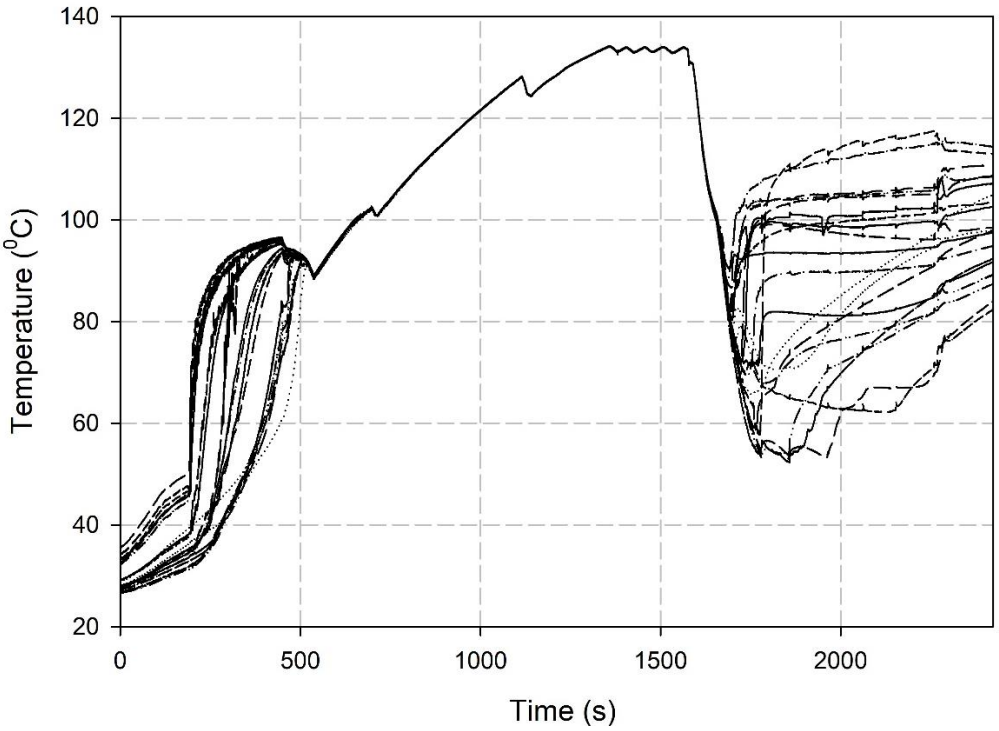

Figure 5.30 Temperature profile in one full sterilization cycle

Figure 5.31 shows the variation of the boiling temperature of water at different absolute pressure values. As it's expected, the boiling temperature drops at lower pressures.

The vacuum created inside the chamber helps in decreasing the temperature at which the water droplets in the pouches start to boil. Heat is transferred from the surface of the tool to the water droplets causing the droplet to evaporate. At some point, the temperature of the tools drops and no more energy is supplied to the water droplet to evaporate. So, evaporation should take place to allow water droplets to vaporize without the need for boiling. Several factors can affect the evaporation rate of water, such as the velocity of the fluid inside the chamber as was suggested by [55]. As the velocity increases, the evaporation rate increases due to forced convection. So, when developing this model, the lower limit of the pressure pulses will be 14 kPa for all the cases.

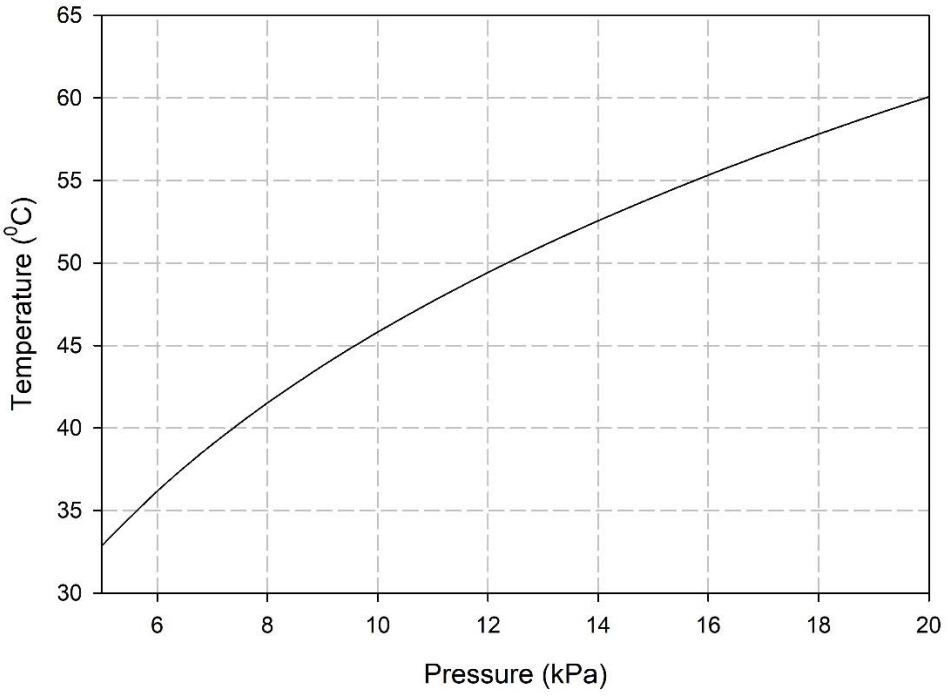

Figure 5.31 Boiling temperature variation with absolute pressure

Eureqa-Formalize software is used to get the correlations that were used in developing the model. Eureqa-Formalize is an artificial intelligence powered modeling engine. These data sets were used to develop the correlations that related the pressure within the chamber with time. Two correlations were obtained, the first one shows the variation of pressure with time during the vacuuming part of process in which steam and air in the chamber are forced to flow out to decrease the pressure as it's shown in Equation 3. The R-value (Regression value) for Equation 3 is 99.98%. The R-value is a statistical

measure of how close the data to the fitted line. The regression value obtained indicates that the model can predict the outputs of the system accurately.

$$P = 191 + 0.0129t^2 + 14.3\exp(-0.127 \times t) - 124\exp(0.00896 \times t) \quad (5.1)$$

The second correlation, Equation 4, shows the variation of pressure with time during the pressurizing process in which air is allowed to flow in the chamber to increase the pressure. The R-value for this correlation is 99.99%. The developed mathematical model is valid between 14 kPa and 80 kPa.

$$P = 15.4 + 4.53t + 0.485\log(1.68 + 17.8t) - 0.0574t^2 \quad (5.2)$$

The developed correlations were solved using EES (Engineering Equations Solver). The results of the model were compared with an actual run in which the drying time took 623 seconds with pressure pulses range of 15.78 kPa to 18.37 kPa. Figure 5.32 compares the developed mathematical model with the actual run. As can be seen, the number of the pulse obtained from the mathematical model is 5 which is the same as the number of pulses occurring in the real run. The average error value of the pressure is 4.4%. The developed model will be used to estimate the number of pressure pulses for each different pressure range and the time it takes to create one complete pressure pulse

Table 5.11 shows the time it takes for the pressurizing phase and vacuuming phase for each range of the pressure pulses.

Table 5.11 Time taken for each range of the pressure pulses used in the simulations

Bottom pressure (kPa)	Top pressure (kPa)	Pressurizing time (s)	Vacuuming time (s)	Total pressure pulse time (s)
14	15	0.3	6.3	6.6
14	16	0.6	13.6	14.2
14	17	0.9	19.1	20.0
14	18	1.2	29.2	30.4
14	19	1.5	36.1	37.6
14	20	1.9	42.1	43.9

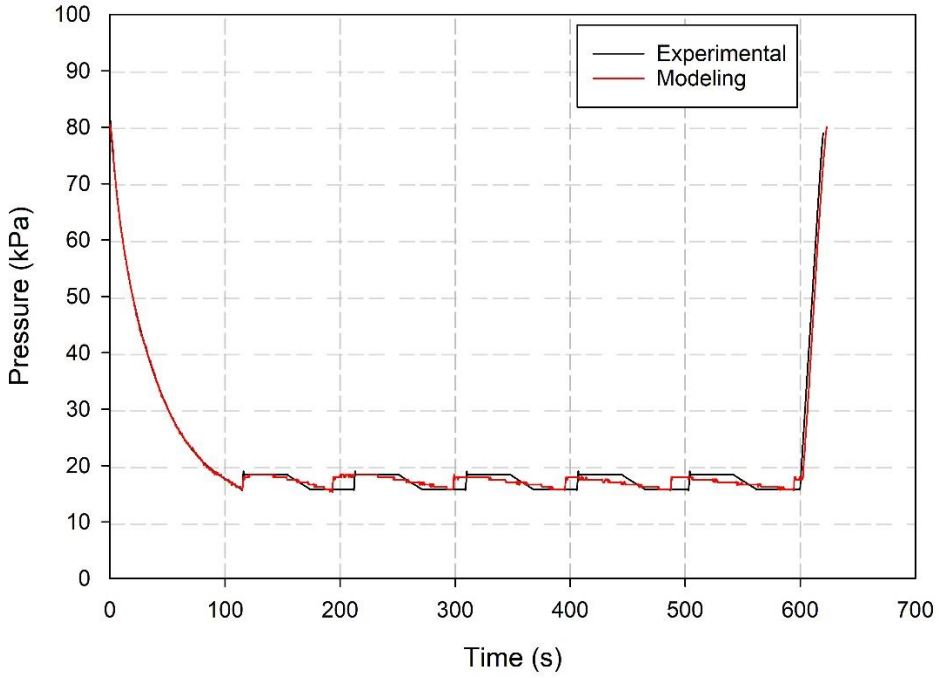

Figure 5.32 Comparison between actual experimental data and the developed mathematical model for the drying phase

5.2.5 The Effects of Pressure Pulses Ranges on Replacing Steam with Air

In this section, the effects of varying the range of pressure pulses and different wall temperatures on the drying performance is examined by simulating a 2d model of the chamber with the real dimensions and conditions. The base pressure in the pressure pulses for all the cases is going to be 14 kPa as suggested by the literature [24]. However, the maximum pressure in the pressure pulses is going to be varied from 15 kPa to 20 kPa to simulate the displacement of steam by air going in the chamber in the pressurizing part during the pressure pulses, while both steam and air mixture leaves the chamber during the vacuuming phase. Figure 5.32 shows the geometry of the chamber with each of the pouches assigned a number. The two holes on the back wall act as inlets during the pressurizing process and outlets during the vacuuming process. On the other hand, the two holes on the bottom wall act only as outlets during the vacuuming process and both of them are closed during the pressurizing process. Each pouch is assigned a different number as it can be shown in Figure 5.33. Before starting the simulation, a mesh independent study is performed to choose the mesh size that will give accurate results with minimum

computational time. Figure 5.34 shows the variation of the average steam fraction of the first pouch after 10 sec. with changing mesh size. As it can be seen, the difference between the results when using 134,402 elements in the mesh size and 148,722 elements in the mesh size is only 0.5%. So, the mesh with 134,402 elements is going to be used in this simulation. Figure 5.35 shows the constructed mesh used in the simulation.

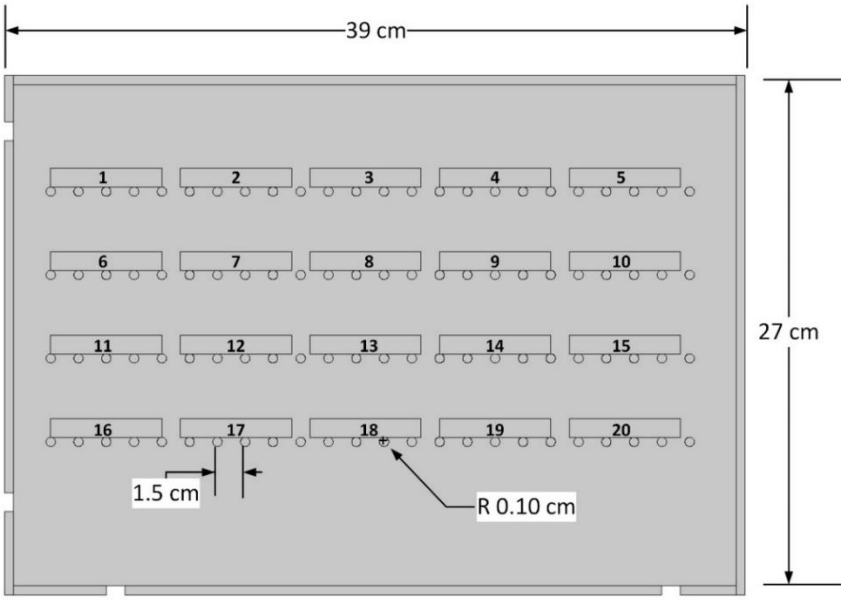

Figure 5.33 2D geometry used in the simulation with dimensions and pouches numbers

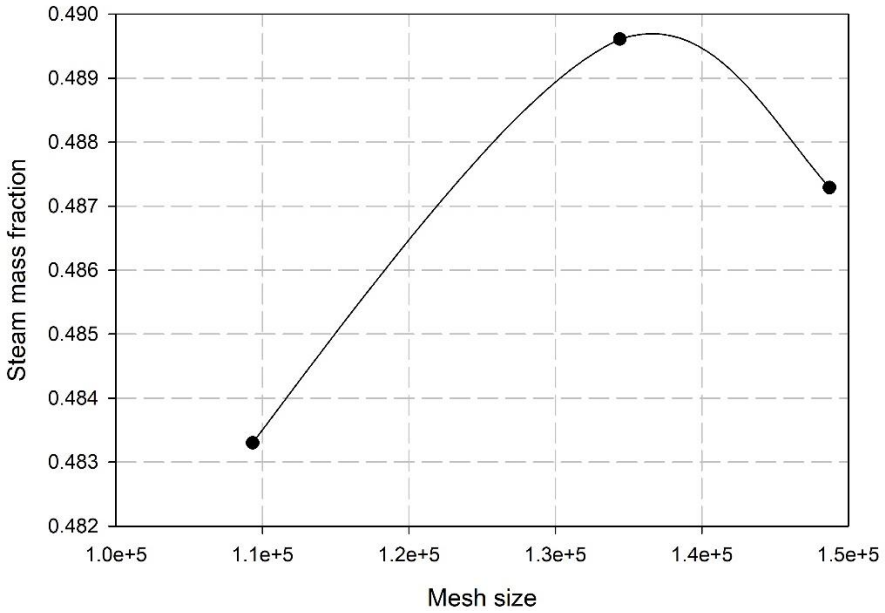

Figure 5.34 Mesh independent study

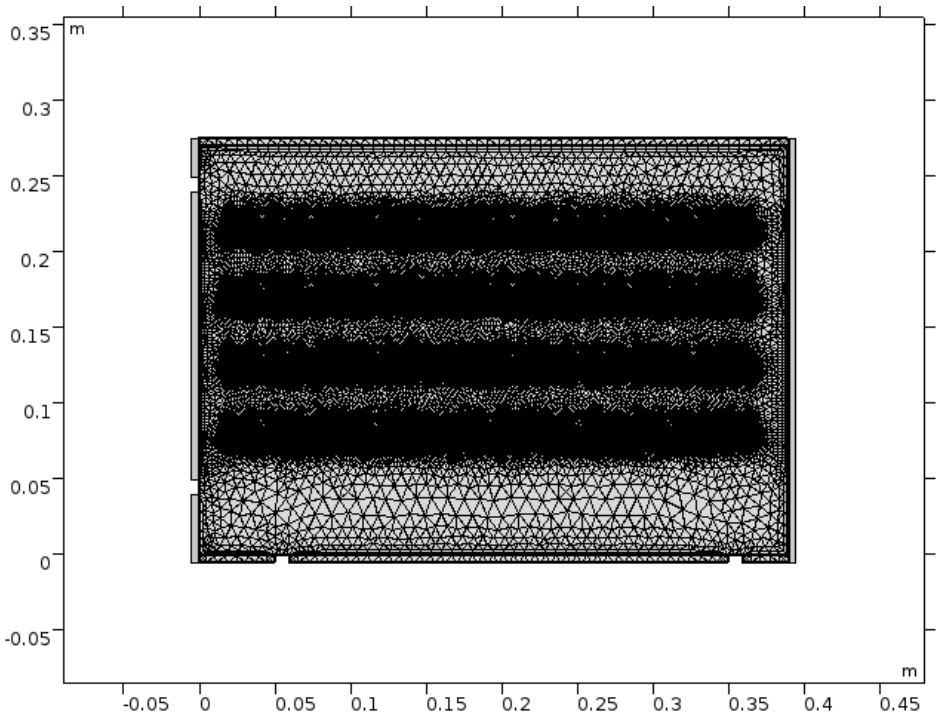

Figure 5.35 The constructed mesh used in the simulation

Water mass fraction variation for the pouches over different pressure pulses ranges and different top and bottom wall temperatures is going to be illustrated. As it's noted, every pressure pulse takes a different time to complete one pressure pulse.

As it can be seen in Table 5.11, the expected total time to create one complete pressure pulse from 14 kPa to 15 kPa is 6.6 seconds. Creating the vacuum takes around 6.3 seconds while pressurizing the chamber takes around 0.3 seconds.

Figure 5.36 shows the drying results after one pressure pulse from 14 kPa to 15 kPa for one pouch in each tray. As it can be seen in Figure 5.36 (a), when the top and bottom walls have the same temperature as 170°C, it results in a better drying quality for pouch No. 5 compared to having different wall temperatures. In the 14-15 (170-170) configuration, the water mass fraction after the first pulse is 0.4978 compared to 0.4983 and 0.4982 for the 14-15 (170-160) and the 14-15 (170-150) configuration, respectively. On the other hand, setting the top wall temperature to 150°C improves the drying quality for pouch No. 8 as it's seen in Figure 5.36 (b). The water mass fraction drops from 0.4984 when the top wall temperature is 170°C to 0.4969 when the top wall temperature is changed

to 150°C, which represents a 0.3% decrease in the water mass fraction. For pouch No. 11 as it's clear in Figure 5.36 (c), having different wall temperatures doesn't improve the drying quality. Having similar wall temperatures as in the 14-15 (170-170) configuration results in 0.4970 water mass fraction compared to 0.4978 and 0.4974 in the 14-15 (170-160) and the 14-15 (170-150) configurations, respectively. While for pouch No. 17, setting the top wall temperature to be less than the bottom wall temperature results in a less water mass fraction as it's shown in Figure 5.36 (d). The behavior is almost the same when the top wall temperature is either 150°C or 160°C. Total water mass fractions are 0.4965 and 0.4968 when the top wall temperature is 150°C and 160°C, respectively. While the water mass fraction is 0.4972 for the 14-15 (170-170) configuration.

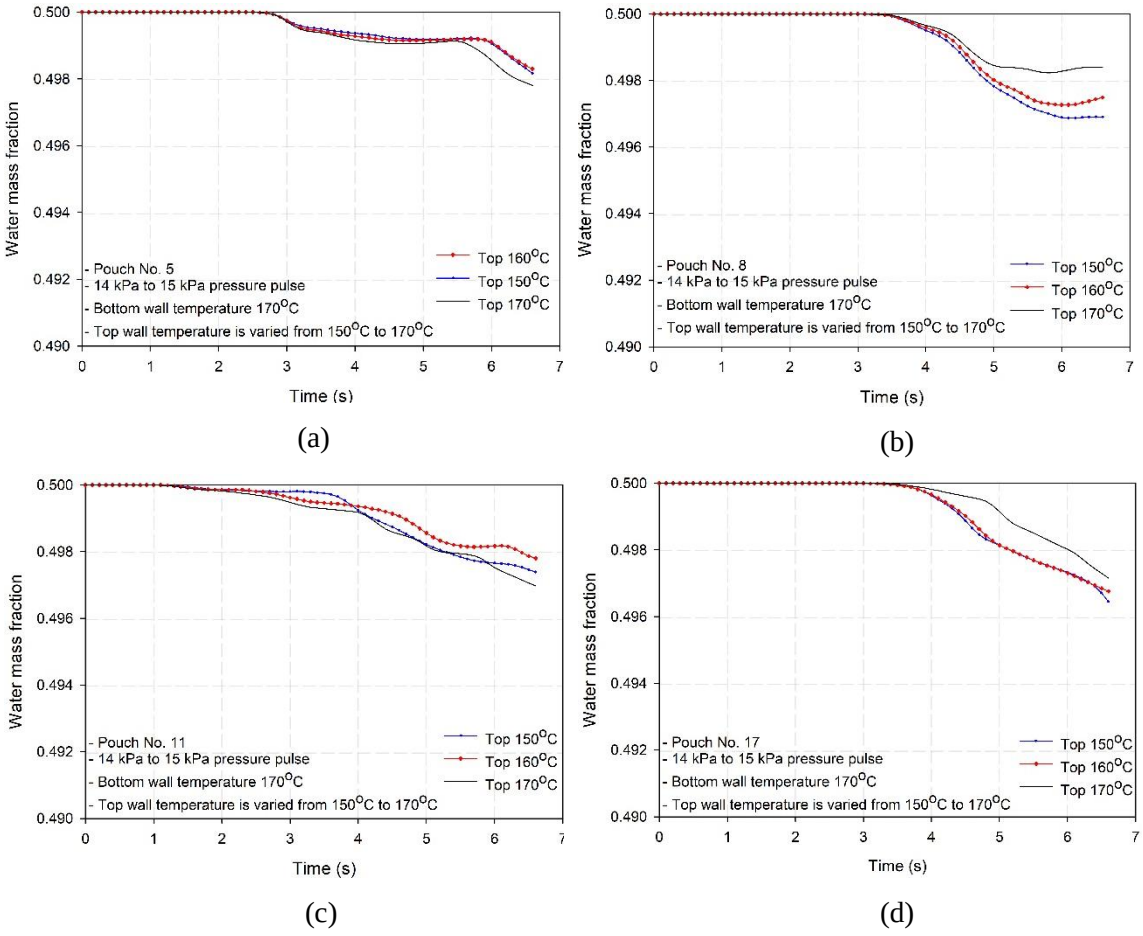

Figure 5.36 Water mass fraction after the first pressure pulse from 14 kPa to 15 kPa for pouches No. 5, 8, 11 and 17

Figure 5.37 shows the average velocity of the fluid inside the chamber with time during one full pressure pulses between 14 kPa and 15 kPa for different top wall

temperatures while the bottom wall temperature is kept at 170°C. The average value of the velocities over the full period of the pressure pulse are 0.089 m/s, 0.095 m/s and 0.094 m/s when the top wall temperatures are 150°C, 160°C and 170°C, respectively. So, setting the top wall temperature as 150°C results in 1.4% decrease in the average velocity of the fluid over the pressure pulse compared to having both the top and the bottom wall temperatures as 170°C. On the other hand, setting the top wall temperature as 160°C results in 0.9% decrease in the average velocity of the fluid over the pressure pulse.

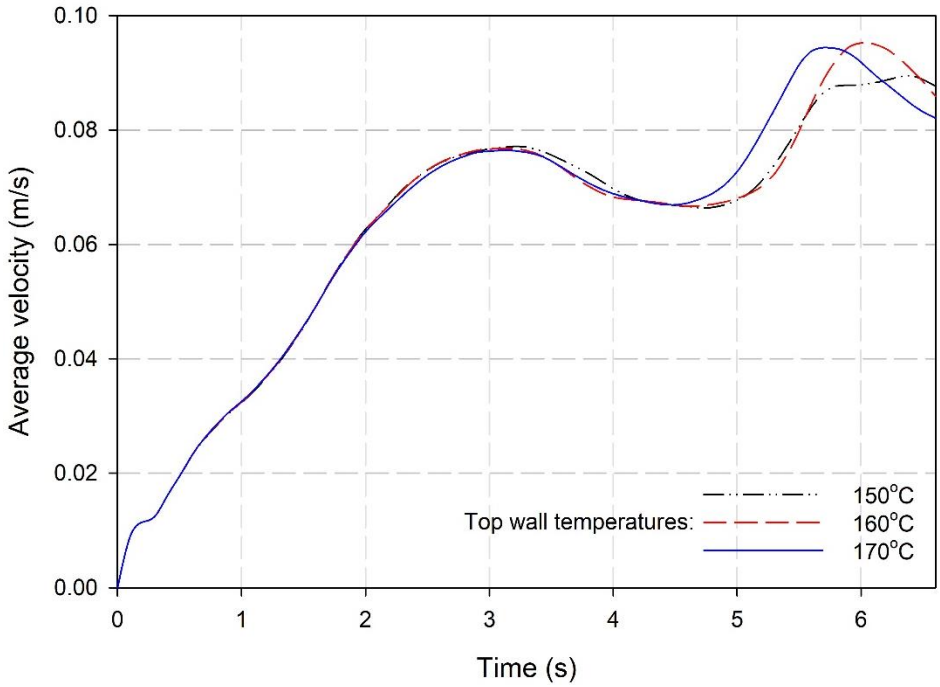

Figure 5.37 Average fluid velocity variation inside the chamber during one full pressure pulse from 14 kPa to 15 kPa for different top wall temperatures

As it can be seen in Table 5.11, the expected total time to create one complete pressure pulse from 14 kPa to 16 kPa is 14.2 seconds. Creating the vacuum takes around 13.6 seconds while pressurizing the chamber takes around 0.6 seconds.

Figure 5.38 shows the drying results after one pressure pulse from 14 kPa to 16 kPa for one pouch in each tray. For pouch No. 2 shown in Figure 5.38 (a), the 14-16 (170-150) configuration results in a better drying quality as the water mass fraction after the first pulse is 0.4877 while it's 0.4899 and 0.4894 for the 14-16 (170-160) and 14-16 (170-170), respectively. However, setting the top wall temperature to be 150°C doesn't always help

in reducing the water mass fraction as it's shown in Figure 5.38 (b) for pouch No. 9. For the 14-16 (170-170) configuration, the water mass fraction after the first pressure pulse is 0.4898 compared to 0.4924 when the top wall temperature is set to 150°C in the 14-16 (170-150) configuration. In some cases, setting the top wall temperature as 160°C results in the least amount of water in the pouch as it's the case for pouch No. 12 shown in Figure 5.38 (c). The water mass fraction for the 14-16 (170-160) configuration after the first pressure pulse is 0.4919 while it's 0.4937 when the top wall temperature is 170°C in the 14-16 (170-150) configuration. This is also the case for pouch No. 16 as it's noted in Figure 5.38 (d). The 14-16 (170-160) results in the least amount of water presented in the pouch after the first pouch while the 14-16 (170-170) results in the most amount of water inside the pouch. The water mass fraction for the 14-16 (170-160) configuration is 0.4849 while it's 0.4906 for the 14-16 (170-170) configuration.

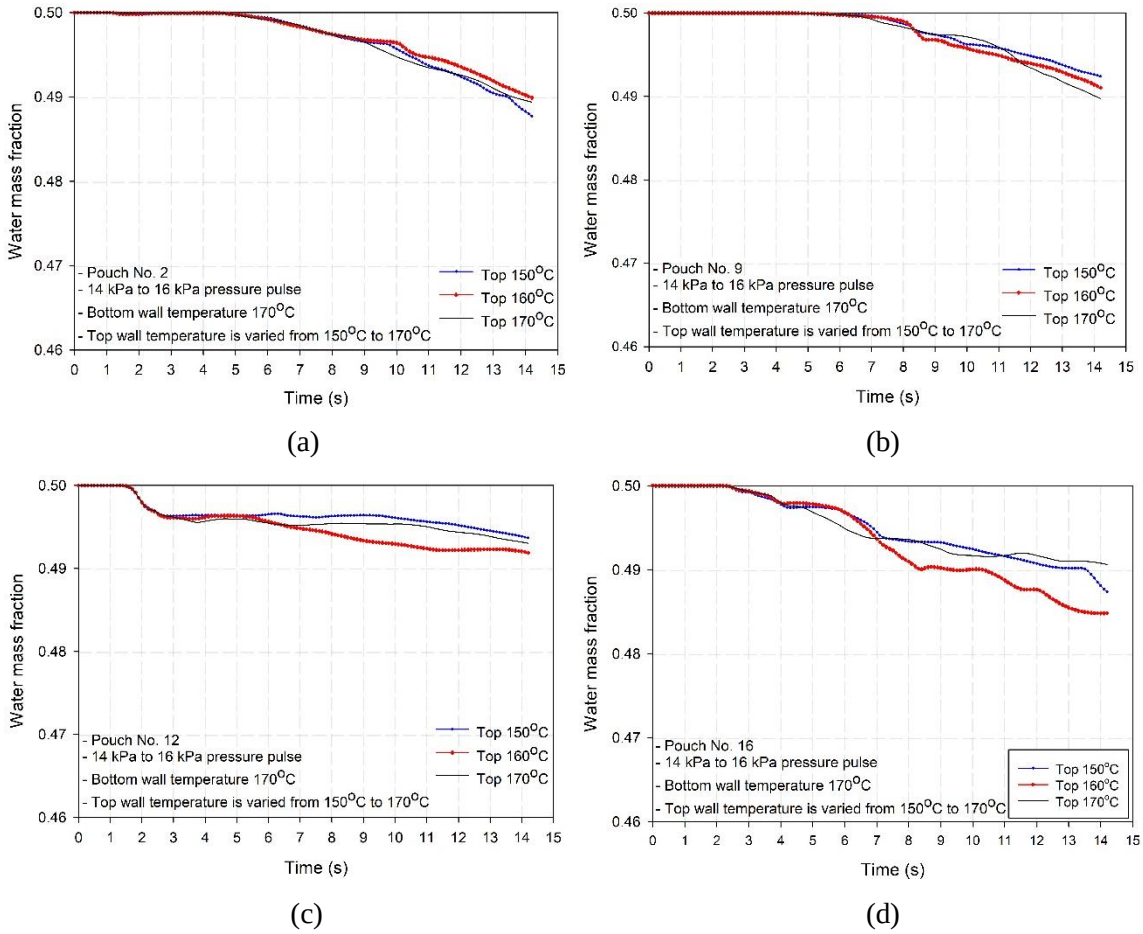

Figure 5.38 Water mass fraction after the first pressure pulse from 14 kPa to 16 kPa for pouches No. 2, 9, 12 and 16

Figure 5.39 shows the average velocity of the fluid inside the chamber with time during one full pressure pulses between 14 kPa and 16 kPa for different top wall temperatures while the bottom wall temperature is kept at 170°C. The average value of the velocities over the full period of the pressure pulse are 0.075 m/s, 0.072 m/s and 0.075 m/s when the top wall temperatures are 150°C, 160°C and 170°C, respectively. So, setting the top wall temperature as 150°C results in 0% increase in the average velocity of the fluid over the pressure pulse compared to having both the top and the bottom wall temperatures as 170°C. On the other hand, setting the top wall temperature as 160°C results in 5% decrease in the average velocity of the fluid over the pressure pulse.

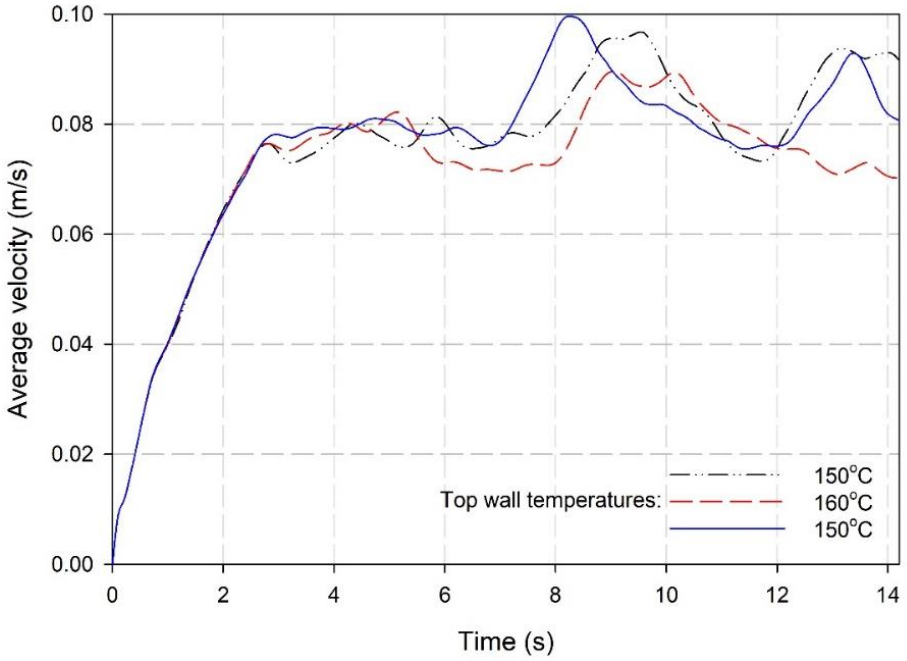

Figure 5.39 Average fluid velocity variation inside the chamber during one full pressure pulse from 14 kPa to 16 kPa for different top wall temperatures

As it can be seen in Table 5.11, the expected total time to create one complete pressure pulse from 14 kPa to 17 kPa is 20 seconds. Creating the vacuum takes around 19.1 seconds while pressurizing the chamber takes around 0.9 seconds.

Figure 5.40 shows the drying results after one pressure pulse from 14 kPa to 17 kPa for one pouch in each tray. The drying results are the same when changing top wall temperature for pouch No. 2 as it's shown in Figure 5.40 (a). Water mass fraction at the end of the first pressure pulse for this pouch is 0.4771, 0.4766 and 0.4755 when the top

wall temperature is 150°C, 160°C, and 170°C, respectively. However, setting the wall temperature as 160°C results in a less water mass fraction in pouch No. 9 compared to the case where the top wall temperature is 150°C as it's clear in Figure 5.40 (b). Water mass fraction at the end of the first pressure pulse for the 14-17 (170-160) configuration is 0.4764 while it's 0.4802 for the 14-17 (170-150). Similar behavior is experienced by pouch No. 15 as it's shown in Figure 5.40 (c). When the top wall temperature is 160°C, water mass fraction 0.4755 while it's 0.4781 and 0.4785 when the top wall temperature is set to 150°C and 170°C, respectively. On the other hand, setting the top wall temperature as 170°C similar to the bottom wall temperature results in the least amount of water mass fraction in pouch No. 18 as it's shown in Figure 5.40 (d). At the end of the first pressure pulse, water mass fraction is 0.4805, 0.4784 and 0.4763 when the top wall temperature is 150°C, 160°C, and 170°C, respectively.

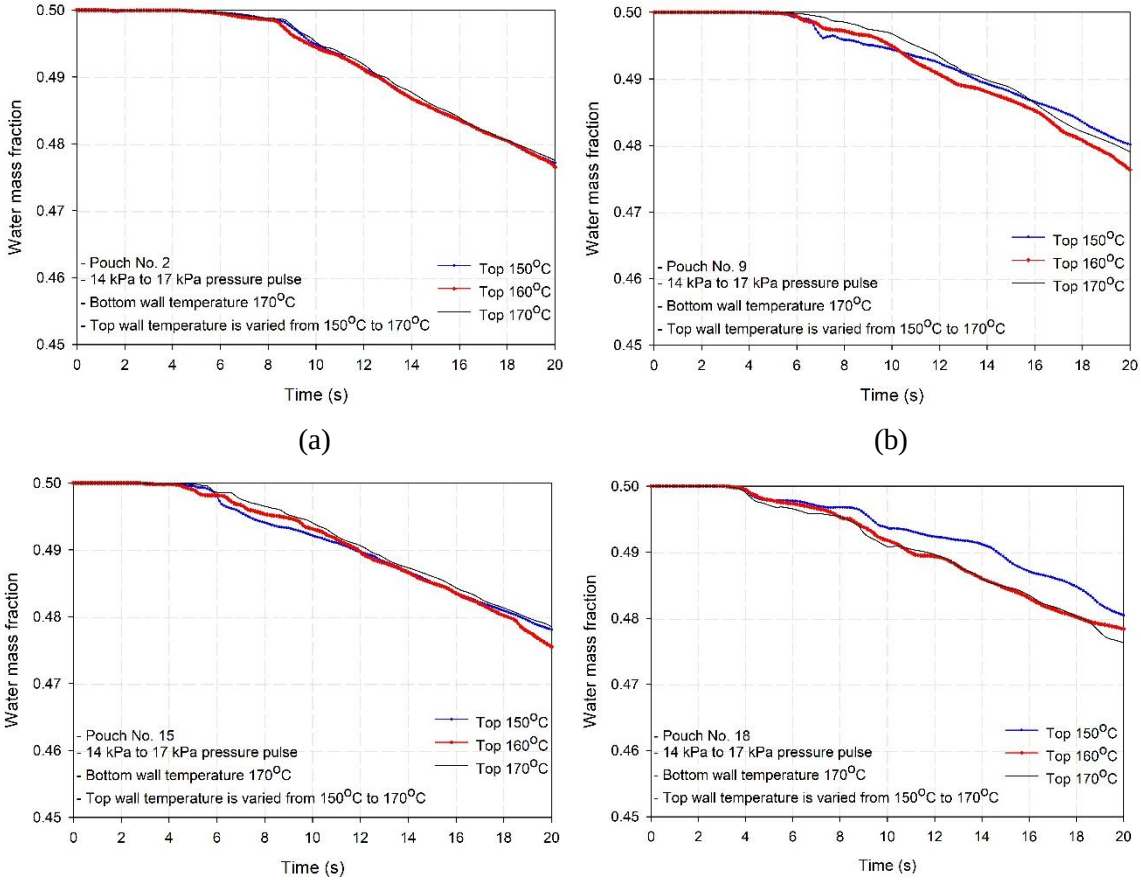

Figure 5.40 Water mass fraction after the first pressure pulse from 14 kPa to 17 kPa for pouches No. 2, 9, 15 and 18

Figure 5.41 shows the average velocity of the fluid inside the chamber with time during one full pressure pulses between 14 kPa and 17 kPa for different top wall temperatures while the bottom wall temperature is kept at 170°C. The average value of the velocities over the full period of the pressure pulse are 0.075 m/s, 0.075 m/s and 0.074 m/s when the top wall temperatures are 150°C, 160°C and 170°C, respectively. So, setting the top wall temperature as 150°C results in 1.4% increase in the average velocity of the fluid over the pressure pulse compared to having both the top and the bottom wall temperatures as 170°C. Also, setting the top wall temperature as 160°C results in 1.4% increase in the average velocity of the fluid over the pressure pulse.

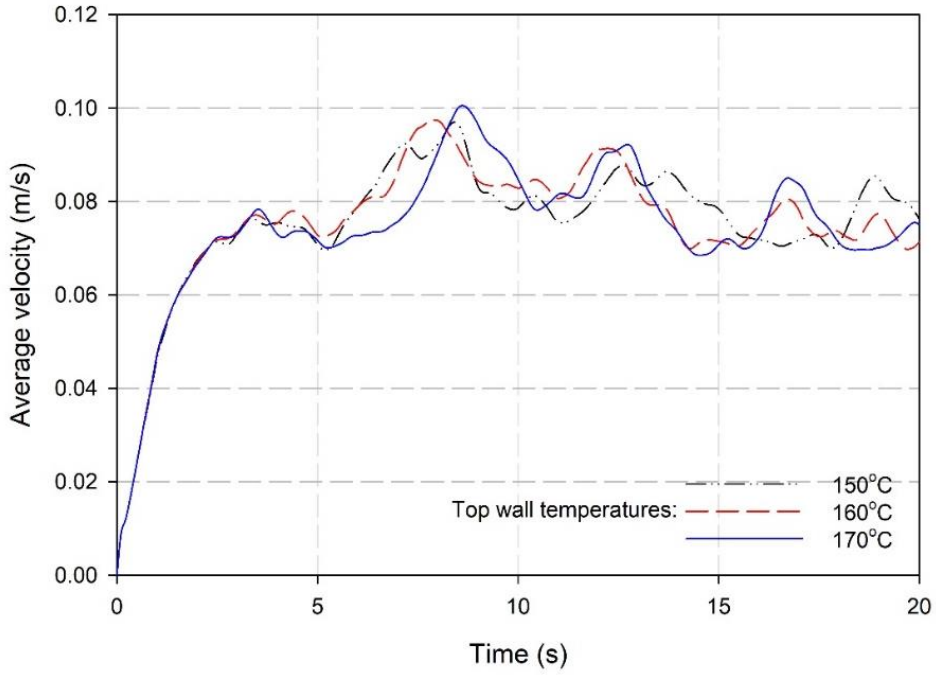

Figure 5.41 Average fluid velocity variation inside the chamber during one full pressure pulse from 14 kPa to 17 kPa for different top wall temperatures

As it can be seen in Table 5.11, the expected total time to create one complete pressure pulse from 14 kPa to 18 kPa is 30.4 seconds. Creating the vacuum takes around 29.2 seconds while pressurizing the chamber takes around 1.2 seconds.

Figure 5.42 shows the drying results after one pressure pulse from 14 kPa to 18 kPa for one pouch in each tray. For pouch No. 1, the performance for both 14-18 (170-160) and 14-18 (170-170) configurations are the same as shown in Figure 5.42 (a). The drying

quality decreases when the top wall temperature is set to 150°C. After the first pressure pulse, the water mass fractions are 0.4626, 0.4507 and 0.4505 when the top wall temperatures are 150°C, 160°C, and 170°C. Similar behavior is experienced by pouch No. 8 as it's shown in Figure 5.42 (b) where the configuration in which the top wall temperature is 150°C shows the most water mass fraction compared to the 14-18 (170-160) and 14-18 (170-170) configurations, respectively. However, setting the top wall temperature to 150°C helps in reducing the water mass fraction for pouch No. 12 that's shown in Figure 5.42 (c). Water mass fraction after the first pressure pulse for pouch No. 12 is 0.4595 compared to 0.4610 and 0.4616 for the 14-18 (170-160) and 14-18 (170-170) configurations, respectively. On the other hand, for pouch No. 18 shown in Figure 5.42 (d), when the top wall temperature is set to 160°C, the water mass fraction is minimized compared to the 14-18 (170-150) and 14-18 (170-170) configurations.

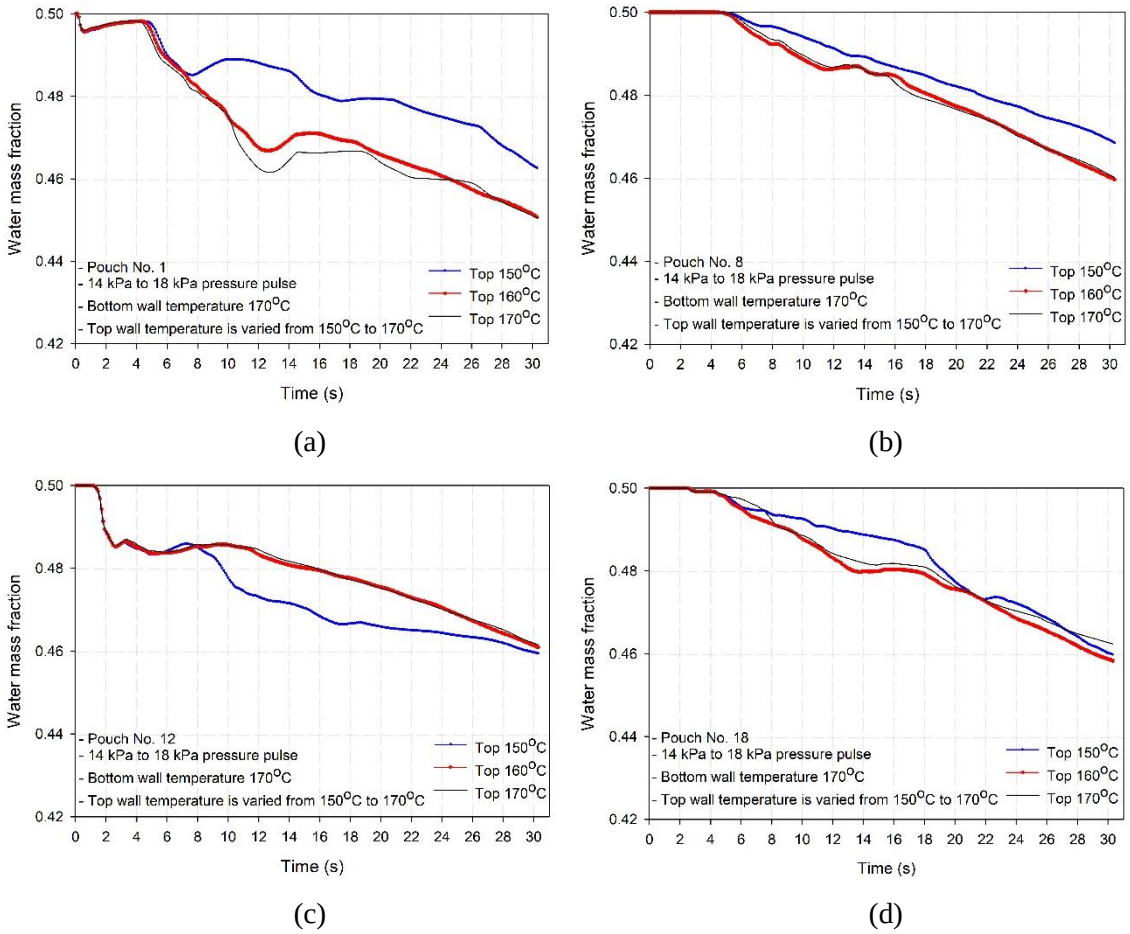

Figure 5.42 Water mass fraction after the first pressure pulse from 14 kPa to 18 kPa for pouches No. 1, 8, 12 and 18

Figure 5.43 shows the average velocity of the fluid inside the chamber with time during one full pressure pulses between 14 kPa and 18 kPa for different top wall temperatures while the bottom wall temperature is kept at 170°C. The average value of the velocities over the full period of the pressure pulse are 0.075 m/s, 0.073 m/s and 0.073 m/s when the top wall temperatures are 150°C, 160°C and 170°C, respectively. So, setting the top wall temperature as 150°C results in 2.7% increase in the average velocity of the fluid over the pressure pulse compared to having both the top and the bottom wall temperatures as 170°C. Also, setting the top wall temperature as 160°C results in 0% increase in the average velocity of the fluid over the pressure pulse.

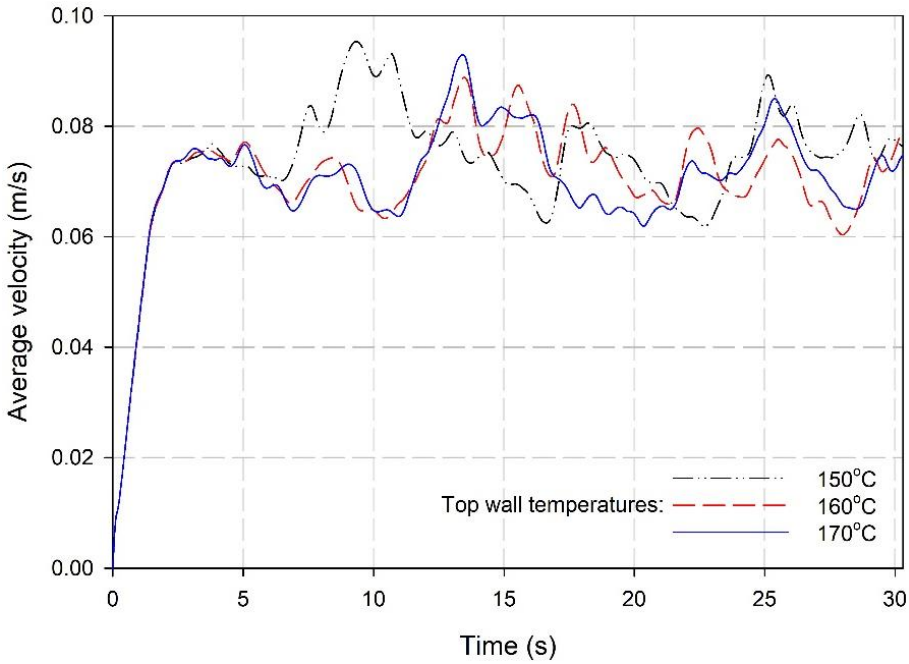

Figure 5.43 Average fluid velocity variation inside the chamber during one full pressure pulse from 14 kPa to 18 kPa for different top wall temperatures

As it can be seen in Table 5.11, the expected total time to create one complete pressure pulse from 14 kPa to 19 kPa is 37.6 seconds. Creating the vacuum takes around 36.1 seconds while pressurizing the chamber takes around 1.5 seconds.

Figure 5.44 shows the drying results after one pressure pulse from 14 kPa to 19 kPa for one pouch in each tray. For all the pouches in the first tray, setting the top wall temperature to 160°C results in the least amount of water vapor inside the pouch. An example is shown in Figure 5.44 (a) for pouch No. 4. The water mass fraction when the

top wall temperature is set to 160°C is 0.4410 while it's 0.4478 when the top wall temperature is 150°C and 0.4467 when the top wall temperature is 160°C. However, for pouch No. 8, setting the top wall temperature to 150°C results in a better drying quality. As it's clear in Figure 5.44 (b), the water mass fraction for the 14-19 (170-150) is 0.4502 while they are 0.4513 and 0.4508 when the top wall temperatures are 160°C and 170°C, respectively. On the other hand, setting the top wall temperature as 150°C or 160°C might have no effect as it is shown in Figure 5.44 (c) for pouch No. 12. The water mass fractions after the first pressure pulse are 0.4507 and 0.4505 when the top wall temperatures are 150°C and 160°C. while it's 0.4518 when the top wall temperature is similar to the bottom one. Similar to the behavior of the pouches in the first tray is shown in Figure 5.44 (d) for pouch No. 18. Setting the top wall temperature as 160°C results in a water mass fraction of 0.4420 while it only reaches to 0.4437 and 0.4517 when the top wall temperatures are 150°C and 170°C.

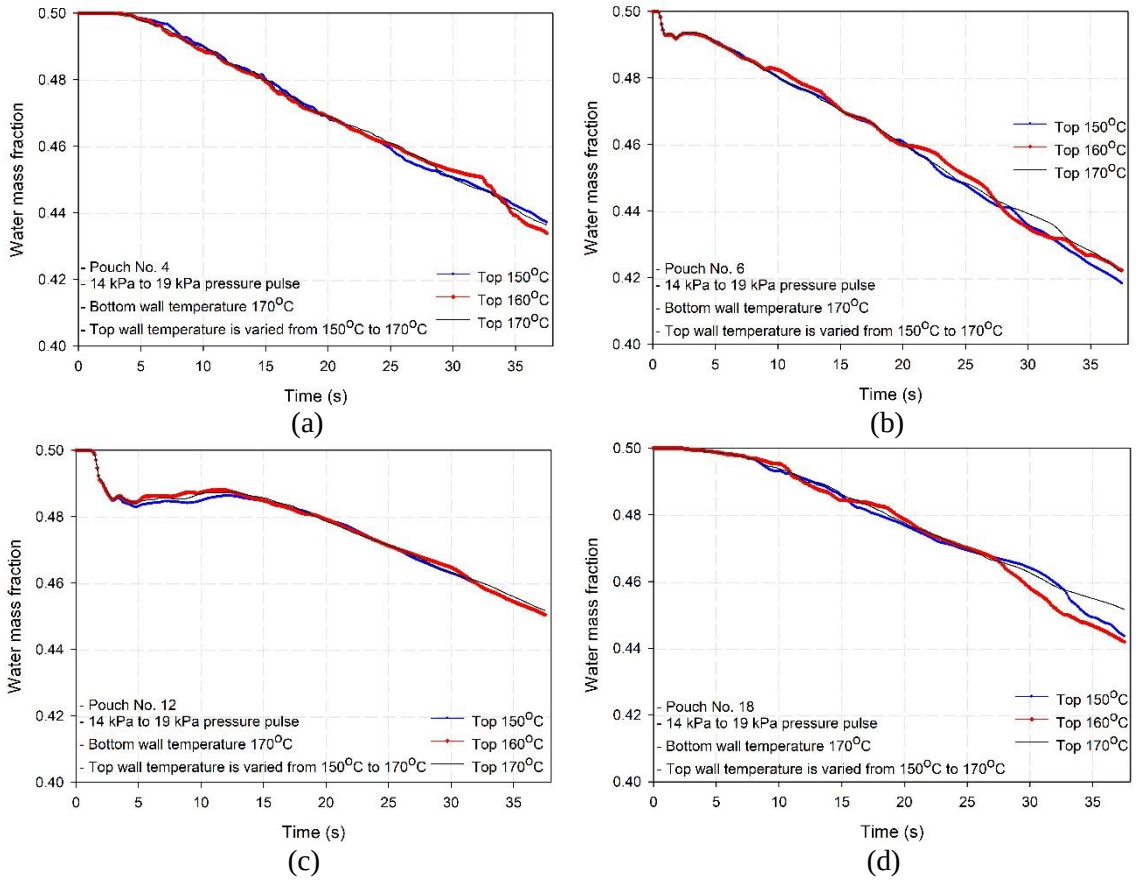

Figure 5.44 Water mass fraction after the first pressure pulse from 14 kPa to 19 kPa for pouches No. 4, 6, 12 and 18

Figure 5.45 shows the average velocity of the fluid inside the chamber variation with time during one full pressure pulses between 14 kPa and 19 kPa for different top wall temperatures while the bottom wall temperature is kept at 170°C. The average value of the velocities over the full period of the pressure pulse are 0.071 m/s, 0.071 m/s and 0.071 m/s when the top wall temperatures are 150°C, 160°C and 170°C, respectively. So, setting the top wall temperatures as 150°C or 160°C results in 0% increase in the average velocity of the fluid over the pressure pulse compared to having both the top and the bottom wall temperatures as 170°C.

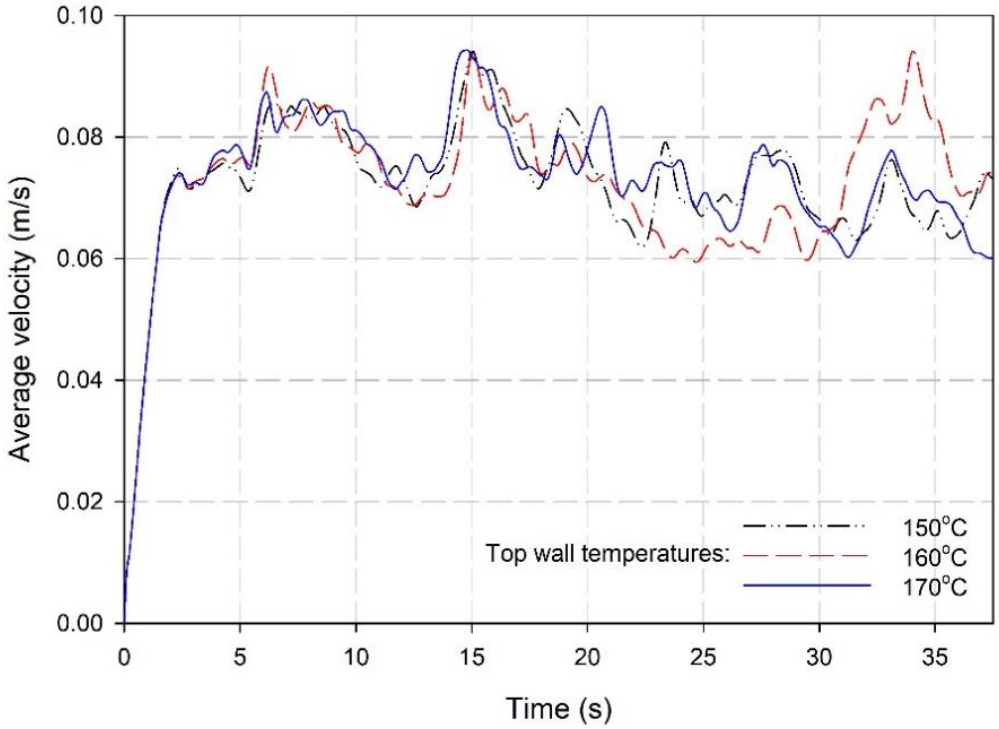

Figure 5.45 Average fluid velocity variation inside the chamber during one full pressure pulse from 14 kPa to 19 kPa for different top wall temperatures

As it can be seen in Table 5.11, the expected total time to create one complete pressure pulse from 14 kPa to 20 kPa is 43.9 seconds. Creating the vacuum takes around 42.1 seconds while pressurizing the chamber takes around 1.9 seconds.

Figure 5.46 shows the drying results after one pressure pulse from 14 kPa to 20 kPa for one pouch in each tray. As it can be seen in Figure 5.46 (a), setting the top wall temperature as 160°C results in the lowest amount of water vapor of 0.4142 in pouch No.

5 while the water mass fractions increase to 0.4222 and 0.4169 when the top wall temperature is 150°C and 170°C, respectively. On the other hand, for pouch No. 6 shown in Figure 5.46 (b), the water mass fraction when the top wall temperature is 150°C is 0.4074 which is lower than 0.4041 and 0.4023 when the top wall temperatures are 160°C and 170°C, respectively. Changing the top wall temperature can have a negligible effect as it's shown in Figure 5.46 (c) for pouch No. 13. The water mass fractions for when the top wall temperatures change as 150°C, 160°C and 170°C are 0.4355, 0.4364, and 0.4349, respectively. Pouch No. 17 undergoes similar effect as the pouches in the first tray as shown in Figure 5.46 (d). Setting the top wall temperature to 160°C results in a lower water mass fraction of 0.4379 compared to 0.4356 and 0.4389 when the top wall temperatures are 150°C and 170°C, respectively.

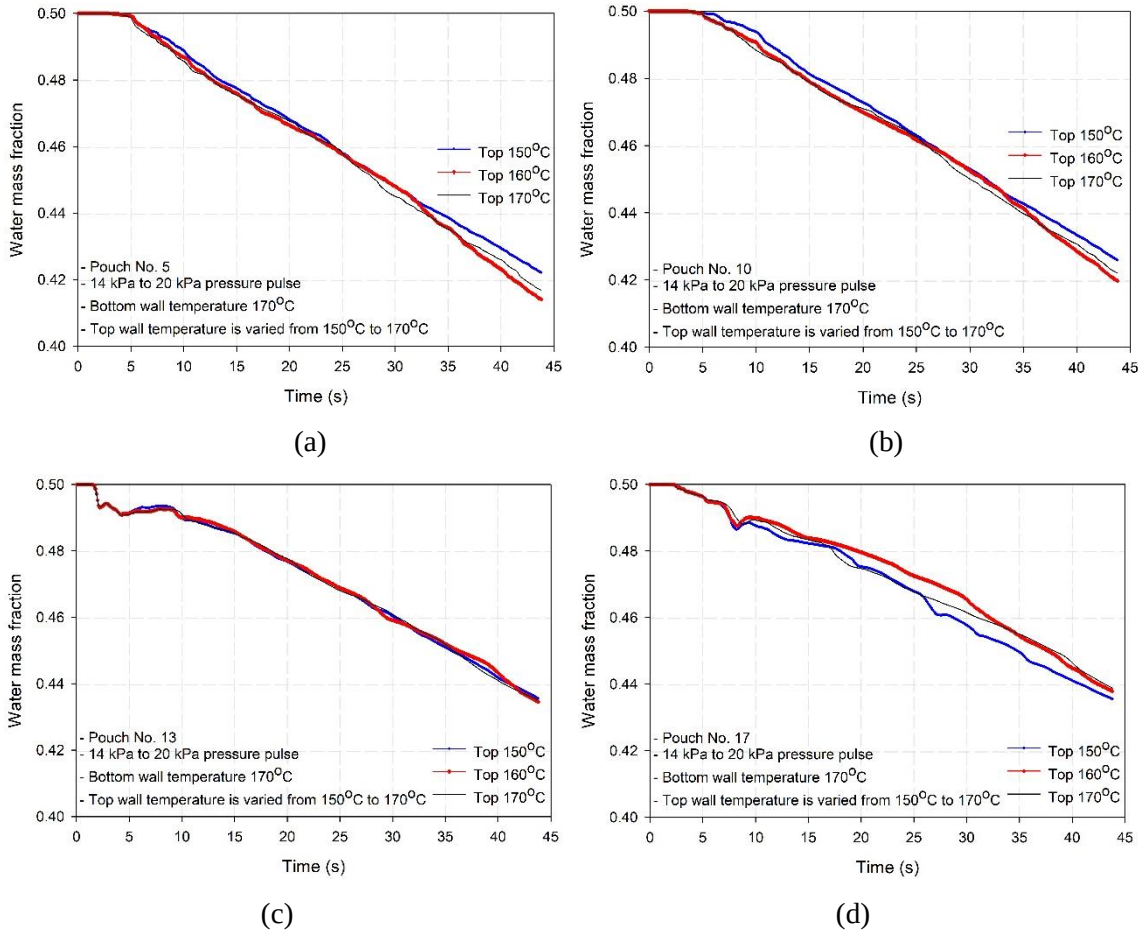

Figure 5.46 Water mass fraction after the first pressure pulse from 14 kPa to 20 kPa for pouches No. 5, 10, 13 and 17

Figure 5.47 shows the average velocity of the fluid inside the chamber variation with time during one full pressure pulses between 14 kPa and 20 kPa for different top wall temperatures while the bottom wall temperature is kept at 170°C. The average value of the velocities over the full period of the pressure pulse are 0.078 m/s, 0.072 m/s and 0.072 m/s when the top wall temperatures are 150°C, 160°C and 170°C, respectively. So, setting the top wall temperature as 150°C results in 8.3% increase in the average velocity of the fluid over the pressure pulse compared to having both the top and the bottom wall temperatures as 170°C. Also, setting the top wall temperature as 160°C results in 0% increase in the average velocity of the fluid over the pressure pulse.

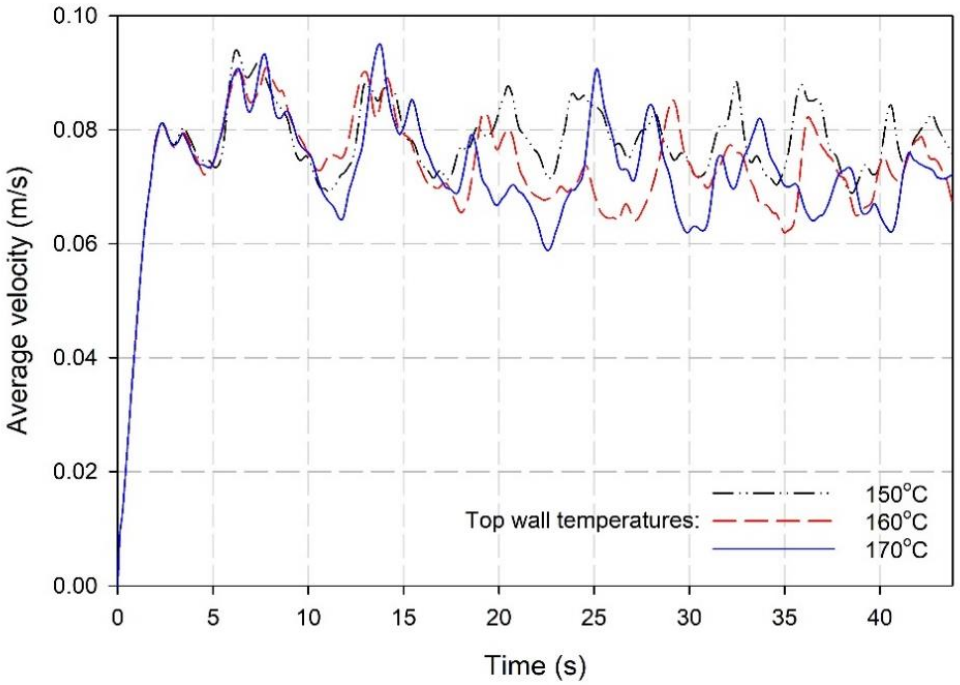

Figure 5.47 Average fluid velocity variation inside the chamber during one full pressure pulse from 14 kPa to 20 kPa for different top wall temperatures

Figure 5.48 shows the average water mass fraction inside all the pouches after one complete pressure pulse for all the different pressure pulses ranges in the simulation withvarying the top wall temperature as 150°C, 160°C to 170°C while the bottom wall temperature remains as 170°C. It's clear that setting the top wall temperature to 160°C results in an overall enhanced circulation and thus lower average water mass fraction inside the pouches after the completion of the first pressure pulse. For the first case where pressure pulse range is from 14 kPa to 15 kPa, changing the top wall temperature has no effect on

the average steam content inside the pouches. However, the only pressure pulse range where setting the top wall temperature as 150°C results in the lowest water mass fraction is when the pressure pulse is 14 kPa to 16 kPa. The average water mass fraction when the top wall temperature is 150°C is 0.4978 which shows a 0.12% improvement compared to the configuration where the top wall temperature is 160°C and 0.08% compared to the 170°C configuration. For all the rest of pressure pulses ranges where the upper limit of the pressure pulse is 17 kPa or higher, setting the top wall temperature as 160°C results in the lowest water mass fraction inside the pouches. The water mass fractions and the percentage improvement of each of them compared to the original configuration in which both the top and bottom wall temperatures are 170°C are shown in Table 5.10. As it can be seen, setting the top wall temperature as 160°C improves the drying quality by decreasing the water mass fraction when the upper limits of the pressure pulses are: 17 kPa, 18 kPa, 19 kPa, and 20 kPa. While setting the top wall temperature to 150°C only improve the drying quality when the upper limits of the pressure pulses are 16 kPa and 19 kPa.

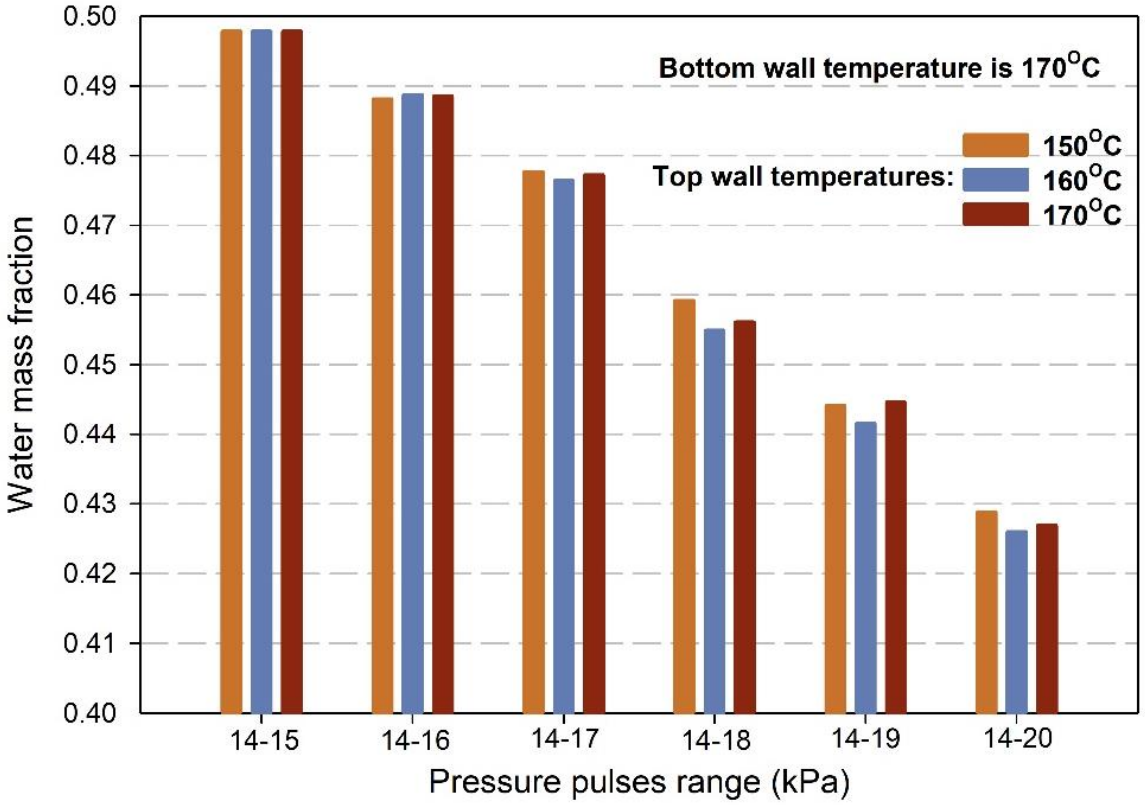

Figure 5.48 Average water mass fraction for the 20 pouches after one complete pressure pulse for different ranges of pressure pulses and different top wall temperatures

Table 5.12 Water mass fractions for different ranges of pressure pulses and different top wall temperatures and percentage improvement of the drying quality

	Water mass fraction	**Water mass fraction**	**% improvement**	**Water mass fraction**	**% improvement**
	170^0C	**160^0C**	**160^0C**	**150^0C**	**150^0C**
14-15 kPa	0.4978	0.4978	0.00	0.4978	0.00
14-16 kPa	0.4885	0.4887	-0.04	0.4881	0.08
14-17 kPa	0.4772	0.4764	0.17	0.4777	-0.10
14-18 kPa	0.4561	0.4549	0.26	0.4592	-0.68
14-19 kPa	0.4446	0.4415	0.70	0.4441	0.11
14-20 kPa	0.4269	0.4260	0.21	0.4288	-0.45

The average chamber temperature should be taken into account while discussing the differences in the performance when changing both the pressure pulses ranges and the top wall temperatures. To aid in the evaporation of any condensed water droplets inside the pouches, the average temperature inside the chamber has to be as high as possible. As changing the top wall temperature to a lower value than the bottom wall temperature which is 170°C help in enhancing the natural circulation of the fluid due to a larger temperature difference, the average temperature inside the chamber is expected to decrease with time as more air is introduced to the chamber. Figure 5.49 shows the variation of the average temperature of the air-steam mixture inside the chamber after one complete pressure pulse for different top wall temperatures and pressure pulses ranges. As can be seen, the average temperature of the fluid inside the chamber drops as the top wall temperature decreases. In addition, the range of the pressure pulses has a great effect on the average temperature of the fluid inside the chamber. The lower the pressure range, the less air introduced to the cycle in one pressure pulses and thus the higher the average temperature is going to be. In addition, the lower the pressure pulse range, the less time the pressure pulses takes to complete and the higher the average temperature of the fluid inside the chamber.

As it was shown earlier, the dry air inlet temperature is assumed to be 30°C as the ambient air passes by the outer surface of the boiler and increases its temperature. In order to maintain higher temperature inside the chamber throughout the drying cycle, one

suggestion is to increase the temperature of the air introduced to the chamber by either increasing the exposed area of the boiler or adding an electric heat the increases the temperature of the dry air before entering the chamber to increase the pressure during the

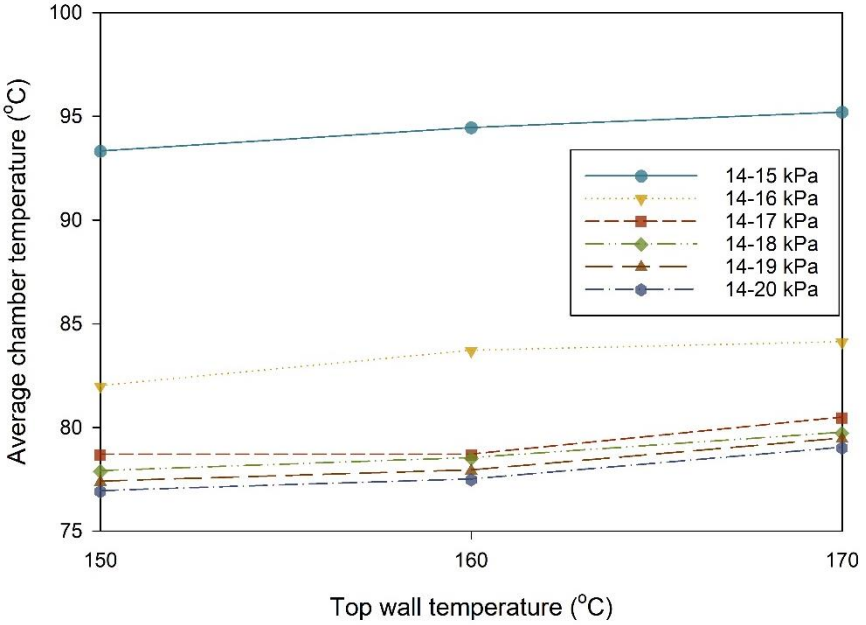

Figure 5.49 Average fluid temperature inside the chamber after one complete pressure pulses for different pressure pulses ranges and top wall temperatures

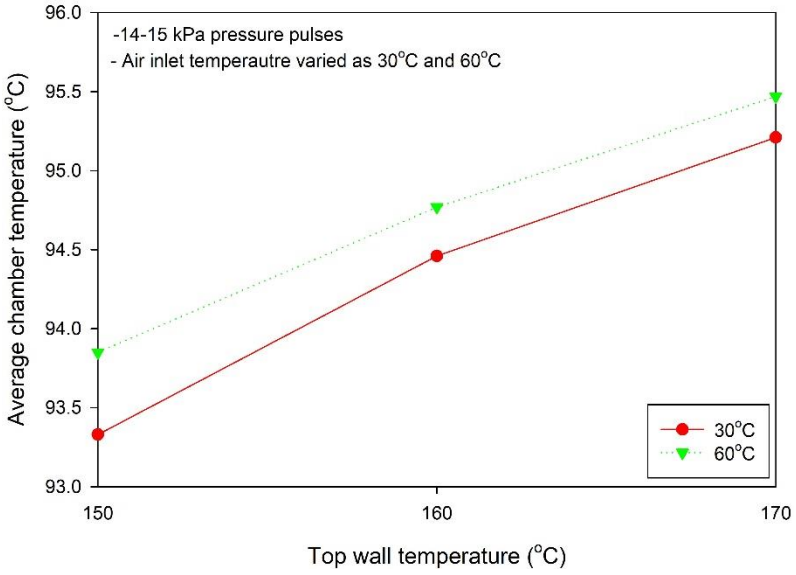

Figure 5.50 The effect of changing dry air inlet temperature on the average fluid temperature inside the chamber after one pressure pulses from 14 kPa to 15 kPa at a different top wall temperature

creation of pressure pulses. Figure 5.50 shows the difference between the average fluid temperatures inside the chamber after one complete pressure pulse from 14 kPa to 15 kPa for different top wall temperature as the dry air inlet temperature is changing from 30°C to 60°C. However, since the mass of the introduced air to the chamber is very small, the expected effect on the temperature is almost negligible as it's shown in Figure 5.51. As the top wall temperature decreases, the effect of the dry air temperature becomes more obvious. The average fluid temperature inside the chamber when the top wall temperature is 150°C is increased from 93.3°C to 93.9°C which represents a 0.64% increase in the average temperature. However, the percentage increase in the average fluid temperature drops to 0.32% and 0.31% when the top wall temperatures are 160°C and 170°C, respectively. So, it's clear that changing the temperature of the dry air introduced to the chamber during the pressurizing process in the pressure pulses has a negligible effect on the average temperature of the fluid inside the chamber.

.

Chapter 6: Conclusions and Recommendations

In this chapter, the main concluding remarks obtained through the experimental and theoretical studies are presented. Furthermore, the recommendations based on the attained expertise are listed for future work.

6.1 Conclusions

This thesis investigated, experimentally, the effects of different ranges of pressure pulses and walls temperatures on the drying quality. Also, the effects of previous parameters on the average velocity, temperature and the homogeneity of the fluid inside the chamber and the drying quality is studied numerically. The main findings can be made of this study are categorized into experimental and numerical results. The main findings obtained from the experimental invistigations are listed as follows:

- When the pressure pulses range is 14 kPa to 16 kPa, the amounts of water remaining on the 16 pouches are 2 gram, 5 grams, and 10 grams when the top wall temperatures are 170°C, 160°C, and 150°C, respectively.
- When the pressure pulses range is 14 kPa to 18 kPa, the amounts of water remaining on the 16 pouches are 12 gram, 11 grams, and 2 grams when the top wall temperatures are 170°C, 160°C, and 150°C, respectively.
- When the pressure pulses range is 14 kPa to 20 kPa, the amounts of water remaining on the 16 pouches are 12 gram, 17 grams, and 16 grams when the top wall temperatures are 170°C, 160°C, and 150°C, respectively.
- When the pressure pulses range is between 14 kPa to 16 kPa, the energy efficiencies are 78.29%, 70.46% and 57.41% while the exergy efficiencies are 30.22%, 27.24% and 22.29% when the top wall temperatures are 170°C, 160°C, and 150°C, respectively.
- When the pressure pulses range is between 14 kPa to 18 kPa, the energy efficiencies are 50.07%, 52.57% and 75.1% while the exergy efficiencies are 20.36%, 21.36% and 30.3% when the top wall temperatures are 170°C, 160°C, and 150°C, respectively.

- When the pressure pulses range is between 14 kPa to 20 kPa, the energy efficiencies are 46.89%, 35.17% and 37.51% while the exergy efficiencies are 20.45%, 15.46% and 16.46% when the top wall temperatures are 170°C, 160°C, and 150°C, respectively.

The main findings obtained from the analytical and numerical studies are listed as follows:

- Increasing the air flow velocity over water increases the amount of evaporated water from 2.4 grams to 49 grams when then the velocity increases from 1.5 m/s to 3 m/s during the 4 minutes of simulation.
- For the 3D geometry of the chamber, after 20 seconds, the simulations show that the average velocity magnitudes of the fluid inside the chamber are: 0.044 m/s, 0.031 m/s, 0.017 m/s 0.014 m/s, 0.024 m/s for the (170-150), (170-160), (160-170), (150-170) and (170-170) configurations, respectively.
- For the 3D geometry of the chamber, after 20 seconds, the simulations show that the steam mass concentrations in the top half of the chamber are: 0.45, 0.46, 0.44, 0.4 and 0.46 for the (170-150), (170-160), (160-170), (150-170) and (170-170) configurations, respectively.
- For the 3D geometry of the chamber, after 20 seconds, the simulations show that the average temperatures of the fluid inside the chamber are: 149.8°C, 154.1°C, 154.4°C, 158.9°C and 158.1°C for the (170-150), (170-160), (160-170), (150-170) and (170-170) configurations, respectively.
- For the 3D geometry of the chamber with a condenser at 20°C, after 20 seconds, the simulations show that the average velocity magnitude of the fluid inside the chamber is 0.142 m/s, the steam mass concentrations in the top half of the chamber is 0.47 and the average temperature of the fluid inside the chamber is 139.8°C.
- After one completer pressure pulse from 14 kPa to 15 kPa, the average water mass fraction remaining inside the 20 pouches in the 2D simulations are 0.4978, 0.4978 and 0.4978 and the average fluid temperatures are 95.2°C, 94.5°C and 93.3°C when the top wall temperatures are 170°C, 160°C, and 150°C

- After one completer pressure pulse from 14 kPa to 16 kPa, the average water mass fraction remaining inside the 20 pouches in the 2D simulations are 0.4885, 0.4887 and 0.4881 and the average fluid temperatures are 84.1°C, 83.7°C and 82.0°C when the top wall temperatures are 170°C, 160°C, and 150°C.
- After one completer pressure pulse from 14 kPa to 17 kPa, the average water mass fraction remaining inside the 20 pouches in the 2D simulations are 0.4772, 0.4764 and 0.4777 and the average fluid temperatures are 80.5°C, 78.7°C and 78.7°C when the top wall temperatures are 170°C, 160°C, and 150°C.
- After one completer pressure pulse from 14 kPa to 18 kPa, the average water mass fraction remaining inside the 20 pouches in the 2D simulations are 0.4561, 0.4549 and 0.4592 and the average fluid temperatures are 77.9°C, 77.6°C and 79.8°C when the top wall temperatures are 170°C, 160°C, and 150°C.
- After one completer pressure pulse from 14 kPa to 19 kPa, the average water mass fraction remaining inside the 20 pouches in the 2D simulations are 0.4446, 0.4415 and 0.4441 and the average fluid temperatures are 79.5°C, 78.0°C and 77.4°C when the top wall temperatures are 170°C, 160°C, and 150°C.
- After one completer pressure pulse from 14 kPa to 20 kPa, the average water mass fraction remaining inside the 20 pouches in the 2D simulations are 4269, 0.4260 and 0.4288 and the average fluid temperatures are 79.1°C, 77.5.0°C and 77.0°C when the top wall temperatures are 170°C, 160°C, and 150°C.
- Increasing the temperature of the dry air inlet during the creation pressures pulses because from 30°C to 60°C results in increasing the average fluid temperature inside the chamber by 0.64%, 0.32% and 0.31% when the top wall temperatures are 170°C, 160°C, and 150°C.

6.2 Recommendations

In this thesis, various parameters are changed to investigate the effects of those parameters on the drying quality. The provided results in this work provide experts in the field with potential solutions to improve the process. The following recommendations were based on the results of this thesis:

- Accurate control of the upper limit of the pressure pulses will help in creating more pulses for the same drying phase time since the average difference of the upper limit of the pressure pulses between the set value and the measured one is around 12.7%.
- Thermocouples must be installed in different places inside the chamber during the drying phase when having different wall temperatures to measure the effect of the wall temperatures on the fluid temperature.
- A more powerful vacuum pump than the already installed venture system is required to create pressure pulses since more pressure pulses can be created at a specific cycle time by reducing the time needed to create the vacuum pulses.
- Detailed full simulation for the full load of pouches to study the whole drying phase including all the pressure pulses is required to better understand the phenomena and find potential solutions.
- The design of the boiler should be improved Improve the overall heat transfer between the drying air and the boiler to increase the temperature of the drying air introduced to the chamber instead of just passing the air over the surface of the boiler.
- Suitable phase change materials should be placed inside the chamber to store some heat during the sterilization phase and release that heat during the drying phase as the average temperature of the fluid drops which will help to increase the temperature of the fluid and thus helps in removing the droplets of water remaining on the pouches.
- The inclusion of moisture wicking material such as sorption materials (silica gel).
- When doing the experiments, the pouches should be placed such that the plastic side is facing upward so the water droplets can escape from the pouch by the help of the gravitational force and thus make the tools inside the pouch dry.
- Increasing the range of the pressure pulses will help in increasing the mass of dry air being introduced to the chamber during each pulse. However, more pulses should be achieved by either enhancing the control of the upper limit of the pressure pulses or replacing the venture system by a more powerful vacuum pump.

References

[1] BP, “BP Statistical Review of World Energy,” 2018.

[2] “Monthly Energy Review – November 2018,” 2018.

[3] BP, “BP Energy Outlook,” 2019.

[4] M. Djaeni and A. J. B. van Boxtel, “PhD Thesis Summary: Energy Efficient Multistage Zeolite Drying for Heat-Sensitive Products,” *Dry. Technol.*, vol. 27, no. 5, pp. 721–722, Apr. 2009.

[5] J. C. Atuonwu, G. van Straten, H. C. van Deventer, and A. J. B. van Boxtel, “Synergistic Process Design: Reducing Drying Energy Consumption by Optimal Adsorbent Selection,” *Ind. Eng. Chem. Res.*, vol. 52, no. 18, pp. 6201–6210, May 2013.

[6] T. Kudra, “Energy Aspects in Drying,” *Dry. Technol.*, vol. 22, no. 5, pp. 917–932, Dec. 2004.

[7] U. Manufacturing, “Energy Use, Loss and Opportunities Analysis,” 2004.

[8] B. Dutta, *Principles of mass transfer and seperation processes*. PHI Learning Pvt. Ltd., 2007.

[9] B. Yilbas, M. Hussain, and I. Dincer, “Heat and moisture diffusion in slab products due to convective boundary condition,” *Heat Mass Transf.*, vol. 39, no. 5, pp. 471–476, Jun. 2003.

[10] J. R. Philip and D. A. De Vries, “Moisture movement in porous materials under temperature gradients,” *Trans. Am. Geophys. Union*, vol. 38, no. 2, p. 222, Apr. 1957.

[11] A. V. Luikov, “Systems of differential equations of heat and mass transfer in capillary-porous bodies (review),” *Int. J. Heat Mass Transf.*, vol. 18, no. 1, pp. 1–14, Jan. 1975.

[12] D. Mukherjee, V. M. Puri, and R. C. Anantheswaran, “Measurement of Coupled Heat and Moisture Transfer Coefficients for Selected Vegetables,” *Dry. Technol.*, vol. 15, no. 1, pp. 71–94, Jan. 1997.

[13] P. Moran, “Sterilization,” in *Encyclopedia of Immigrant Health*, New York, NY: Springer New York, 2012, pp. 1384–1385.

[14] J. B. Epstein, G. Rea, L. Sibau, and C. H. Sherlock, “Rotary dental instruments and the potential risk of transmission of infection: herpes simplex virus.,” *J. Am. Dent. Assoc.*, vol. 124, no. 12, pp. 55–9, Dec. 1993.

[15] J. B. Epstein, G. Rea, L. Sibau, C. H. Sherlock, and N. D. Le, “Assessing viral retention and elimination in rotary dental instruments.,” *J. Am. Dent. Assoc.*, vol. 126, no. 1, pp. 87–92, Jan. 1995.

[16] A. Smith, G. Smith, D. F. Lappin, H. C. Baxter, A. Jones, and R. L. Baxter, “Dental

handpiece contamination: a proteomics and surface analysis approach," *Biofouling*, vol. 30, no. 1, pp. 29–39, Jan. 2014.

[17] G. Smith and A. Smith, "Microbial contamination of used dental handpieces," *Am. J. Infect. Control*, vol. 42, no. 9, pp. 1019–1021, Sep. 2014.

[18] M. Kellett and W. P. Holbrook, "Bacterial contamination of dental handpieces," *J. Dent.*, vol. 8, no. 3, pp. 249–253, Sep. 1980.

[19] S. Winter, A. Smith, D. Lappin, G. McDonagh, and B. Kirk, "Investigating steam penetration using thermometric methods in dental handpieces with narrow internal lumens during sterilizing processes with non-vacuum or vacuum processes," *J. Hosp. Infect.*, vol. 97, no. 4, pp. 338–342, Dec. 2017.

[20] I. Dincer and C. Zamfirescu, *Drying Phenomena: Theory and Applications*. Wiley, 2015.

[21] E. A. S. Mujumdar, "Book Review : Handbook of Industrial Drying , Third Edition Handbook of Industrial Drying , Third Edition," vol. 3937, no. 2007, 2010.

[22] O. Espinoza and B. Bond, "Vacuum Drying of Wood — State of the Art," *Curr. For. Reports*, pp. 223–235, 2016.

[23] A. Gray, "Process of drying timber," US763482, 1904.

[24] S. Kirckof, S. Flynn, and M. Young, "Are You Running the Correct Steam Sterilization Cycles for Your Loads ? Understanding the challenges of extended steam sterilization cycles," *Manag. Infect. Control*, no. March, pp. 72–89, 2009.

[25] S. Jaya and P. H. Das, "A Vacuum Drying Model for Mango Pulp," vol. 3937, 2007.

[26] M. A. Sahari, H. Samadlui, M. A. Sahari, and H. Samadlui, "Optimization of Vacuum Drying Characteristics of Date Powder Optimization of Vacuum Drying Characteristics of Date Powder," vol. 3937, no. May, 2008.

[27] M. F. Zotarelli, B. D. A. Porciuncula, and J. B. Laurindo, "A convective multi-flash drying process for producing dehydrated crispy fruits," *J. Food Eng.*, vol. 108, no. 4, pp. 523–531, Feb. 2012.

[28] M. Dion and W. Parker, "Steam Sterilization Principles," *Pharm. Eng.*, vol. 33, no. 6, pp. 1–8, 2013.

[29] SATO VAC INC., "What is Vacuum drying?" [Online]. Available: http://www.satovac.co.jp/en/seminar/dryness.html.

[30] "Guideline for Disinfection and Sterilization in Healthcare Facilities," 2008. [Online].Available: https://www.cdc.gov/infectioncontrol/guidelines/disinfection/tables/table7.html.

[31] A. Abhat, "Low temperature latent heat thermal energy storage: Heat storage materials," *Sol. Energy*, vol. 30, no. 4, pp. 313–332, 1983.

[32] G. A. Lane, "Low temperature heat storage with phase change materials," *Int. J.*

Ambient Energy, vol. 1, no. 3, pp. 155–168, Jul. 1980.

[33] S. Mondal, "Phase change materials for smart textiles–An overview," *Appl. Therm. Eng.*, vol. 28, pp. 1536–1550, 2008.

[34] M. Farid, A. Khudhair, S. Razack, and S. Al-Hallaj, "A review on phase change energy storage: materials and applications," *Elsevier*.

[35] M. Liu, W. Saman, F. B.-R. and S. E. Reviews, and undefined 2012, "Review on storage materials and thermal performance enhancement techniques for high temperature phase change thermal storage systems," *Elsevier*.

[36] S. M. Hasnain, "Review on sustainable thermal energy storage technologies, Part I: heat storage materials and techniques," *Energy Convers. Manag.*, vol. 39, no. 11, pp. 1127–1138, Aug. 1998.

[37] I. Dincer and M. Rosen, *Thermal energy storage systems and applications*. Wiley, 2002.

[38] H. Baumann and J. Heckenkamp, "Latentwärmespeicher," *Nachrichten aus Chemie, Tech. und Lab.*, vol. 45, no. 11, pp. 1075–1081, Nov. 1997.

[39] A. Kaizawa *et al.*, "Thermophysical and heat transfer properties of phase change material candidate for waste heat transportation system," *Heat Mass Transf.*, vol. 44, no. 7, pp. 763–769, May 2008.

[40] X. Wang, E. Lu, W. Lin, and C. Wang, "Micromechanism of heat storage in a binary system of two kinds of polyalcohols as a solid–solid phase change material," *Energy Convers. Manag.*, vol. 41, no. 2, pp. 135–144, Jan. 2000.

[41] Q. Yan and C. Liang, "The thermal storage performance of monobasic, binary and triatomic polyalcohols systems," *Sol. Energy*, vol. 82, no. 7, pp. 656–662, Jul. 2008.

[42] D. Chandra, R. Chellappa, and W.-M. Chien, "Thermodynamic assessment of binary solid-state thermal storage materials," *J. Phys. Chem. Solids*, vol. 66, no. 2–4, pp. 235–240, Feb. 2005.

[43] X. Wang *et al.*, "Heat storage performance of the binary systems neopentyl glycol/pentaerythritol and neopentyl glycol/trihydroxy methyl-aminomethane as solid–solid phase change materials," *Energy Convers. Manag.*, vol. 41, no. 2, pp. 129–134, Jan. 2000.

[44] W. A. Rutala and D. J. Weber, "Disinfection and sterilization: an overview.," *Am. J. Infect. Control*, vol. 41, no. 5 Suppl, pp. S2-5, May 2013.

[45] W. A. Rutala and D. J. Weber, "Guideline for Disinfection and Sterilization in Healthcare Facilities," 2008.

[46] S. BP, "CDC guidelines for the prevention and control of nosocomial infections. Guideline for hospital environmental control.," no. 11, pp. 97–120, 1983.

[47] R. WA, "1994, 1995, and 1996 APIC Guidelines Committee. APIC guideline for selection and use of disinfectants. Association for Professionals in Infection Control

and Epidemiology, Inc.," *Am J Infect Control*, no. 24, pp. 313–342, 1996.

[48] E. L. Ussler, *Diffusion: Mass Transfer in Fluid Systems*, 2nd ed. New York: Cambridge University Press, 1997.

[49] D. Basu, "Reason behind wet pack after steam sterilization and its consequences: An overview from Central Sterile Supply Department of a cancer center in eastern India," *J. Infect. Public Health*, vol. 10, no. 2, pp. 235–239, 2017.

[50] "Guideline for Disinfection and Sterilization in Healthcare Facilities," 2008. [Online].Available: https://www.cdc.gov/infectioncontrol/guidelines/disinfection/sterilization/steam.html.

[51] F. Pask, J. Sadhukhan, P. Lake, S. McKenna, E. B. Perez, and A. Yang, "Systematic approach to industrial oven optimisation for energy saving," *Appl. Therm. Eng.*, vol. 71, no. 1, pp. 72–77, Oct. 2014.

[52] M. Al-Ali and I. Dincer, "Energetic and exergetic studies of a multigenerational solar–geothermal system," *Appl. Therm. Eng.*, vol. 71, no. 1, pp. 16–23, Oct. 2014.

[53] I. Dincer and M. Rosen, *Exergy: energy, environment and sustainable development*. 2012.

[54] "COMSOL Multiphysics® v. 5.4. www.comsol.com. COMSOL AB, Stockholm, Sweden." [Online]. Available: https://www.comsol.com/.

[55] P. K. Bansal and N. Zealand, "A unified empirical correlation for evaporation of water at low air velocities," vol. 25, no. 2, pp. 183–190, 1998.